REFERENCE:	SAF/AC/AUTH-RMI/VR/001
ISSUE:	1/2020
DATE:	3 July 2020
PAGES:	112

SAF/AC VALIDATION REPORT

Validated products:

Identifier	Name	Acronym
O3M-68, O3M-78, O3M-69	NRT Absorbing Aerosol Height products	NRT/AAH
O3M-79, O3M-364, O3M-365	Offline Absorbing Aerosol Height products	Offline/AAH
O3M-170	Data Record Absorbing Aerosol Height products	DR/AAH

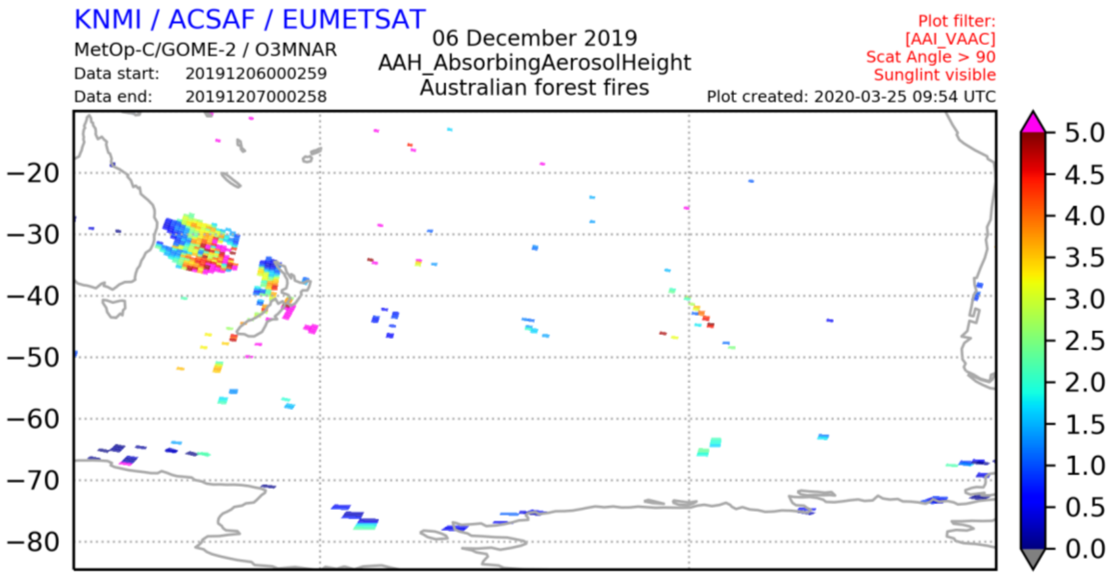

Authors:

Name	Institute
V. De Bock and A. Delcloo	Royal Meteorological Institute of Belgium (RMI)
K. Michailidis, M. Koukouli and D. Balis	Laboratory of Atmospheric Physics, Aristotle University of Thessaloniki

Reporting period: 2007-2019

Table of contents:

Contents

1 Introduction

1.1 General EUMETSAT information

EUMETSAT is the European operational satellite agency for monitoring weather, climate and the environment. It operates a system of meteorological satellites that observe the atmosphere and ocean and land surfaces – 24 hours a day, 365 days a year. This data is supplied to the National Meteorological Services of the organization's Member and Cooperating States in Europe, as well as other users worldwide. The service provided by EUMETSAT helps to enhance and safeguard the daily lives of European citizens. They aid meteorologists in identifying and monitoring the development of potentially dangerous weather situations and in issuing timely forecasts and warnings to emergency services and local authorities, helping to mitigate the effects of severe weather and protecting human life and property. This information is also critical to the safety of air travel, shipping and road traffic, and to the daily business of farming, construction and many other industries.

Utilizing specialist expertise from the Member States**, Satellite Application Facilities** (SAFs) are dedicated centers of excellence for processing satellite data. They form an integral part of the distributed EUMETSAT Application Ground Segment. The eight EUMETSAT SAFs provide users with operational data and software products, each one for a dedicated user community and application area.

1.2 Atmospheric Composition Satellite Application Facility (AC SAF) information

Background
The monitoring of atmospheric chemistry is essential due to several human caused changes in the atmosphere, like global warming, loss of stratospheric ozone, increasing UV radiation, and pollution. Furthermore, the monitoring is used to react to the threads caused by the natural hazards as well as follow the effects of the international protocols.
Therefore, monitoring the chemical composition and radiation of the atmosphere is a very important duty for EUMETSAT and the target is to provide information for policy makers, scientists and general public.

Objectives
The main objectives of the AC SAF is to process, archive, validate and disseminate atmospheric composition products (O_3, NO_2, SO_2, BrO, HCHO, H_2O, OClO, CO, NH_3), aerosol products and surface ultraviolet radiation products utilizing the satellites of EUMETSAT. The majority of the AC SAF products are based on data from the GOME-2 and IASI instruments onboard MetOp satellites.
Another important task besides the near real-time (NRT) and offline data dissemination is the provision of long-term, high-quality atmospheric composition products resulting from reprocessing activities.

Product categories, timeliness and dissemination
Near Real-Time (NRT) products are available in less than three hours after measurement. These products are disseminated via EUMETCast, WMO GTS or internet.

- Near real-time trace gas columns (total and tropospheric O3 and NO2, total SO2, total HCHO, CO) and ozone profiles
- Near real-time absorbing aerosol indexes from main science channels and polarization measurement detectors
- Near real-time UV indexes, clear-sky and cloud-corrected

Offline products are available within two weeks after measurement and disseminated via dedicated web services at EUMETSAT and AC SAF.

- Offline trace gas columns (total and tropospheric O3 and NO2, total SO2, total BrO, total HCHO, total H2O) and ozone profiles
- Offline absorbing aerosol indexes from main science channels and polarization measurement detectors
- Offline surface UV, daily doses and daily maximum values with several weighting functions

Data records (DR) are available after reprocessing activities from the EUMETSAT Data Centre and/or the AC SAF archives.

- Data records generated in reprocessing
- Surface Lambertian-equivalent reflectivity
- Total OClO

Users can access the AC SAF offline products and data records (free of charge) by registering at the AC SAF web site.

More information about the AC SAF project, products and services: http://acsaf.org/
AC SAF Helpdesk: helpdesk@acsaf.org
Twitter: https://twitter.com/Atmospheric SAF

1.3 Absorbing Aerosol Height

The Global Ozone Monitoring Experiment (GOME)-2 Absorbing Aerosol Height (AAH) product is a new product developed by Koninklijk Nederlands Meteorologisch Instituut (KNMI) within EUMETSAT's AC SAF. This product builds on a previously developed product, the Absorbing Aerosol Index (AAI; Tuinder et al., 2019), and derives the actual height of the absorbing aerosol layer in the O2-A band using the Fast Retrieval Scheme for Clouds from the Oxygen A band (FRESCO) algorithm. The AAH product can be used to monitor volcanic eruptions globally and provide the height of the ash layers (Balis et al., 2016). The AAH is very sensitive to cloud contamination. However, aerosols and clouds can prove difficult to distinguish and the AAH is computed for different FRESCO cloud fractions. Not only is FRESCO able to determine the height of an absorbing aerosol layer in the absence of clouds, but under certain conditions also in the presence of clouds. Further details and more information associated with the AAH product are available in the Product User Manual (PUM) and Algorithm Theoretical Basis Document (ATBD).

In summary, the AAH algorithm retrieves, from the GOME-2 level-1b Product Dissemination Unit (PDU), the following parameters:
– CF: effective aerosol/cloud fraction
– CH: aerosol/cloud height
– SA: scene albedo
– SH: scene height
Two different aerosol/cloud layer heights (CH and SH) are determined by the AAH algorithm. It is up to the algorithm to decide which of the two is the best candidate to represent the actual AAH.

To determine whether CH or SH should be reported as the AAH, the algorithm distinguishes three situations (regimes):

A:	CF ≤ 0.25	→ AAH = CH (high reliability)
B:	0.25 < CF < 0.75	→ AAH = max(SH,CH) (medium reliability)
C:	CF ≥ 0.75	→ AAH = CH (low reliability)

The effective cloud fraction is used to check in which of these regimes inside the parameter space the solution is likely to be found. The scheme is based on the results of the study presented in Wang et al. (2012). Regime A refers to the situation in which there is only a low degree of cloud cover or if the AOD is sufficiently large to compensate for the presence of a cloud layer below the aerosol layer. In this case the results reported in Wang et al. (2012) clearly show that the cloud height is close to the real height of the aerosol layer in almost all cases. Exceptions are cases with low aerosol amounts, but these scenes were filtered out beforehand by demanding that the AAI must be higher than the threshold value of 4.0 index points. Regime C is the situation of a thick cloud layer present in the scene. In this case, an aerosol layer is only retrieved successfully when the aerosol layer is sufficiently thick. According to the results presented in Wang et al. (2012), the best value for the AAH is that of the cloud height. In most cases, however, the AAH is severely underestimated. The reliability is therefore characterized as “low”. Finally, regime B is an intermediate regime, and the best estimate is the highest value from cloud height and scene height. The AAH found this way is likely to underestimate the AAH in some cases, and the reliability attributed to this regime is “medium”. The accuracy requirements for the AAH product are defined in Table 1.

Table 1. Accuracy requirements defined for the AAH product

	Layer height < 10 km	**Layer height > 10 km**
Threshold	3 km	4 km
Target	2 km	3 km
optimal	1 km	2 km

The GOME-2 AAH product is available in Near-Real time (NRT) and offline processing, from the Level-1 data generated from the GOME-2 instruments onboard the MetOp-A, MetOp-B and MetOp-C satellite platforms. The format of the AAH product Level-2 file is HDF-5. The organized data group contains all the appropriate information about AAI, AAH and FRESCO. The list of the aerosol data products used in the study is shown in Table 2.

Table 2. Overview of the AAH NRT & offline data products produced by the MetOp satellites

Product ID	Satellite Platform	Type
O3M-68	GOME-2 MetOp-A	NRT
O3M-69	GOME-2 MetOp-A	Offline
O3M-78	GOME-2 MetOp-B	NRT
O3M-79	GOME-2 MetOp-B	Offline
O3M-364	GOME-2 MetOp-C	NRT
O3M-365	GOME-2 MetOp-C	Offline
O3M-170	GOME-2 MetOp-A/B/C	DR

2 Aim and scope of the work

The purpose of this document is to present the validation of the EUMETSAT AC SAF AAH product. This validation was independently performed by teams from two different institutes: the Royal Meteorological Institute of Belgium (RMI) and the Aristotle University of Thessaloniki (AUTH). Both teams took a different approach towards this validation exercise. RMI compared the GOME-2 AAH with the aerosol layer height determined by Cloud-Aerosol Lidar with Orthogonal Polarization (CALIOP) for different specific case studies, while AUTH compared the GOME-2 AAH with the aerosol layer height (ALH) retrieved from Light Detection and Ranging (LIDAR) instruments in the European Aerosol Research Lidar Network (EARLINET). Both teams will compare their results with the accuracy requirements defined in section 1.3.

3 Data and methodology

3.1 RMI validation approach

The GOME-2 AAH product is validated by RMI using aerosol layer height information provided by the CALIOP Vertical Feature Mask product (V4.20) data (downloaded from the Atmospheric Science Data Center located at NASA's Langley Research Center at https://eosweb.larc.nasa.gov/project/calipso/cal_lid_l2_vfm_standard_v4_20). The CALIOP data consists of latitude, longitude, profile time, day/night flag, land/water flag and feature classification flags. These feature classification flags define the type of a feature as either clear air, aerosol, cloud, stratospheric feature, surface, subsurface or no signal. A quality flag is assigned to this type classification. A subtype is also defined. For the tropospheric aerosol type, CALIOP defines clean marine, dusty marine, clean continental, polluted continental, dust, polluted dust and smoke. For the stratospheric aerosol type, CALIOP defines volcanic ash, sulfate and elevated smoke. The subtype classification also receives a quality flag.

RMI decided to validate the GOME-2 AAH for specific cases of volcanic eruptions. A list of confirmed volcanic eruptions can be found on the website of the Global Volcanism Program of the Smithsonian Institution (https://volcano.si.edu/). From this list, cases with a 'clear' signal (AAI>4) on AAI maps (available from the TEMIS website: http://www.temis.nl/airpollution/absaai/) were chosen to further investigate. Figure 1 shows an example of such an AAI map with the signal of the Calbuco eruption (41.33°S/72.62°W).

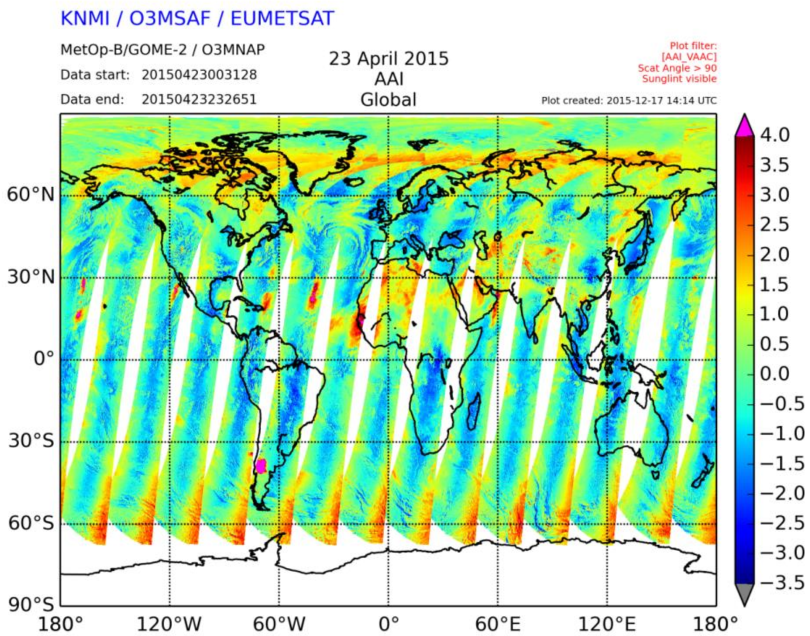

Figure 1: AAI map of GOME-2B for the 23rd of April 2015. In Chili, a zone of high AAI values (> 4) can be observed which coincides with the location of the Calbuco volcano which erupted on this day.

The final list of studied volcanic eruptions can be found in Table 3. GOME-2 and CALIOP pixels were compared when the distance between the center pixel of GOME-2 and CALIOP was maximum 100 km. There was no threshold used to limit the time difference between both satellite overpasses. Only AAH data for AAI>4 are validated to assure that there are enough absorbing aerosols. Especially the layer height of volcanic species (volcanic ash and sulfate) was looked at. However, as it is known that volcanic aerosols in the troposphere are often misclassified by CALIOP as dust or polluted dust, the height of these aerosol layers will also be compared to the AAH.

Table 3: List of studied volcanos together with their geographical coordinates, the study period and the available GOME-2 overpasses.

Volcano (Country)	Latitude/Longitude	Studied dates	GOME-2 A/B/C
Barren Island (India)	12.278°N/93.858°E	25-26 September 2018	B
Bulusan (Philipines)	12.769°N/124.056°E	1-3 May 2015	A/B
Calbuco (Chile)	41.33°S/72.62°W	23-24 April 2015	A/B
Eyjafjallajokull (Iceland)	63.633°N/19.633°W	14-17 April 2010	A
Grimsvotn (Iceland)	64.416°N/17.316°W	22-24 May 2011	A
Kasatochi (United States)	52.177°N/175.508°W	7-9 August 2008	A
Krakatau (Indonesia)	6.102°S/105.423°E	19-24 February 2017	A/B
Mount Kelud (Indonesia)	7.93°S/112.31°E	13-15 February 2014	A/B
Nishinoshima (Japan)	27.247°N/140.874°E	12-15 July 2018	A/B
Paluweh (Indonesia)	8.32°S/121.71°E	2-11 February 2013	A/B
Puyehue-Cordon Caulle (Chili)	40.59°S/72.12°W	5 June 2011	A
Raikoke (Russia)	48.29°N/153.25°E	22-23 June 2019	B/C
Rinjani (Indonesia)	8.42°S/116.47°E	25-27 October 2015	A/B
Sarychev Peak (Russia)	48.092°N/153.20°E	14-17 June 2009	A
Ubinas (Peru)	16.355°S/70.903°W	13-14 September 2016	A/B

Apart from case studies from volcanic eruptions, the recent bush fires in Australia were also investigated as large amounts of absorbing aerosols were emitted into the atmosphere. It is important to note that the CALIOP V4.20 Vertical Feature Mask data is not yet available for November and December 2019. It was decided to use the older version 3.40 data to have a first look at the agreement between the height of the smoke layers detected by CALIOP and the AAH from GOME-2C. A big difference is that V3.40 data does define stratospheric aerosol types, such as elevated smoke. Only tropospheric subtypes are defined, so only the height of tropospheric smoke layers can be tracked.

3.2 AUTH validation approach

AUTH used the aerosol layer height retrieved from LIDARS within EARLINET to validate the GOME-2 AAH product.

The European Aerosol Research Lidar Network, EARLINET, was founded in 2000 as a research project for establishing a quantitative, comprehensive, and statistically significant database for the horizontal, vertical, and temporal distribution of aerosols on a continental scale (Bösenberg et al., 2003; Pappalardo et al., 2014). Since then EARLINET has continued to provide the most extensive collection of ground-based data for the aerosol vertical distribution over Europe. EARLINET observations are performed on a regular schedule of one daytime measurement per week (Monday) around noon, when the Planetary Boundary Layer (PBL) is usually well developed, and two nighttime measurements per week (Monday and Thursday), with low background light, in order to perform Raman extinction measurements (Figure 2). In addition to these systematic measurements for the consolidation of a European aerosol climatology, further observations are devoted to monitoring special events over the continent, such as Saharan dust outbreaks, forest fires, photochemical smog, and volcanic eruptions.

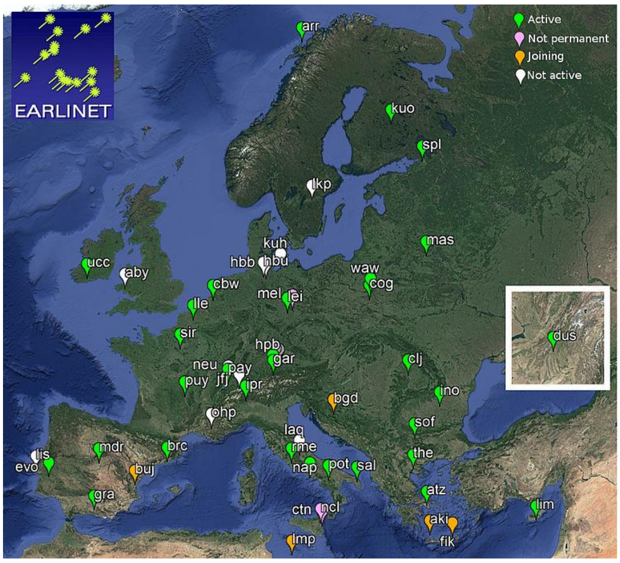

Figure 2:Geographical distribution of current EARLINET stations (Last update: 03/03/2020)

Consequently, EARLINET data have already been used for climatological studies (Amiridis et al., 2005, Balis et al., 2003, Giannakaki et al., 2010), long-range transport analysis (Ansman et al., 2003, Papayannis et al., 2008, Pappalardo et al., 2013), aerosol characterization of dust weather forecast modeling (Perez et al., 2006). Furthermore, retrieval algorithms related to aerosol microphysical properties were developed with real multi-wavelength lidar data (Balis et al., 2010, Mamouri et al., 2012, Tesche et al, 2008, Veselovski et al., 2002). Apart from climatological measurements, EARLINET also performs specific observations during special events such as Saharan dust outbreaks (Balis et al., 2004, Fernández et al., 2018, Papayannis et al., 2008), volcanic eruptions (Balis et al., 2016, Pappalardo et al., 2013) and biomass burning (Amiridis et al., 2009, Balis et al., 2003). Some of the EARLINET systems perform 24/7 continuous measurements as, for example, the PollyXT systems (Baars et al., 2016, Engelmann et al., 2016). EARLINET consists of quite different lidar systems regarding the number of measured wavelengths and signal channels, the detection range, which is mainly determined by laser power and telescope size and number, the optical design and the electronic signal detection techniques. The EARLINET stations can be classified in the following categories according to their measurement capabilities: (a) Backscatter lidar stations, (b) Raman lidar stations and (c) Multi-wavelength Raman lidar stations. Typical operating wavelengths of EARLINET are 355, 532 and 1064 nm. Furthermore, many stations operate depolarization channels that measure the depolarization of the emitted linearly polarized radiation, yielding as product the aerosol particle linear depolarization ratio which enhances the aerosol typing capabilities by providing information on the particle shape. A list of the EARLINET stations used for the validation of GOME-2 AAH and their geographical coordinates are given in Table 4 and presented in Figure 3.

Table 4. Locations of EARLINET lidar stations and their geographical coordinates. D: aerosol depolarization measurement capability; MWRL: multi-wavelength Raman lidar; RL: Raman lidar

Site	EARLINET code		Altitude a.s.l (m)	Latitude (°N)	Longitude (°E)
Barcelona, Spain	**BRC**	MWRL (D)	115	41.39	2.11
Granada, Spain	**GRA**	MWRL (D)	680	37.16	-3.60
Évora, Portugal	**EVO**	MWRL (D)	293	38.56	-7.91
Thessaloniki, Greece	**THE**	MWRL (D)	60	40.63	22.95
Minsk, Belarus	**MAS**	MWRL (D)	200	53.91	27.60
Bucharest, Romania	**INO**	MWRL (D)	93	44.34	26.03
Limassol, Cyprus	**LIM**	RL (D)	10	34.67	33.04

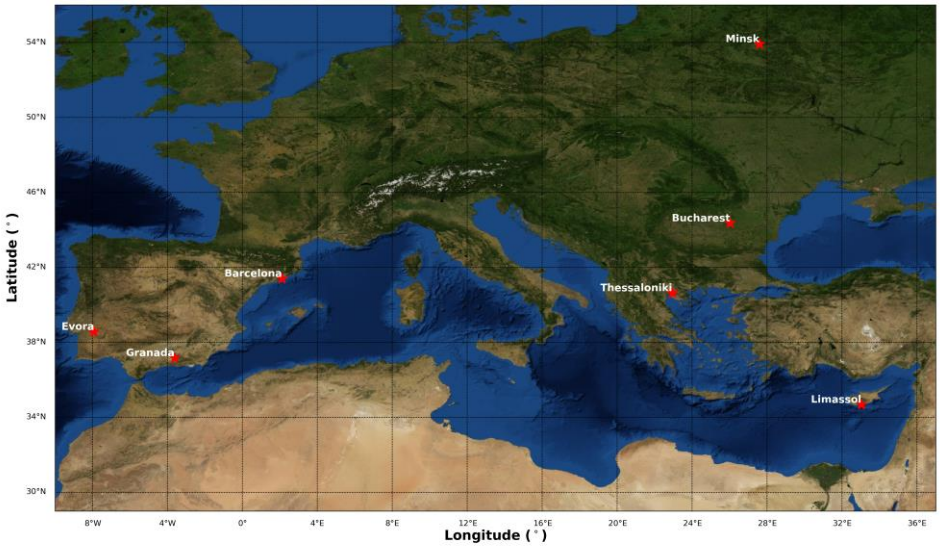

Figure 3. Map of EARLINET and stations involved in this validation report.

The EARLINET database represents the largest collection of ground-based data of the vertical aerosol distribution on a continental scale. EARLINET members, as well as external users, get access to the database through a web interface. This web portal is accessible through a corresponding link on the EARLINET web pages (www.earlinet.org). The main information stored in the files of the EARLINET database is the vertical distribution backscatter and aerosol extinction coefficients. Additionally, there are more optional variables included in the files, such as the lidar ratio, the particle linear depolarization ratio and the water vapor mixing ratio profiles. The EARLINET database stores only quantitative information.

In this study we use the backscatter profiles for aerosol layer height retrieval. The backscatter files contain at least a profile of the aerosol backscatter coefficient ($m^{-1}sr^{-1}$) derived from the elastic backscatter signal. The backscatter profile may be accompanied by an extinction coefficient profile. All lidar data in the database are stored in netCDF format and metadata is also provided in the netCDF files. In this study we use the vertical information of backscatter profiles (at 1064 nm and 532 nm in some case) for the selected EARLINET stations.

3.2.1 Wavelet covariance transform (WCT) method

This section discusses the algorithmic processes that are required in order to extract geometrical features from the lidar signals. Further details can be found in Siomos (2018). The aerosol geometrical properties carry information about the structure of lidar profiles, such as the boundary layer height (PBL) and the features of the lofted aerosol layers. They can be obtained from any lidar profile. Some lidar optical products however are more reliable to use than others. For example, the longer wavelengths typically magnify the differences in the vertical distribution of the aerosol load, resulting in layers that are easier to identify. Furthermore, the Raman inversion always results in profiles that are less structured for the extinction coefficients than the backscatter coefficients. This is the reason why we prioritize them in order to produce geometrical properties. The product with the highest potential to magnify the layer structure available is selected for each measurement. More specifically, the backscatter products are prioritized over the extinction products and the longer wavelengths over the shorter ones. For this study, backscatter profiles at 1064 nm have been prioritized but in some cases backscatter profiles at 532 nm have also been used.

The analysis is based on the method of Baars et al. (2008) that applies the wavelet covariance transform (WCT) to the raw lidar data in order to extract geometrical features such as the PBL height and the cloud boundaries. Many methods have been proposed for the calculation of the PBL height from lidar data (e.g., Brooks, 2003, Flamant et al., 1997). The WCT transformation has also been applied successfully in the past on other lidar products. Siomos et al. (2017), for example, used an adaptation of the WCT method and calculated the geometrical features from the aerosol concentration profiles. The wavelet covariance transform was defined as a means of detecting step changes in a signal. It is based upon a compound step function, the Haar function ***h***, defined as:

$$h\left(\frac{z-b}{a}\right)=\begin{cases}+1: b-\frac{a}{2}\leq z\leq b\\ -1: b\leq z\leq b+\frac{a}{2}\\ 0: elsewhere,\end{cases}$$

Here, h[(z-b)/a] is the Haar function, a is the dilation of the Haar function indicating the size of the window (or dilation), b is the center of the Haar function (or the translation) and z is the altitude range. The covariance transform of the Haar function, W_f (a,b), is defined as:

$$W_f(a,b) = a^{-1}\int_{zb}^{zt} f(z)h\left(\frac{z-b}{a}\right)dz$$

where f(z) is the backscatter lidar signal, z_b and z_t are the lowest altitude and the highest altitude of possible layers heights. The W_f(a,b) is refered to as the wavelet coefficient. These variables define the window function. Based on the defined lower and upper limits the Haar transform is calculated. The obtained Haar values are subjected to covariance transform. The maximum negative value of covariance transform provides the aerosol layer top. The key issues of performing the WCT are the determination of the dilation value of the Haar function. A small dilation value can detect many small aerosol layers. With the increase of the dilation value, these small features may be invisible from the wavelet coefficient. A dilation of 0.4 km is used in this study for the lofted aerosol layer height calculations, similar to Siomos et al. (2017). An example of an EARLINET backscatter profile with the resulting WCT profile from Barcelona lidar station is shown in Figure 4, where multiple layers are detected.

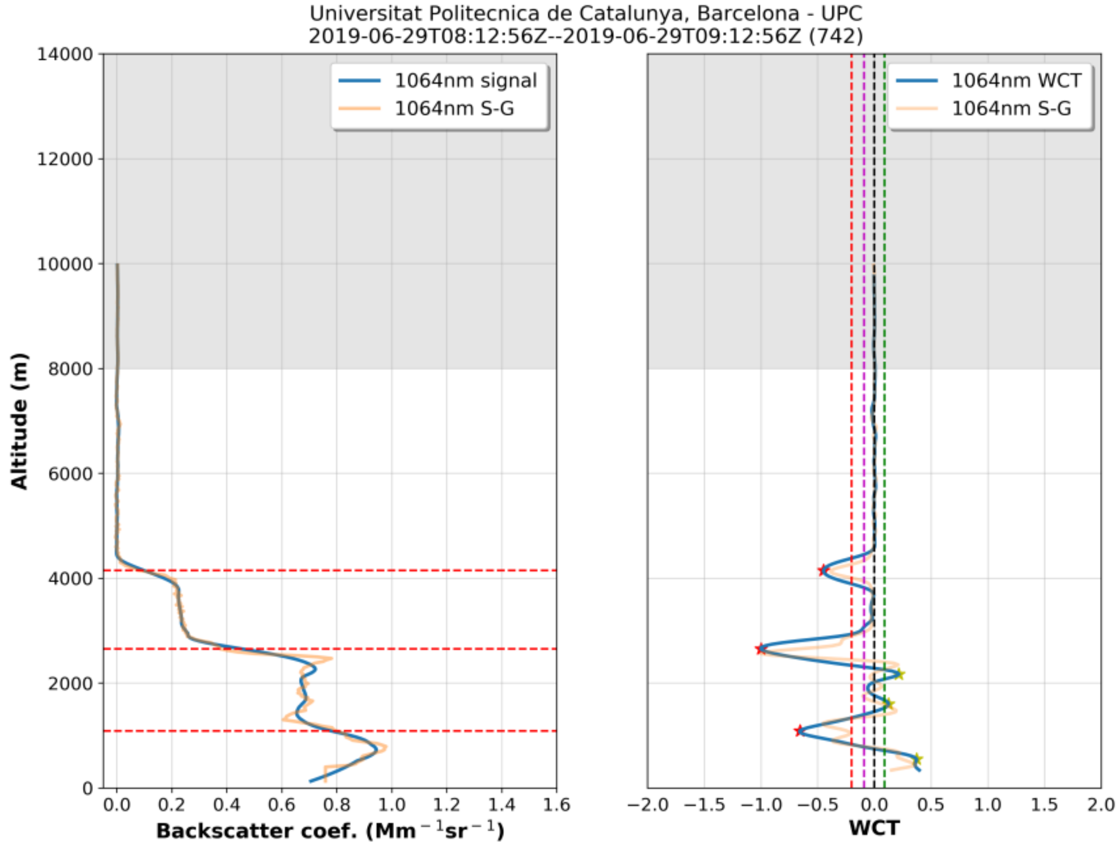

Figure 4 (Left) Lidar backscatter profile at 1064nm and (right) resulting WCT profile from the Barcelona lidar station on June 29, 2019.

The Lidar system is, as shown in Figure 4, capable of sensing multiple layers using the automated identification algorithm. When many layers are captured by a lidar signal, the top-most layer is manually chosen for this study as this would be the one also viewed by the top-down nadir-sensing GOME2 instrument. In this report, we performed sensitivity studies on more appropriate collocation scenarios where the heights sensed by both types of sensor are pre-screened for their applicability. A large amount of GOME-2 AAH heights below the 1km level are reported, which in most cases are unlikely to be captured from a lidar backscatter profile. Due to limitations of a lidar system in the near range, related to the overlap of each system (the height where the laser beam is fully within the field of view of the telescope), the archived backscatter profiles usually start at heights between 0.7-1km. In more detail, the backscatter profiles archived in the EARLINET database have a variable height range which typically extends from 0.7-1km up to 5-6 km depending on the system overlap- and the signal-to-noise ratio. As a result, those very low GOME-2 AAH heights are not considered for the collocation dataset since, even if they depict a true layer the ground-based instrument cannot sense it. Furthermore, a number of cases were found where GOME2 reported AAH heights above 7.5km. However, for heights above 5-6km the Lidar has usually a low signal-to-noise ratio, and thus the archived profiles report values only up to these heights. This is further testified by the fact that for some of those GOME2 AAH>7.5km cases, the Lidar reports an aerosol layer far below 4km, clearly sensing a different part of the atmospheric structure. Those collocations were also excluded from further analysis, because they would be misleading.

3.2.2 Validation method

As the UV-VIS satellite instruments provide daytime observations, only the lidar measurements temporally close to the satellite overpass are used in this comparison. The lidar backscatter profiles are used to retrieve aerosol layer height information of the aerosol vertical profile, while the AAH product is extracted by the GOME-2 algorithm. For the comparison of the GOME-2 AAH against aerosol height from EARLINET lidars, the coincidence criteria are set to a 150 km search radius between the satellite pixel center and the geolocation of the ground-based station. The LIDAR measurement nearest to the GOME-2 overpass time within a 5h temporal interval is selected for every available day of measurement, to ensure a sufficiently large collocation database. For each ground based measurement, only the spatially closest GOME-2 measurements are included in the comparison study. Certain criteria for ensuring the quality and representativeness of the satellite measurements, such as sun glint, solar eclipse flags and AAI values greater than 2 need to be taken into account.
Figure 5 shows the individual comparisons between the GOME-2 AAH and the lidar aerosol layer height for Barcelona [left] and Thessaloniki [right.] All collocations at a 5h temporal interval and a 150km spatial difference are shown for the period 2007 to 2019. The concentric red circle denotes the region of 150 km around the location of the stations. The aim of these maps is to show the mean bias as a function of the spatial distance (in km) between ground station and satellite pixel.

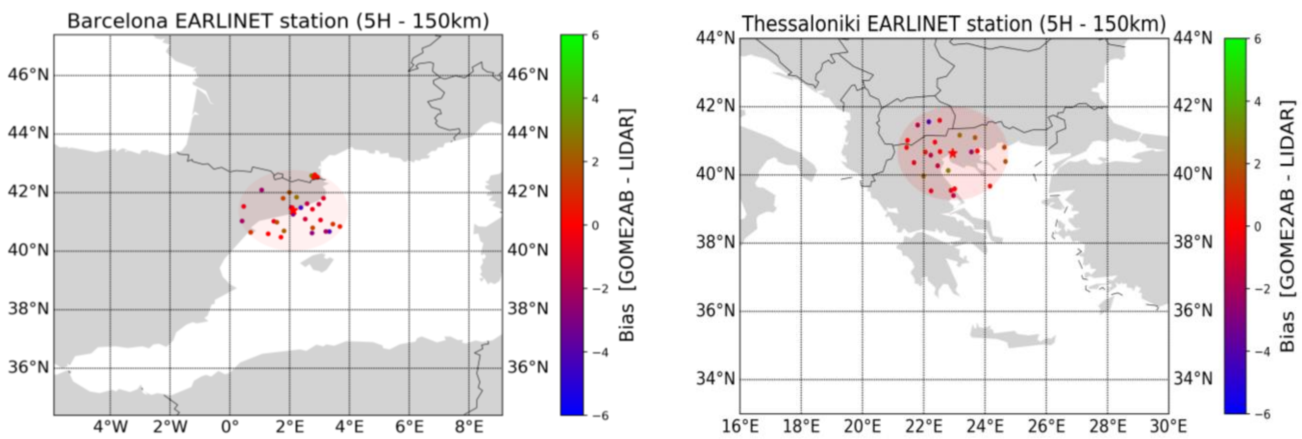

Figure 5. Spatial distribution of collocated layers from 2007 to 2019. The concentric red circle denotes the 150 km distance from the location of Barcelona, Spain (32 collocations) [left] and Thessaloniki, Greece (24 collocations) [right].

4 Results

The results from the two validation teams (RMI and AUTH) will be presented separately in the following sections. Each team presents a general summary followed by case studies.

4.1 RMI results

4.1.1 General summary

For the selected case studies, all GOME-2 and CALIOP pixels within 100 km distance from each other were compared (AAH versus minimum and maximum CALIOP layer height).
The results (height difference in function of the distance) are shown in Figure 6 for GOME-2A, GOME-2B and GOME-2C. Similarly, the height difference in function of difference in overpass time for GOME-2A, GOME-2B and GOME-2C is presented in Figure 7. From Figure 6, it can be concluded that for all three GOME-2 instruments, there is a large spread in the difference between the AAH and the CALIOP layer heights and there is no clear relation in function of the distance between overpasses. The same can be said for the spread in function of time difference between overpasses (Figure 7). It needs to be specified that care needs to be taken in comparing the three instruments as the plots are not based on the same data for each instruments. E.g. for GOME-2C, only data from the Raikoke eruption have been used. A list of used data is given in Table 5.

The overall performance of the three GOME-2 instruments is shown in Table 6. GOME-2A, GOME-2B and GOME-2C are able to represent the minimum CALIOP layer height with a mean error of -2.5 ± 5 km, -1.2 ± 5.9 km and -2 ± 5.8 km respectively. For the maximum CALIOP layer height, the mean errors are -3.3 ± 5.1 km, -2.1 ± 5.9 km and -2.6 ± 5.9 km respectively. The high standard deviation is due to the inclusion of stratospheric aerosol species. Figure 8 also shows that there is a difference in performance of GOME-2 AAH in function of the aerosol type observed by CALIOP. It is clear that for the 'stratospheric' aerosol types (volcanic ash, sulfate and elevated smoke), the AAH is in most cases not able to represent the height of these layers. The performance for the tropospheric aerosol subtypes is much better. If the stratospheric aerosol are removed from the data, the errors become -0.2 ± 3.6 km, -0.1 ± 5.4 km and -0.8 ± 3.8 km for GOME-2A, GOME-2B and GOME-2C respectively for the minimum CALIOP layer height and -1.0 ± 3.6 km, -1.0 ± 5.4 km and -1.4 ± 3.9 km for GOME-2A, GOME-2B and GOME-2C respectively for the maximum CALIOP layer height. Only the height of dust layers seems to be problematic. The height of the other species is approximated by GOME-2 to within about 5 km. For GOME-2B, the differences tend to be a bit higher, but as not exactly the same data set was used, it could be due to the contents of the dataset.

In the GOME-2 AAH product, reliability flags are used to define the confidence level of the AAH. The above analysis is repeated but now instead of making a distinction between subtypes, the different confidence levels are presented in Figure 9 and Table 7. It could be expected that the high confidence AAH pixels have a better agreement with the CALIOP layer height, however, this is not the case.

For each AAH pixel, the error on the AAH is also given. Figure 10 shows the AAH plus and minus this error and the minimum and maximum CALIOP layer height in function of the GOME-2 AAH for all three instruments. In the plots, the height of the CALIOP layers is limited to 15 km, which is the detection limit of GOME-2 as a result of the application of the FRESCO algorithm. On average, the errors are quite small: 0.4 km, 0.4 km and 0.3 km for GOME-2A, -2B and -2C respectively.

The data set validated by RMI was analyzed further to check its agreement with the accuracy requirements defined in Table 1. The results are shown in Table 8 (all data) and Figure 11 (height limited to 15 km). This shows that for the investigated data sets for GOME-2A and GOME-2B, less than 60% of the points are within the threshold limits. As the dataset is focused on volcanic case studies, this might give a biased view. Only taking into account tropospheric aerosol species improves the results, which can be seen by looking at the percentages between brackets in Table 8.

Figure 12 shows the boxplots of the differences between the AAH from each GOME-2 instrument and the minimum CALIOP layer height for the different aerosol types (as defined by CALIOP). All boxplot results need to be analyzed with caution as they are based only on specific case studies. Especially in the case of GOME-2C, only a very limited amount of data was examined. However, even with only case studies, a clear difference can be seen between the tropospheric and stratospheric aerosol species, where differences between GOME-2 AAH and CALIOP layer height are clearly higher for volcanic ash, sulfate and elevated smoke. Within the tropospheric aerosol species, differences are also obvious. Dust and polluted dust have a larger spread compared to aerosol types that typically occur very close to the surface (e.g. clean marine).

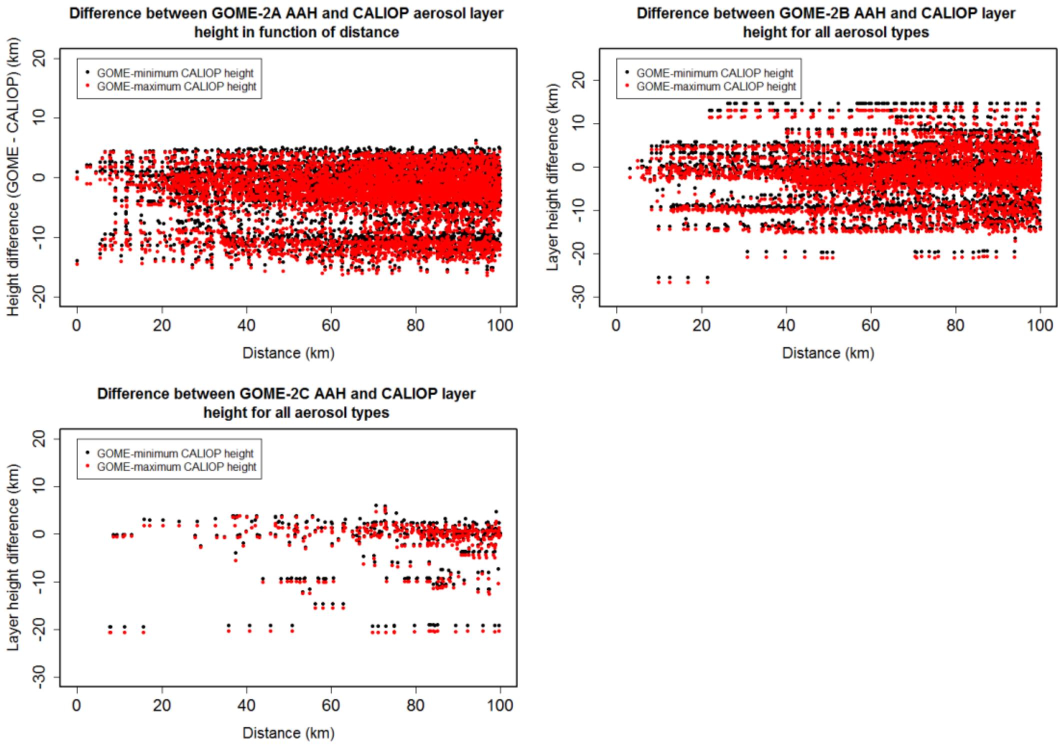

Figure 6: Difference between GOME-2 AAH and the minimum (in black) and maximum (in red) CALIOP layer height in function of the distance between the GOME-2 and CALIOP pixel. The upper left plot shows the results for GOME-2A, the upper right plot shows the results for GOME-2B and the lower left plot shows the results for GOME-2C.

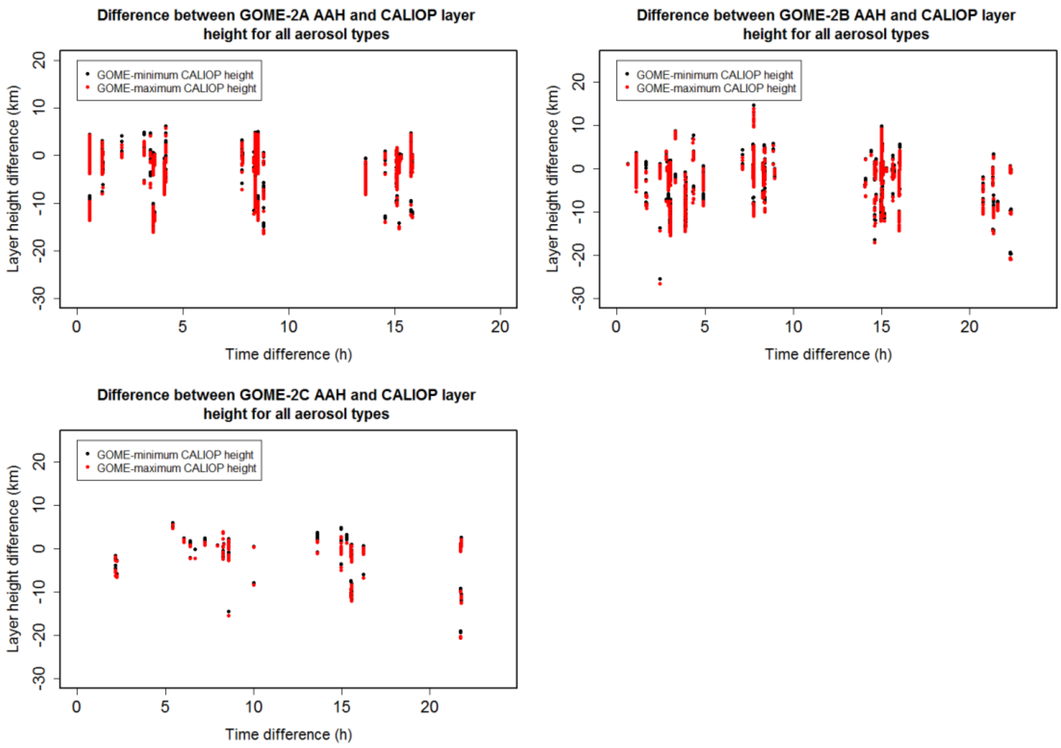

Figure 7: Difference between GOME-2 AAH and the minimum (in black) and maximum (in red) CALIOP layer height in function of the time difference between overpasses from GOME-2 and CALIOP. The upper left plot shows the results for GOME-2A, the upper right plot shows the results for GOME-2B and the lower left plot shows the results for GOME-2C.

Table 5: Overview of used case studies for the three GOME-2 instruments

GOME-2A	GOME-2B	GOME-2C
	Barren Island: 25/9/2018 Barren Island: 26/9/2018	
	Bulusan: 3/5/2015	
Calbuco: 23/4/2015 Calbuco: 24/4/2015	Calbuco: 23/4/2015 Calbuco: 24/4/2015	
Eyjafjallajokull: 15/4/2010 Eyjafjallajokull: 16/4/2010		
Grimsvotn: 23/5/2011		
Kasatochi: 8/8/2008		
	Krakatau: 22/2/2017	
	Mount Kelud: 14/2/2014 Mount Kelud: 15/2/2014	
Nishinoshino: 13/7/2018 Nishinoshino: 14/7/2018	Nishinoshino: 13/7/2018 Nishinoshino: 14/7/2018	
Paluweh: 3/2/2013 Paluweh: 4/2/2013 Paluweh: 8/2/2013 Paluweh: 11/2/2013	Paluweh: 9/2/2013 Paluweh: 10/2/2013	
Puyehue: 5/6/2011		
	Raikoke: 22/6/2019 Raikoke: 23/6/2019	Raikoke: 22/6/2019 Raikoke: 23/6/2019
Rinjani: 27/10/2015	Rinjani: 26/10/2015	
Sarychev: 14/6/2009 Sarychev: 16/6/2009		
Ubinas: 14/9/2016	Ubinas: 13/9/2016	

Table 6: Overview of the mean difference (mean) and its standard deviation (stdev) between GOME-2 AAH and CALIOP minimum and maximum layer height

GOME-2A				
	min_dif (km)		**max_dif (km)**	
TYPE	**mean**	**stdev**	**mean**	**stdev**
ALL	-2.5	5	-3.3	5.1
Only tropospheric	-0.2	3.6	-1.0	3.6
clean marine	0.8	1.6	-0.1	1.7
dust	-1.4	4.3	-2.3	4.2
polluted continental	1.1	2	0.1	1.8
clean continental	-1.1	1.4	-1.5	1.6
polluted dust	1.4	2.7	0.8	2.9
smoke	-1.4	1.6	-2.3	1.4
dusty marine	-0.8	2	-1.6	2
volcanic ash	-7.9	3.5	-8.9	3.4
sulfate	-8.3	1.6	-9.8	1.3
elevated smoke	-8.2	3.7	-8.7	3.7
GOME-2B				
	min_dif (km)		**max_dif (km)**	
TYPE	**mean**	**stdev**	**mean**	**stdev**
ALL	-1.2	5.9	-2.1	5.9
Only tropospheric	-0.1	5.4	-1.0	5.4
clean marine	3.9	3.4	3.1	3.3
dust	-3.1	5.4	-4	5.5
polluted continental	3.8	5.3	2.9	5.1
clean continental	-0.8	1.1	-1.3	0.9
polluted dust	0.9	6.1	0.2	5.9
smoke	-1	2.4	-2	2.6
dusty marine	1.7	3.3	0.8	3.6
volcanic ash	-5.9	4.8	-6.9	4.8
sulfate	-9.7	7	-10.5	6.9
elevated smoke	-5.5	5.1	-6.2	5
GOME-2C				
	min_dif (km)		**max_dif (km)**	
TYPE	**mean**	**stdev**	**mean**	**stdev**
ALL	-2	5.8	-2.6	5.9
Only tropospheric	-0.8	3.8	-1.4	3.9
clean marine	1.5	1	0.9	1.1
dust	-2.3	4.5	-2.9	4.7
polluted continental	1.1	1.5	0.3	1
clean continental	-0.8	0.1	-1.1	0.2
polluted dust	0	3.5	0.8	3.5
smoke	-0.7	2.2	-1.3	2.2
dusty marine	0.5	0.5	0.3	0.6
volcanic ash	-19.2	0.1	-20.5	0.1
sulfate	-14.6	0	-15.4	0
elevated smoke	NO DATA	NO DATA	NO DATA	NO DATA

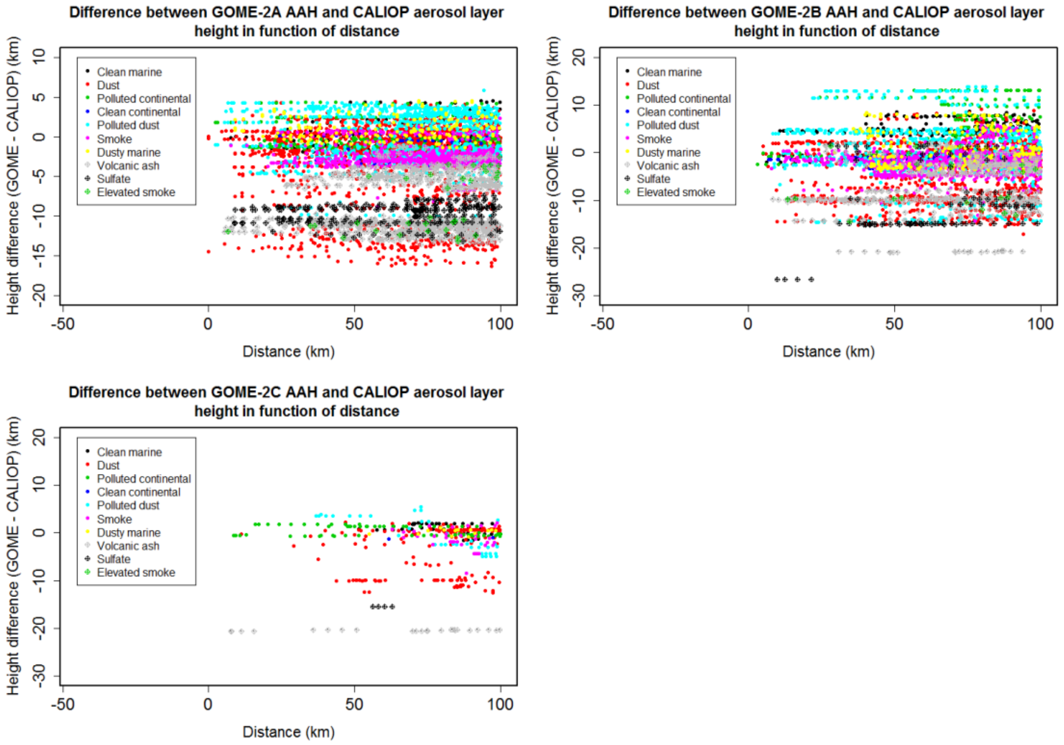

Figure 8: Difference between GOME-2 AAH and the minimum (in black) and maximum (in red) CALIOP layer height in function of the distance between overpasses from GOME-2 and CALIOP. The different colors represent the different aerosol subtypes as observed by CALIOP. The upper left plot shows the results for GOME-2A, the upper right plot shows the results for GOME-2B and the lower left plot shows the results for GOME-2C.

Table 7: Overview of the mean difference (mean) and its standard deviation (stdev) between GOME-2 AAH and CALIOP minimum and maximum layer height for the different reliability levels.

GOME-2A				
	min_dif (km)		**max_dif (km)**	
	mean	**stdev**	**mean**	**stdev**
High reliability	-2.5	5.9	-3.4	6.0
Medium reliability	-2.5	4.3	-3.4	4.4
Low reliability	-1.3	3.1	-2.3	3.1
GOME-2B				
	min_dif (km)		**max_dif (km)**	
	mean	**stdev**	**mean**	**stdev**
High reliability	0.8	6.4	-0.2	6.2
Medium reliability	-1.6	5.7	-2.4	5.7
Low reliability	-3.4	4.5	-4.3	4.6
GOME-2C				
	min_dif (km)		**max_dif (km)**	
	mean	**stdev**	**mean**	**stdev**
High reliability	-0.2	4.8	-0.7	4.8
Medium reliability	-2.2	6.1	-2.9	6.3
Low reliability	-1.7	2.7	-2.2	2.6

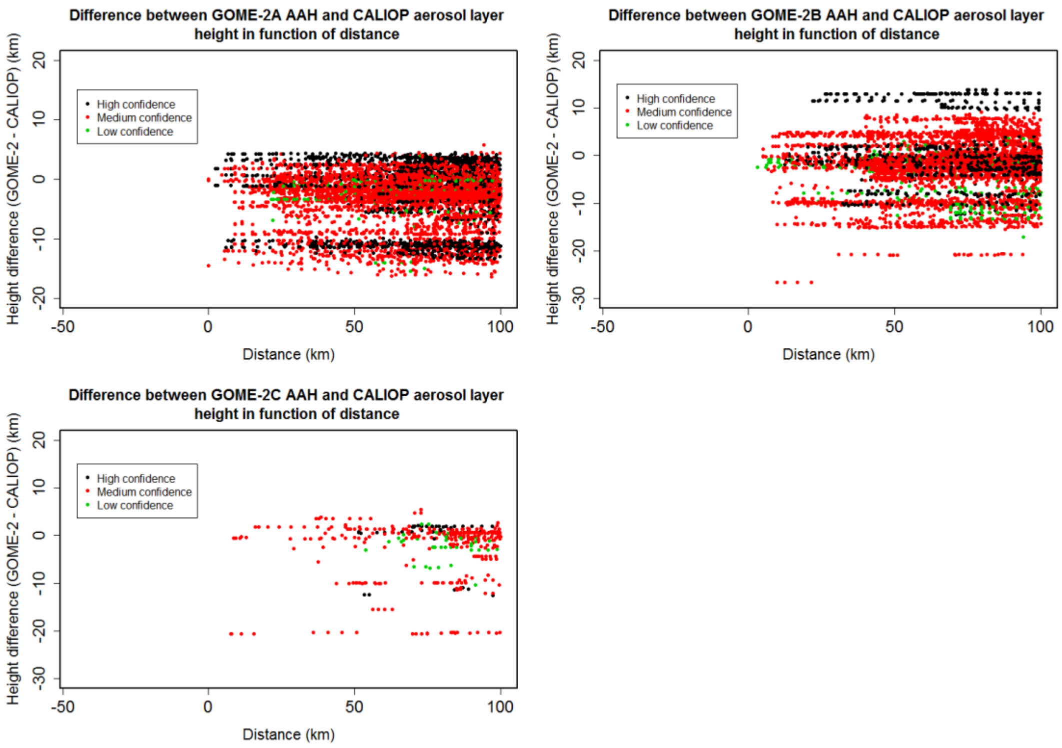

Figure 9: Difference between GOME-2 AAH and the maximum CALIOP layer height in function of the distance between overpasses from GOME-2 and CALIOP. The different colors represent the different AAH confidence levels. The upper left plot shows the results for GOME-2A, the upper right plot shows the results for GOME-2B and the lower left plot shows the results for GOME-2C.

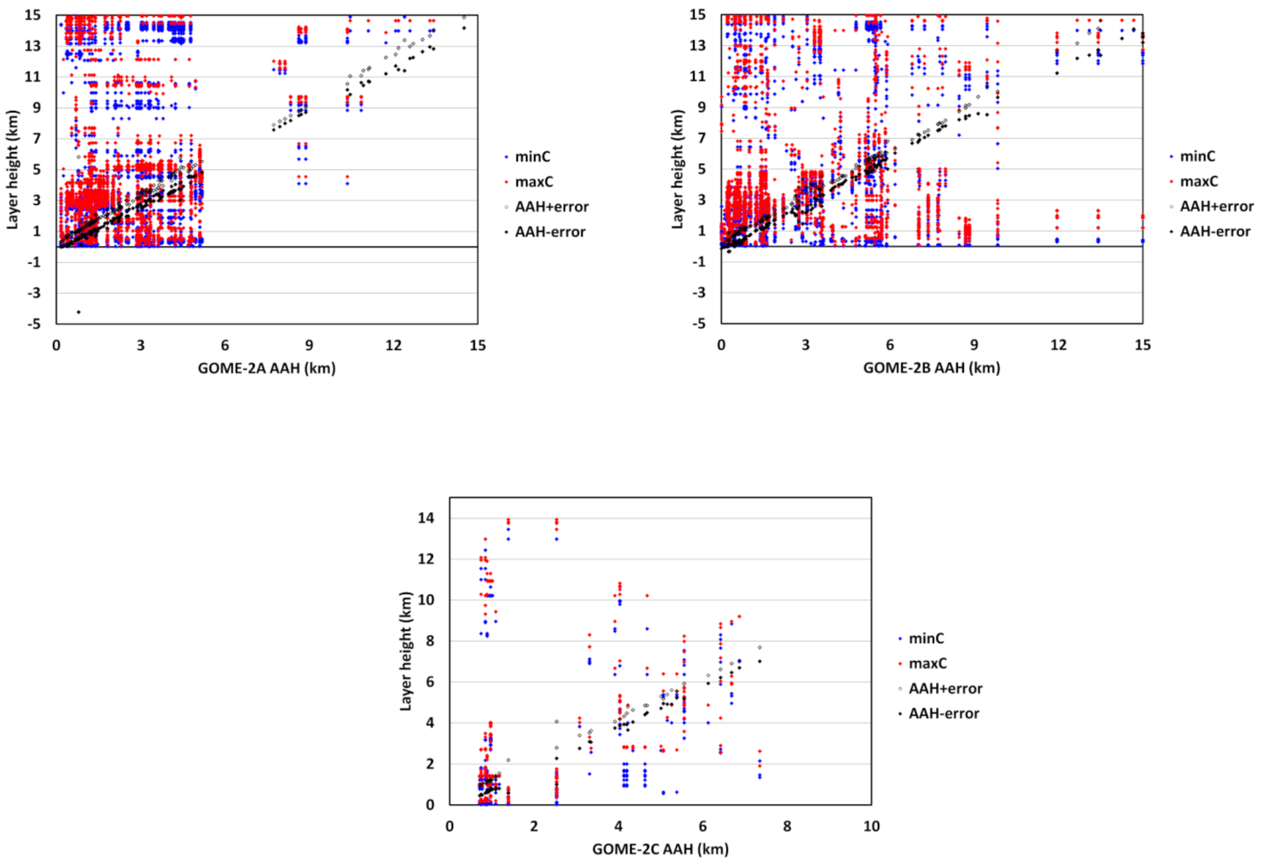

Figure 10: GOME-2 AAH plus (in grey) and minus (in black) its error and the minimum (in blue) and maximum (in red) CALIOP layer height in function of GOME-2 AAH for GOME-2A (upper left), GOME-2B (upper right) and GOME-2C (lower middle). CALIOP pixels are only shown up to a height of 15 km, which is the detection limit of GOME-2.

Table 8.: % of data for each GOME-2 instrument that reached the threshold, target and optimal requirements. Values obtained when only considering the tropospheric aerosol species are shown between brackets.

GOME-2A				
		Layer height <10 km	**Layer height >10 km**	**Total**
Threshold	**AAH-minC**	57.8 % (74.0 %)	59.7 % (87.5 %)	58.0 % (74.1 %)
	AAH-maxC	57.4 % (73.5 %)	29.4 % (87.5 %)	54.7 % (73.5 %)
Target	**AAH-minC**	40.2 % (51.5 %)	28.5 % (87.5 %)	39.1 % (51.5 %)
	AAH-maxC	38.2 % (48.9 %)	11.7 % (87.5 %)	35.6 % (49 %)
Optimal	**AAH-minC**	17.8 % (22.9 %)	12.6 % (75 %)	17.3 % (22.9 %)
	AAH-maxC	18.1 % (23.1 %)	3.0 % (87.5 %)	16.6 % (23.2 %)
GOME-2B				
		Layer height <10 km	**Layer height >10 km**	**Total**
Threshold	**AAH-minC**	50.8 % (56.8 %)	71.1 % (11.4 %)	53.2 % (54.9 %)
	AAH-maxC	48.6 % (54.4 %)	49.8 % (11.4 %)	48.8 % (52.5 %)
Target	**AAH-minC**	43.6 % (48.8 %)	53.0 % (4.6 %)	44.7 % (46.8 %)
	AAH-maxC	34.6 % (38.7 %)	44.1 % (11.4 %)	44.7 % (37.5 %)
Optimal	**AAH-minC**	28.2 % (31.5 %)	29.3 % (4.6 %)	28.3 % (30.3 %)
	AAH-maxC	19.3 % (21.6 %)	20.4 % (4.6 %)	19.4 % (20.8 %)
GOME-2C				
		Layer height <10 km	**Layer height >10 km**	**Total**
Threshold	**AAH-minC**	70.0 % (74.9 %)	No data (No data)	70.0 % (74.9 %)
	AAH-maxC	72.4 % (77.4 %)	No data (No data)	72.4 % (77.4 %)
Target	**AAH-minC**	53.4 % (57.1 %)	No data (No data)	53.4 % (57.1 %)
	AAH-maxC	64.9 % (69.4 %)	No data (No data)	64.9 % (69.4 %)
Optimal	**AAH-minC**	41.5 % (44.4 %)	No data (No data)	41.5 % (44.4 %)
	AAH-maxC	43.3 % (46.4 %)	No data (No data)	43.3 % (46.4 %)

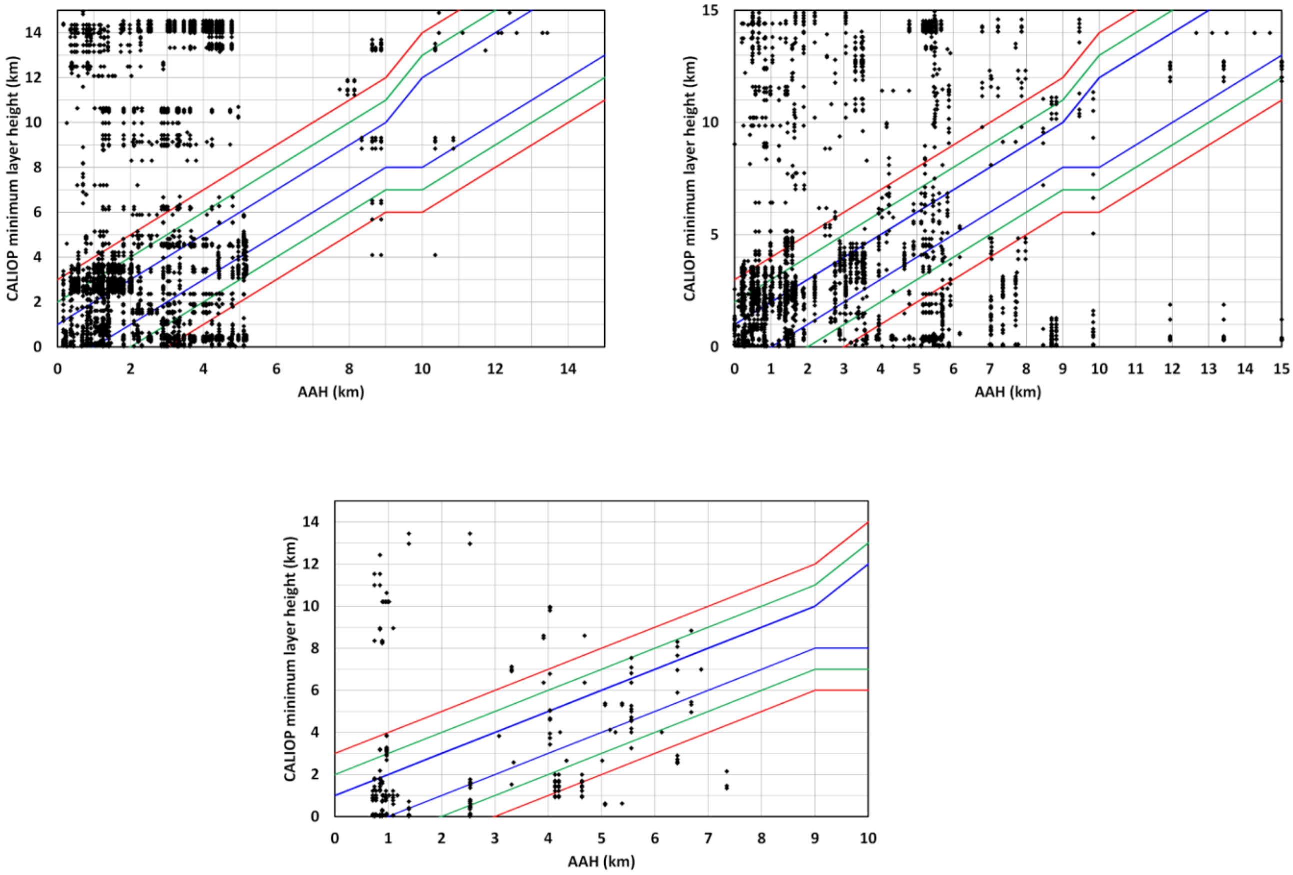

Figure 11: Requirement plots for GOME-2A (upper left), GOME-2B (upper right) and GOME-2C (lower middle).The red, green and blue line represent the threshold, target and optimal requirement lines. CALIOP pixels are only shown up to a height of 15 km, which is the detection limit of GOME-2.

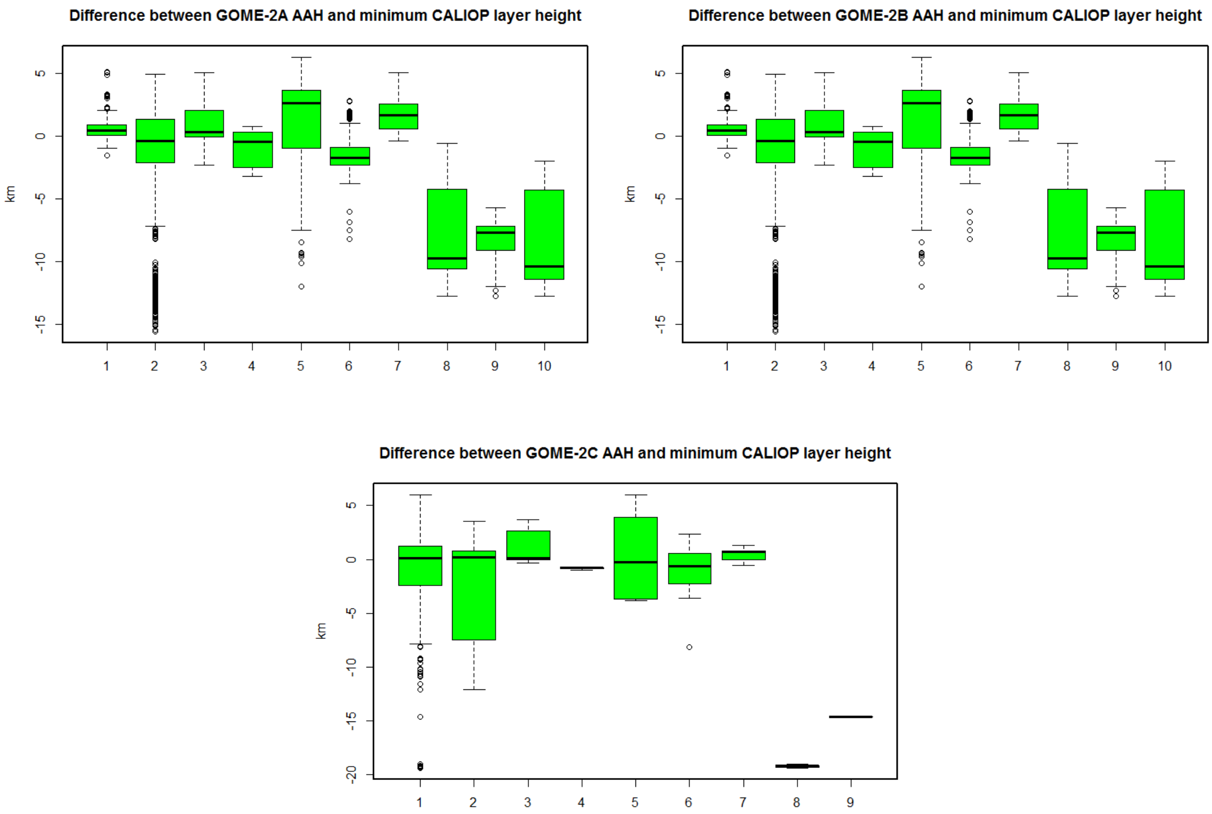

Figure 12: Boxplot of differences between GOME-2A (upper left), GOME-2B (upper right) and GOME-2C (lower middle) AAH and CALIOP minimum layer height for the different aerosol species (1: clean marine; 2: dust; 3: polluted continental; 4: clean continental; 5: polluted continental; 6: smoke; 7: dusty marine; 8: volcanic ash; 9: sulfate; 10: elevated smoke)

In the following section, the most interesting case studies will be highlighted. Other case studies can be consulted in Appendix A.

4.1.2 Case studies

4.1.2.1 Calbuco eruption

The Servicio Nacional de Geología y Minería reported that an eruption from Calbuco occurred on the 23rd of April 2015 around 01h00, which lasted six hours and generated an ash plum that rose higher than 15 km and drifted towards the N, NE and E[1]. On the 24th of April 2015 the ash plume continued to rise 2 km and explosions were detected. Data from the 23rd until the 24th of April 2015 have been analyzed for both GOME-2A and GOME-2B.

4.1.2.1.1 GOME-2A

On the 23rd of April 2015, CALIOP detected a layer of volcanic ash between 13.2 and 18.6 km. Figure 13 shows the location of the overpass pixels of GOME-2A and CALIOP located within 100 km from each other.

[1] https://volcano.si.edu/volcano.cfm?vn=358020#April2015

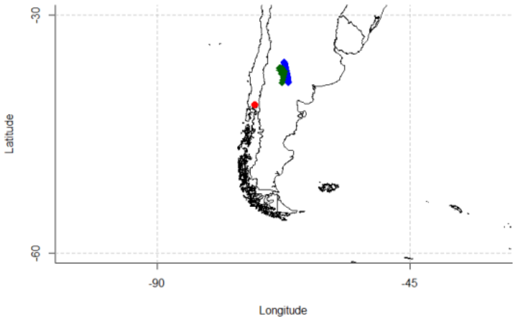

Figure 13: The location of the volcano is shown in red. The location of the CALIOP and GOME-2A overpasses on the 23rd of April 2015 are shown in blue and green respectively.

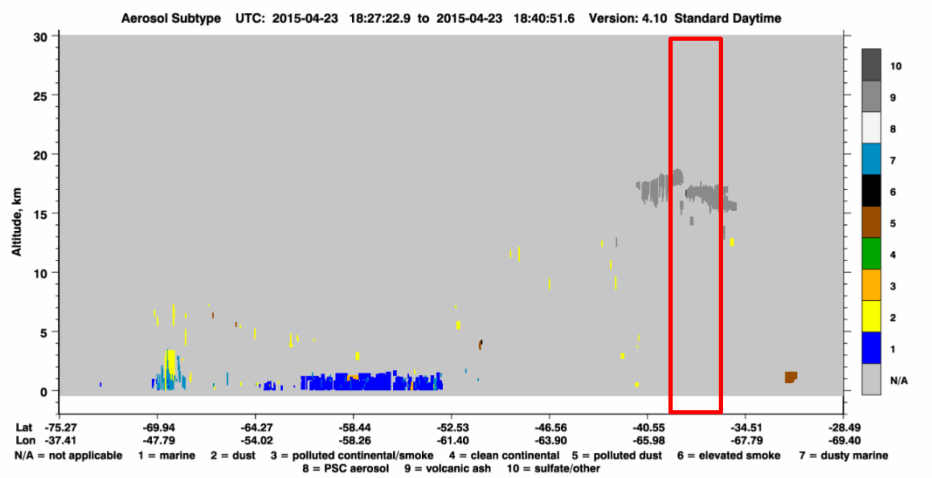

Figure 14: CALIOP overpass on the 23rd of April 2015 from 18:27:22 to 18:40:51. The approximate part of the overpass within 100 km of GOME-2A overpasses is highlighted by the red box.

Figure 15 shows the observed aerosol layer height from CALIOP and the AAH detected by GOME-2A in function of latitude. All CALIOP pixels from Figure 15 were classified as volcanic ash (with the exception of one pixel classified as elevated smoke). The AAH detected by GOME-2A was between 10.5-14.5 km (Table 9). The time difference between the CALIOP and GOME-2A overpass was around 4 h and the closest GOME-2A pixel was located about 26 km from a CALIOP pixel. GOME-2A was not entirely able to capture the volcanic ash layer detected by CALIOP as it was located at an altitude higher than 15 km. Due to the use of the FRESCO algorithm, GOME-2 is limited to a maximum height of 15 km for the AAH retrieval and hence cannot detect layers higher than 15 km.

Table 9: Height of the aerosol layer detected by CALIOP for the different aerosol species compared to the AAH detected by GOME-2A for pixels located within 100 km distance for the 23rd of April 2015.

	CALIOP	**AAH**
Volcanic ash	13.2-18.6 km	10.5-14.5 km
Elevated smoke	15.4-16.9 km	10.5-13.4 km

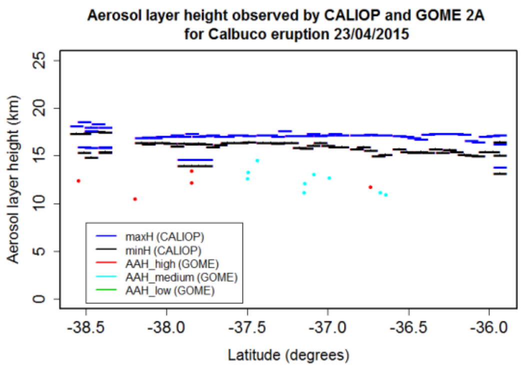

Figure 15: The aerosol layer height detected by CALIOP is shown in blue (maximum layer height) and black (minimum layer height) as a function of latitude for the 23rd of April 2015. The GOME-2A AAH pixels located within 100 km of a CALIOP overpass pixel are presented in red (high reliability), cyan (medium reliability) and green (low reliability).

On the 24th of April 2015, CALIOP detected volcanic ash at heights between 13.1-17.5 km, dust between 0.2-5.6 km, polluted dust between 0.2-5.5 km, sulfate and elevated smoke between 14.5-14.9 km (Figure 16 and Table 10). Figure 17 shows the location of the overpass pixels of GOME-2A and CALIOP located within 100 km from each other and Figure 18Figure 18 shows the observed aerosol layer height from CALIOP and the AAH detected by GOME-2A in function of latitude. The time difference between both overpasses is around 8 h and the closest GOME-2A pixel is located ~5 km from a CALIOP pixel. For this case it seems as though GOME-2A does not see the volcanic species, but probably the tropospheric dust and/or the polluted dust detected by CALIOP (Figure 18 and Figure 19).

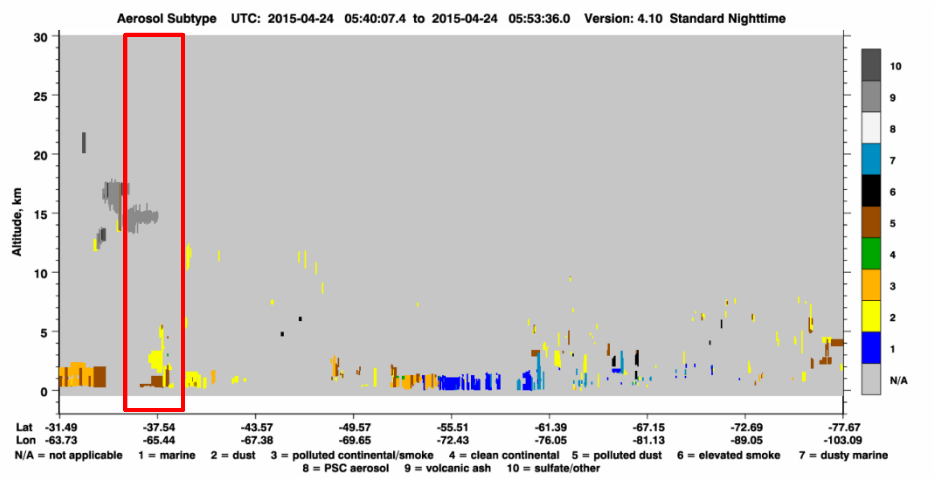

Figure 16: CALIOP overpass on the 24th of April 2015 from 05:40:07 to 05:53:36. The approximate part of the overpass within 100 km of GOME-2 overpasses is highlighted by the red box.

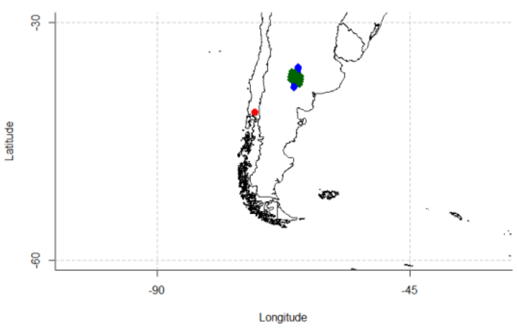

Figure 17: The location of the volcano is shown in red. The location of the CALIOP and GOME-2A overpasses on the 24rd of April 2015 are shown in blue and green respectively.

Table 10: Height of the aerosol layer detected by CALIOP for the different aerosol species compared to the AAH detected by GOME-2A for pixels located within 100 km distance for the 24th of April 2015.

	CALIOP	**AAH**
Dust	0.2-5.6 km	1.8-4.8 km
Polluted dust	0.2-5.5 km	1.8-4.8 km
Volcanic ash	13.1-17.5 km	1.8-4.8 km
Sulfate	14.5-14.9 km	1.8-4.2 km
Elevated smoke	14.5-14.9 km	1.8-4.8 km

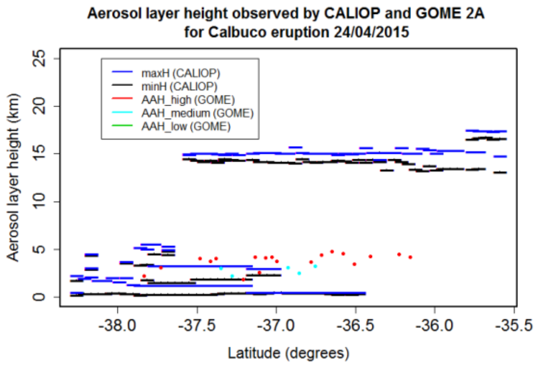

Figure 18: The aerosol layer height detected by CALIOP is shown in blue (maximum layer height) and black (minimum layer height) as a function of latitude for the 24th of April 2015. The GOME-2A AAH pixels located within 100 km of a CALIOP overpass pixel are presented in red (high reliability), cyan (medium reliability) and green (low reliability).

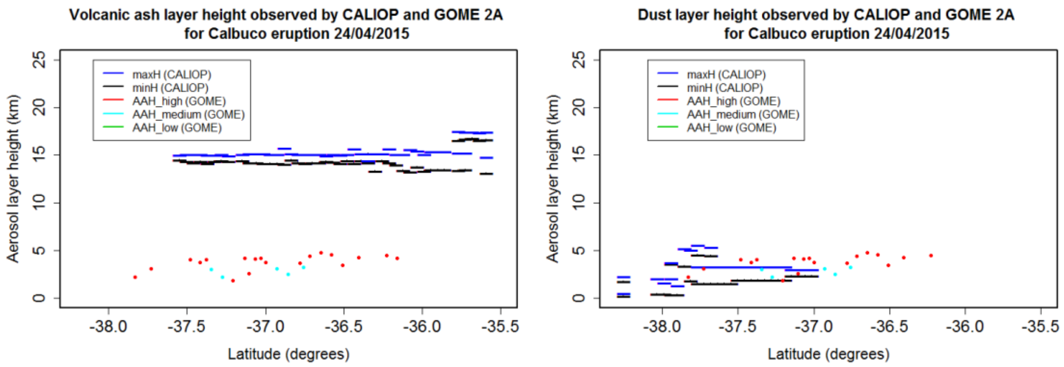

Figure 19: Detail of the volcanic ash (left) and dust (right) layer detected by CALIOP. The maximum and minimum layer heights are shown in blue and black respectively as a function of latitude for the 24th of April 2015. The GOME-2A AAH pixels located within 100 km of a CALIOP overpass pixel are presented in red (high reliability), cyan (medium reliability) and green (low reliability).

4.1.2.1.2 GOME-2B

Figure 20 shows the location of the overpass pixels of GOME-2B and CALIOP located within 100 km from each other and Figure 21 shows the observed aerosol layer height from CALIOP and the AAH detected by GOME-2B in function of latitude for the 23rd of April 2015. All CALIOP pixels from Figure 21 were classified as volcanic ash (with the exception of one pixel of elevated smoke). The AAH detected by GOME-2B was between 9.1-14.7 km (Table 11). The time difference between the CALIOP and GOME-2B overpass was between 4 and 5 h and the closest GOME-2B pixel is located ~40 km away from a CALIOP pixel. Again, due to the inability of GOME-2 to observe layers higher than 15 km, the volcanic ash layer's height was underestimated by the AAH from GOME-2B.

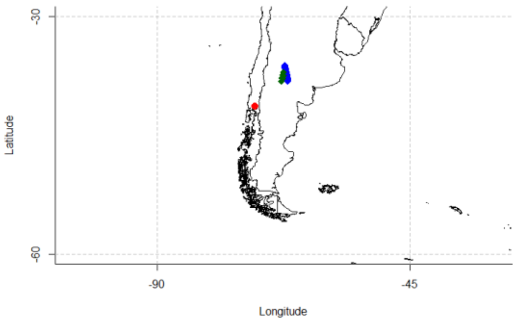

Figure 20: The location of the volcano is shown in red. The location of the CALIOP and GOME-2B overpasses on the 23rd of April 2015 are shown in blue and green respectively.

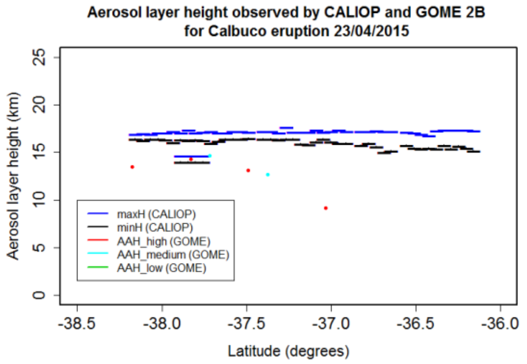

Figure 21: The aerosol layer height detected by CALIOP is shown in blue (maximum layer height) and black (minimum layer height) as a function of latitude for the 23rd of April 2015. The GOME-2B AAH pixels located within 100 km of a CALIOP overpass pixel are presented in red (high reliability), cyan (medium reliability) and green (low reliability).

Table 11: Height of the aerosol layer detected by CALIOP for the different aerosol species compared to the AAH detected by GOME-2B for pixels located within 100 km distance for the 23rd of April 2015.

	CALIOP	**AAH (all conf.)**
Volcanic ash	13.2-18.6 km	9.1-14.7 km
Elevated smoke	15.4-16.9 km	10.5-14.3 km

Figure 22 shows the location of the overpass pixels of GOME-2B and CALIOP located within 100 km from each other and Figure 23 shows the observed aerosol layer height from CALIOP and the AAH detected by GOME-2B in function of latitude for the 24th of April 2015. The time difference between both overpasses is around 8 h and the closest GOME-2B pixel is located ~8 km away from a CALIOP pixel. The exact layer heights can be found in Table 12. Here, the high reliability AAH pixels of GOME-2B follow the height of the volcanic ash layer, whereas the medium reliability AAH agrees with the tropospheric dust and/or the polluted dust layers (Figure 24).

Table 12: Height of the aerosol layer detected by CALIOP for the different aerosol species compared to the AAH detected by GOME-2B for pixels located within 100 km distance for the 24th of April 2015.

	CALIOP	**AAH (all conf.)**
Dust	0.2-12.7 km	1.8-15 km
Polluted continental	0.3-2.3 km	11.9-15 km
Clean continental	2.9-3.1 km	2.2-3.1 km
Polluted dust	0.2-5.5 km	1.8-15 km
Volcanic ash	12-17.9 km	1.8-15 km
Sulfate	12.6-21.7 km	1.8-15 km
Elevated smoke	12.7-17.5 km	1.8-15 km

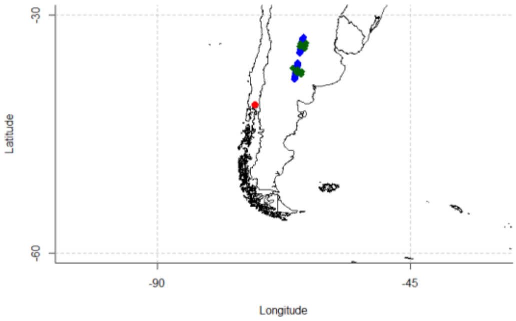

Figure 22: The location of the volcano is shown in red. The location of the CALIOP and GOME-2B overpasses on the 24rd of April 2015 are shown in blue and green respectively.

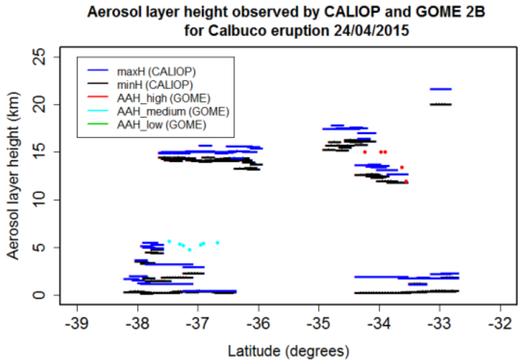

Figure 23: The aerosol layer height detected by CALIOP is shown in blue (maximum layer height) and black (minimum layer height) as a function of latitude for the 24th of April 2015. The GOME-2B AAH pixels located within 100 km of a CALIOP overpass pixel are presented in red (high reliability), cyan (medium reliability) and green (low reliability).

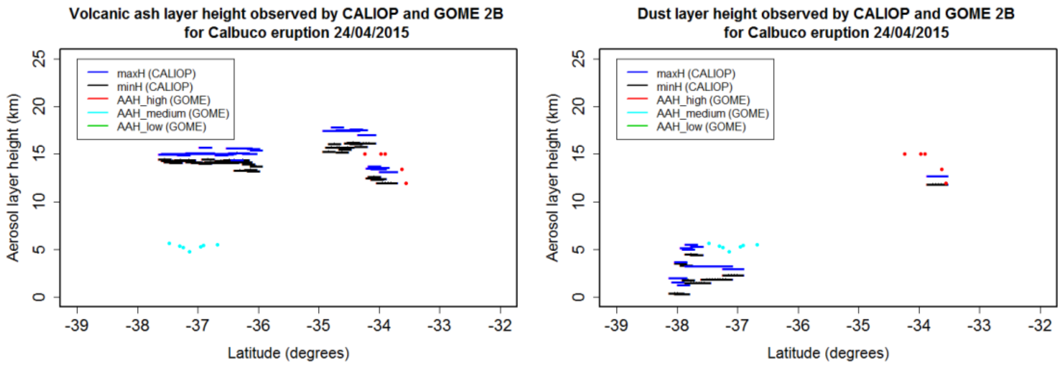

Figure 24: Detail of the volcanic ash (left) and dust (right) layer detected by CALIOP. The maximum and minimum layer heights are shown in blue and black respectively as a function of latitude for the 24th of April 2015. The GOME-2B AAH pixels located within 100 km of a CALIOP overpass pixel are presented in red (high reliability), cyan (medium reliability) and green (low reliability).

4.1.2.2 Mount Kelud

It was reported that a major eruption took place on the 13th of February 2014 at 22h50, followed by another large explosion at 23h30[2]. Ash plumes rose to an altitude of 17 km a.s.l. Data from both GOME-2 instruments from 14-15 February 2014 were studied.

[2] http://volcano.si.edu/volcano.cfm?vn=263280#February2014

4.1.2.2.1 GOME-2A

GOME-2A has no data within 100 km of a CALIOP overpass near the volcano on the 14th and 15th of February 2014.

4.1.2.2.2 GOME-2B

On the 14th of February 2014, CALIOP detects mainly dust and volcanic ash (apart from a few pixels with polluted dust, sulfate and elevated smoke) (Figure 26 and Table 13). GOME-2B is unable to capture the height of the volcanic ash layer as it was located at an altitude above 15 km where GOME-2 has no detection sensitivity (Figure 27 and Figure 28). GOME-2B also underestimates the height of the dust layer. The time difference between both overpasses is only 3 h, so it is very likely that they are observing the same air mass. The distance between the closest GOME-2B and CALIOP pixels is ~16 km.

Table 13: Height of the aerosol layer detected by CALIOP for the different aerosol species compared to the AAH detected by GOME-2B for pixels located within 100 km distance for the 14th of February 2014.

	CALIOP	**AAH**
Dust	9.8-15.5 km	5.5-9.5 km
Polluted dust	10.6-11.1 km	5.5-9.5 km
Volcanic ash	17.4-20.0 km	5.5-9.5 km
Sulfate	17.0-21.0 km	6.8-9.5 km
Elevated smoke	19.0-19.9 km	5.5-9.5 km

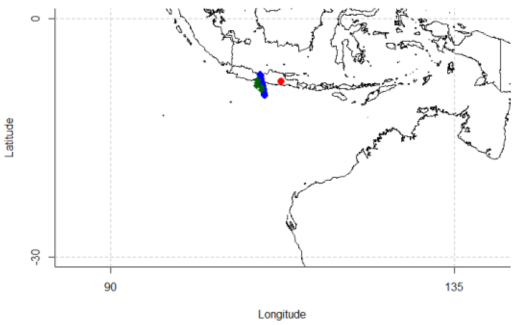

Figure 25: The location of the volcano is shown in red. The location of the CALIOP and GOME-2B overpasses for the 14th of February 2014 are shown in blue and green respectively.

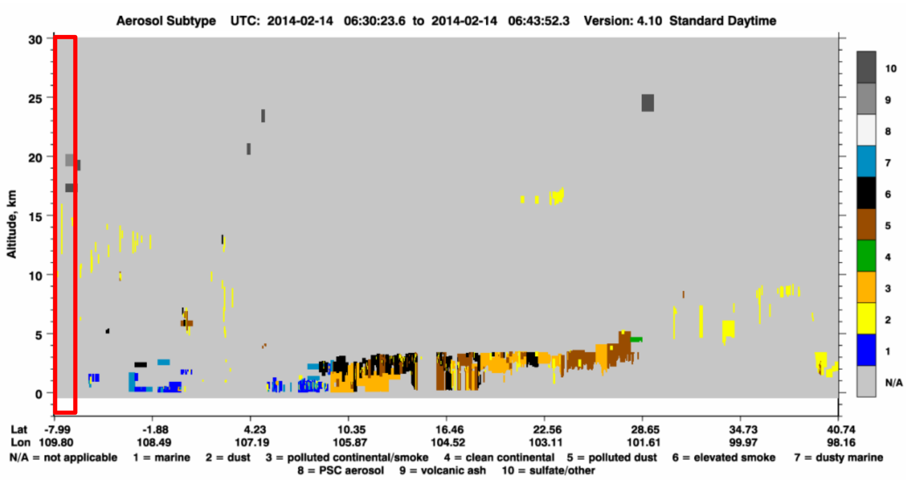

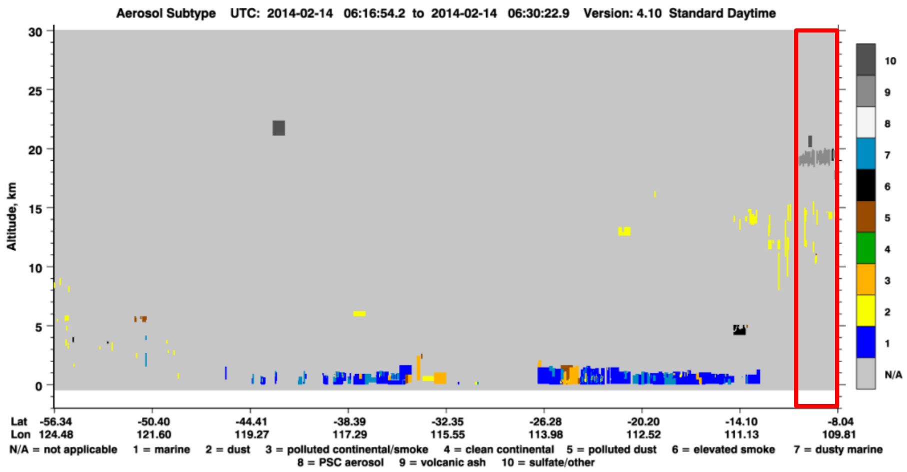

Figure 26: CALIOP overpass on the 14th of February 2014 from 06:30:23 to 06:43:52 and from 06:16:54 to 06:30:22. The approximate parts of the overpass within 100 km of GOME-2B overpasses are highlighted by the red boxes.

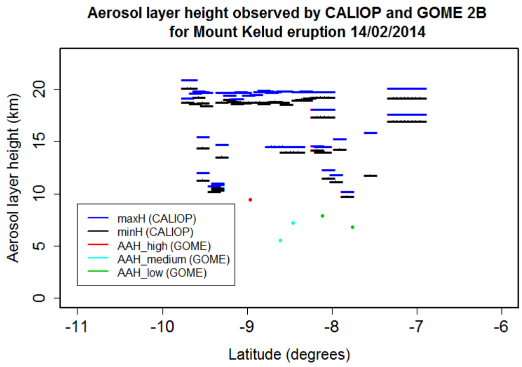

Figure 27: The aerosol layer height detected by CALIOP is shown in blue (maximum layer height) and black (minimum layer height) as a function of latitude for the 14th of February 2014. The GOME-2B AAH pixels located within 100 km of a CALIOP overpass pixel are presented in red (high reliability), cyan (medium reliability) and green (low reliability).

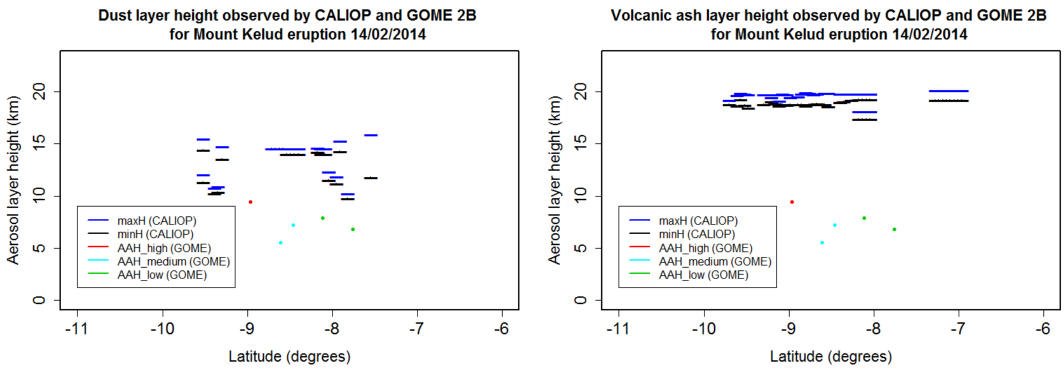

Figure 28: Detail of the dust (left) and volcanic ash (right) layer detected by CALIOP. The maximum and minimum layer heights are shown in blue and black respectively as a function of latitude for the 14th of February 2014. The GOME-2B AAH pixels located within 100 km of a CALIOP overpass pixel are presented in red (high reliability), cyan (medium reliability) and green (low reliability).

On the 15th of February 2014, CALIOP detected only dust and polluted dust (Figure 30 and Table 14). There is only 1 GOME-2B pixel nearby and its AAH is equal to 5.5 km, which is too low compared to the layer heights detected by CALIOP. The time difference between both overpasses is quite large (~20 h), so both satellites might not be looking at the same air mass which may explain the difference in detected aerosol layer height.

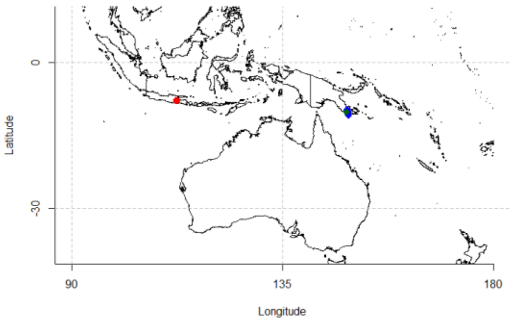

Figure 29: The location of the volcano is shown in red. The location of the CALIOP and GOME-2B overpasses for the 15th of February 2014 are shown in blue and green respectively.

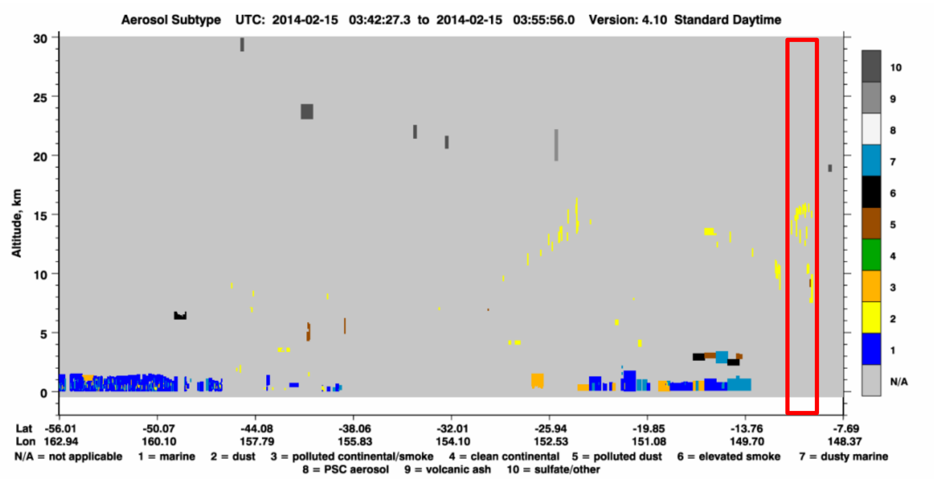

Figure 30: CALIOP overpass on the 15th of February 2014 from 03:42:27 to 03:55:56. The approximate part of the overpass within 100 km of GOME-2B overpasses is highlighted by the red box.

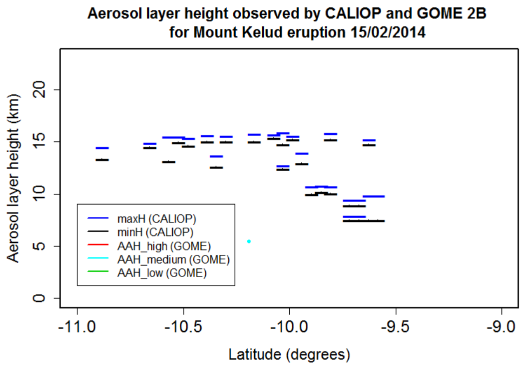

Figure 31: The aerosol layer height detected by CALIOP is shown in blue (maximum layer height) and black (minimum layer height) as a function of latitude for the 15th of February 2014. The GOME-2B AAH pixels located within 100 km of a CALIOP overpass pixel are presented in red (high reliability), cyan (medium reliability) and green (low reliability).

Table 14: Height of the aerosol layer detected by CALIOP for the different aerosol species compared to the AAH detected by GOME-2B for pixels located within 100 km distance for the 15th of February 2014.

	CALIOP	**AAH**
Dust	7.5-15.9 km	5.5 km
Polluted dust	8.9-9.4 km	5.5 km

4.1.2.3 Australian bush fires

The focus is on the final days of 2019 (27-31 December), a period during which the fires in Australia intensified.

4.1.2.3.1 GOME-2C

GOME -2C and CALIOP overpasses within 100 km of each other on the 27th of December 2019 are shown in Figure 32. The location of the smoke layers is also specified on the right side of the figure. The height of all aerosol types and more specifically of the smoke layer is shown together with the GOME-2C AAH in Figure 33 and in Table 15. For some GOME-2C pixels, the AAH agrees quite well with the height of the smoke layer detected by CALIOP. The 'undefined' CALIOP subtype could be elevated smoke, but this is just an assumption.

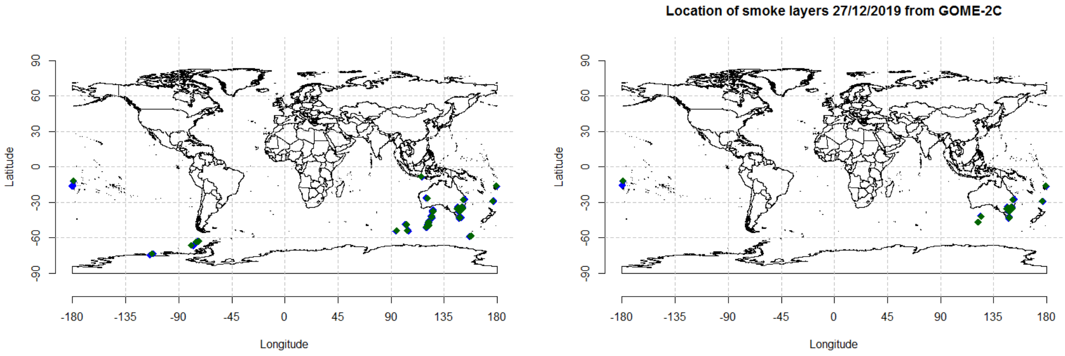

Figure 32: The location of the CALIOP and GOME-2C overpasses for the 27th of December 2019 are shown in blue and green respectively on the left plot. The plot on the right side shows where CALIOP detected smoke layers.

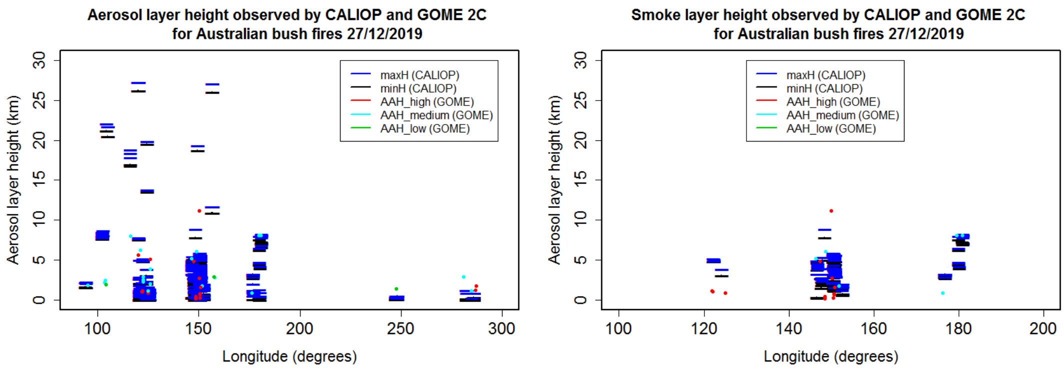

Figure 33: The aerosol (left) and smoke (right) layer height detected by CALIOP is shown in blue (maximum layer height) and black (minimum layer height) as a function of longitude for the 27th of December 2019. The GOME-2C AAH pixels located within 100 km of a CALIOP overpass pixel are presented in red (high reliability), cyan (medium reliability) and green (low reliability). The western latitudes (which are normally negative) are plotted between 180 and 360°.

Table 15: Height of the aerosol layer detected by CALIOP for the different aerosol species compared to the AAH detected by GOME-2C for pixels located within 100 km distance for the 27th of December 2019.

	CALIOP	**AAH**
Clean marine	0.0-4.1 km	0.2-8.1 km
Dust	0.0-3.7 km	0.2-6.1 km
Polluted continental	0.0-4.2 km	0.2-11.1 km
Clean continental	0.1-4.4 km	0.8-11.1 km
Polluted dust	0.0-6.8 km	0.2-11.1 km

Smoke	0.3-8.8 km	0.2-11.1 km
Undefined	7.6-28.2 km	0.2-8.0 km

GOME -2C and CALIOP overpasses within 100 km of each other on the 28th of December 2019 are shown in Figure 34. The location of the smoke layers is also specified on the right side of the figure. The height of all aerosol types and more specifically of the smoke layer is shown together with the GOME-2C AAH in Figure 35. The AAH from two out of three GOME-2C pixels shows a decent agreement with the height of the smoke layer detected by CALIOP.

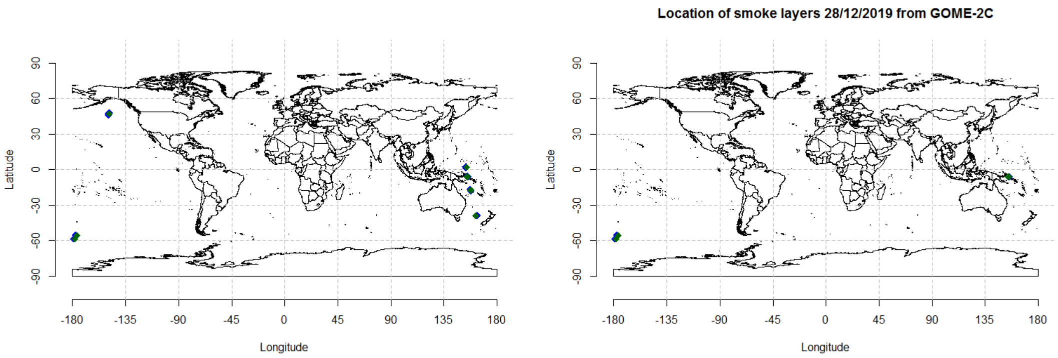

Figure 34: The location of the CALIOP and GOME-2C overpasses for the 28th of December 2019 are shown in blue and green respectively on the left plot. The plot on the right side shows where CALIOP detected smoke layers.

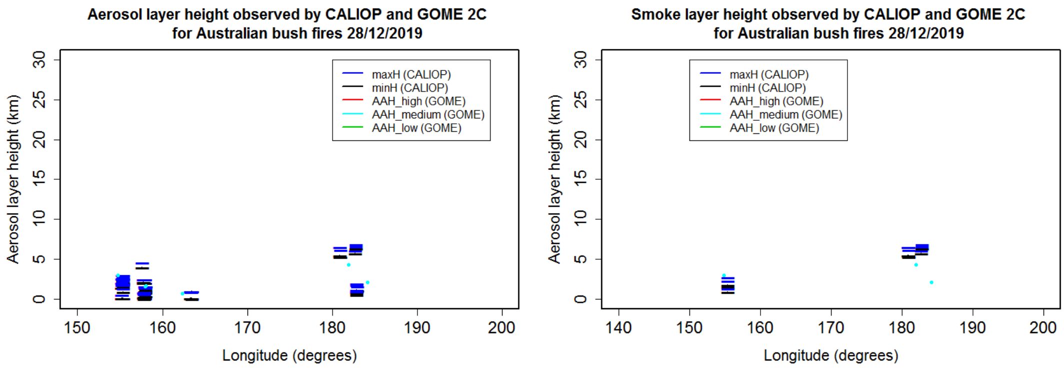

Figure 35: The aerosol (left) and smoke (right) layer height detected by CALIOP is shown in blue (maximum layer height) and black (minimum layer height) as a function of longitude for the 28th of December 2019. The GOME-2C AAH pixels located within 100 km of a CALIOP overpass pixel are presented in red (high reliability), cyan (medium reliability) and green (low reliability). The western latitudes (which are normally negative) are plotted between 180 and 360°.

GOME -2C and CALIOP overpasses within 100 km of each other on the 29th of December 2019 are shown in Figure 36. The location of the smoke layers is also specified on the right side of the figure. The height of all aerosol types and more specifically of the smoke layer is shown together with the GOME-2C AAH in Figure 35. The AAH from the high reliability GOME-2C pixel agrees nicely with the height of the smoke layer detected by CALIOP. The medium reliability GOME-2C pixel overestimates the height of the smoke layer and probably detects a higher absorbing aerosol layer.

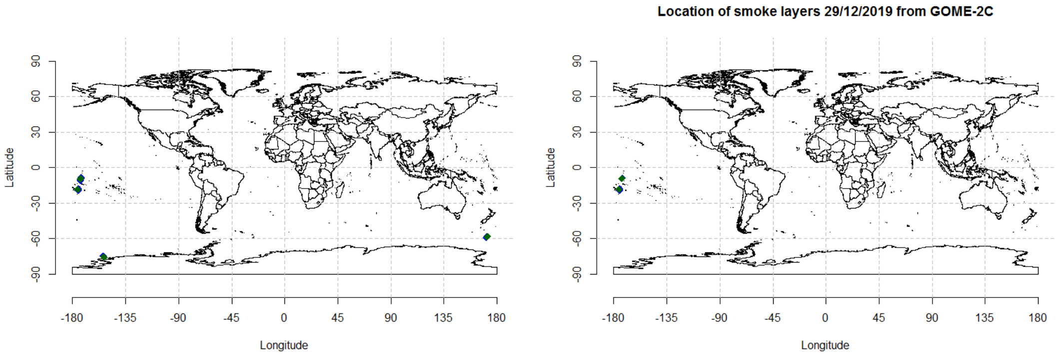

Figure 36: The location of the CALIOP and GOME-2C overpasses for the 29th of December 2019 are shown in blue and green respectively on the left plot. The plot on the right side shows where CALIOP detected smoke layers.

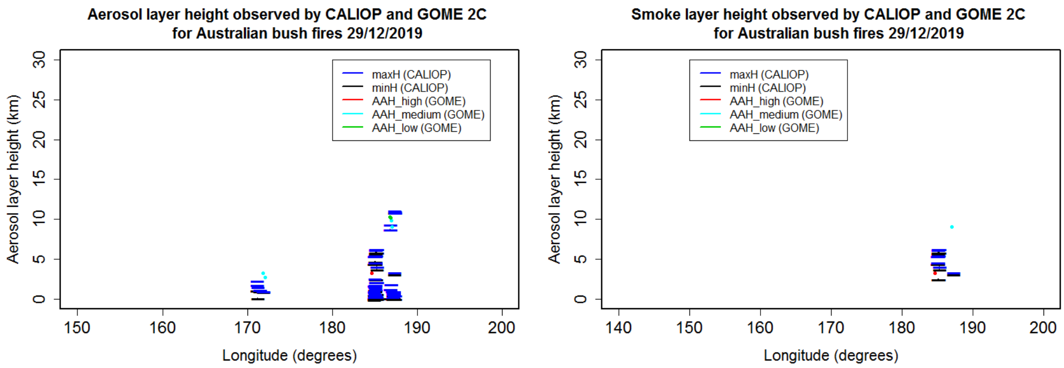

Figure 37: The aerosol (left) and smoke (right) layer height detected by CALIOP is shown in blue (maximum layer height) and black (minimum layer height) as a function of longitude for the 29th of December 2019. The GOME-2C AAH pixels located within 100 km of a CALIOP overpass pixel are presented in red (high reliability), cyan (medium reliability) and green (low reliability). The western latitudes (which are normally negative) are plotted between 180 and 360°.

GOME -2C and CALIOP overpasses within 100 km of each other on the 31st of December 2019 are shown in Figure 38. The location of the smoke layers is also specified on the right side of the figure. The height of all aerosol types and more specifically of the smoke layer is shown together with the GOME-2C AAH in Figure 39. The AAH from the GOME-2C pixel mostly agrees with the height of the smoke layer detected by CALIOP.

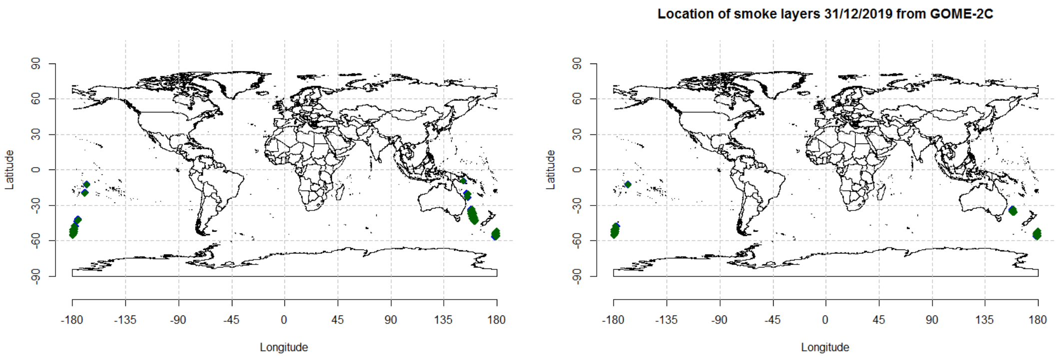

Figure 38: The location of the CALIOP and GOME-2C overpasses for the 31st of December 2019 are shown in blue and green respectively on the left plot. The plot on the right side shows where CALIOP detected smoke layers.

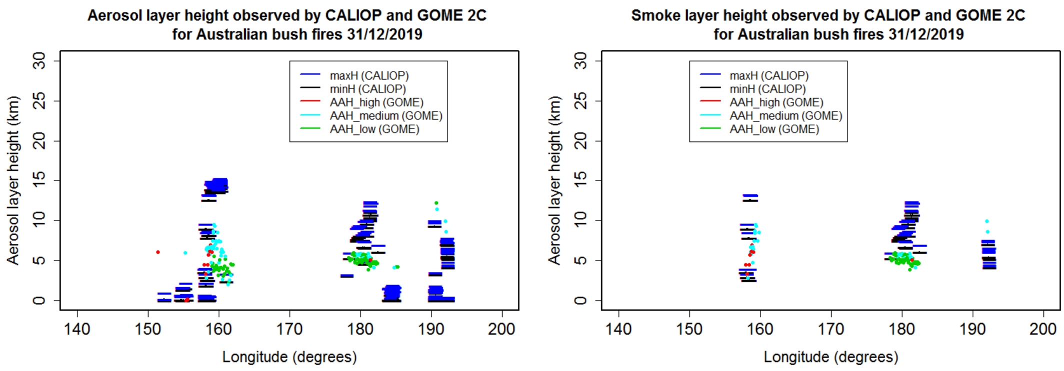

Figure 39: The aerosol (left) and smoke (right) layer height detected by CALIOP is shown in blue (maximum layer height) and black (minimum layer height) as a function of longitude for the 31st of December 2019. The GOME-2C AAH pixels located within 100 km of a CALIOP overpass pixel are presented in red (high reliability), cyan (medium reliability) and green (low reliability). The western latitudes (which are normally negative) are plotted between 180 and 360°.

The first results for the Australian bush fire case show promising results. The height of the smoke layer could in most cases be captured by the AAH from GOME-2C.

4.2 AUTH results

4.2.1 General summary

For the comparison of GOME-2 AAH against aerosol height from EARLINET lidars, the coincidence criteria are set to a 150 km search radius between the satellite pixel center and the geolocation of the ground-based station. The lidar measurements nearest to the GOME-2 overpass time within a 5 hour temporal interval were selected for every available day of measurement, to ensure a sufficiently large collocation database. It should also be noted that the temporal criterion is enforced since most of the EARLINET lidar observations occur at noon or night while the MetOp orbits are in the morning. For each ground based measurement, only the spatially closest GOME-2 measurements were selected in the comparison study. Furthermore, for the validation of GOME-2 AAH values, the AAI is taken into accounts. Observation pixels with AAI values below 2.0 correspond to scenes with a too low aerosol amount which results in an unreliable AAH retrieval. Furthermore, for AAI values larger than 2.0 but smaller than 4.0, the aerosol layer is not in all cases thick enough for a reliable retrieval. However, in this study, most aerosol cases are reported for AAI below the 4.0 level. In Appendix B, the AAI and AAH time series from the GOME-2 satellite measurements for each satellite platform are plotted. Observation pixels with AAI values below 2.0 correspond to scenes with a too low amount of aerosols to result in a reliable AAH retrieval and for this reason these pixels are excluded from the time series.

As discussed in detail in Section 3.2, a large amount of GOME-2 AAH heights below the 1km level are reported, which in most cases are unlikely to be captured from a lidar backscatter profile since the archived backscatter profiles usually start at heights between 0.7-1km. As a result, those very low GOME-2 AAH heights are not considered for the collocation. Furthermore, a number of cases were found where GOME2 reported AAH heights above 7.5km. However, for heights above 5-6km the Lidar has usually a low signal-to-noise ratio and those collocations were also excluded from further analysis, because they would be misleading. Therefore, as can also be seen for the last bar – for heights above 6km- of Figure 41(right), there are very few cases where the lidars report heights above that altitude.

Quality flags are very important indicators for the correctness of both the input and the retrieved values of the AAI. The GOME-2 AAI products are, like another AAI product, affected by sun glint.

The primary and most direct problem of sun glint is that it results in of abnormally high AAI estimates and observations affected by sun glint should therefore not be used. The sun glint flag provided as information in the GOME-2 AAI product (Tuinder and Tilstra, 2016) is used to filter potential sun glint cases. Secondly, solar eclipse events lead to abnormally low values for the retrieved Earth reflectance. Observations taken during a solar eclipse should not be used and the affected measurements should be removed from the analysis study and a solar eclipse flag is determined for each observation. Figure 40 (right) shows the number of available lidar backscatter profiles and (left) the total number of the retrieved GOME-2 pixels (after flags were applied) used to find collocations with the lidars for each MetOp satellite and for each EARLINET station.

In Figure 41 (left) the distribution of reliability category (Regime) of collocated observations is presented, including the contribution of clouds. The effective cloud fraction (CF) is a primary indicator for the AAH algorithm and is used to check which of these regimes is more reliable for retrieving the AAH. It is clear that most of collocated cases belong to the high (regime A) and medium (regime B) reliability categories.

Figure 42 shows the distribution of GOME-2 AAH and EARLINET aerosol layer height differences for each EARLINET station individually. The left panels present the scatter plots between GOME-2 AAH and ground-based lidar aerosol layer height and the right panels show histograms of the absolute bias for the collocated cases. The GOME-2 AAH performance is also quantified through the linear correlation coefficient between the GOME-2 AAH and EARLINET aerosol layer height distributions for collocated observation cases. The statistics of the intercomparison between GOME-2 and EARLINET are summarized in Table 16. The mean bias (GOME-2 AAH – EARLINET aerosol layer height) falls in the ±1 km range with an associated standard deviation between 1 and 2 km. Considering the differences mainly in the temporal collocation, the difference between the satellite pixel size and the point view of the ground-based observations and, these results are quite promising as the stable aerosol layers are well captures by the satellite sensors.

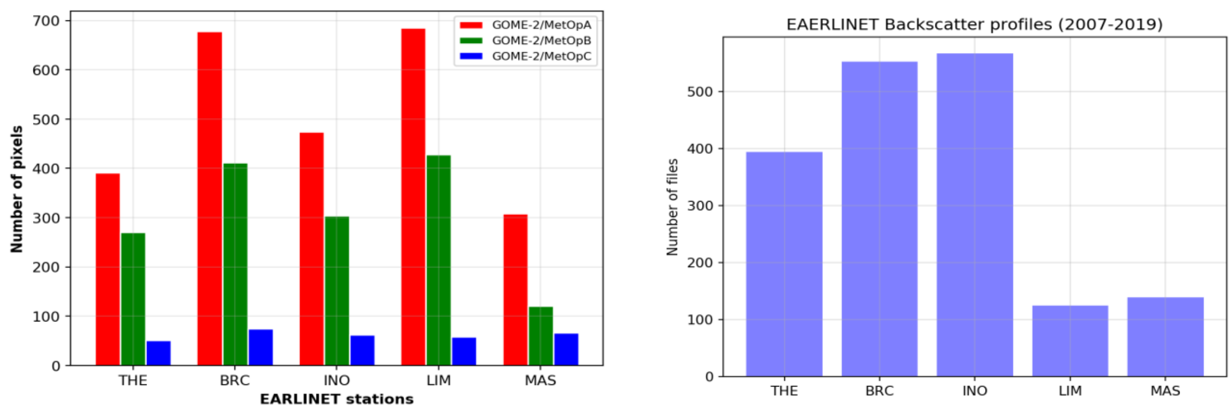

Figure 40. (left) Number of the spatially closest GOME2 pixels within a radial distance of 150 km around each EARLINET station and (right) number of lidar backscatter profiles used in this study for the period 2007-2019 [THE: Thessaloniki, BRC: Barcelona, INO: Bucharest, LIM: Limassol, MAS: Minsk].

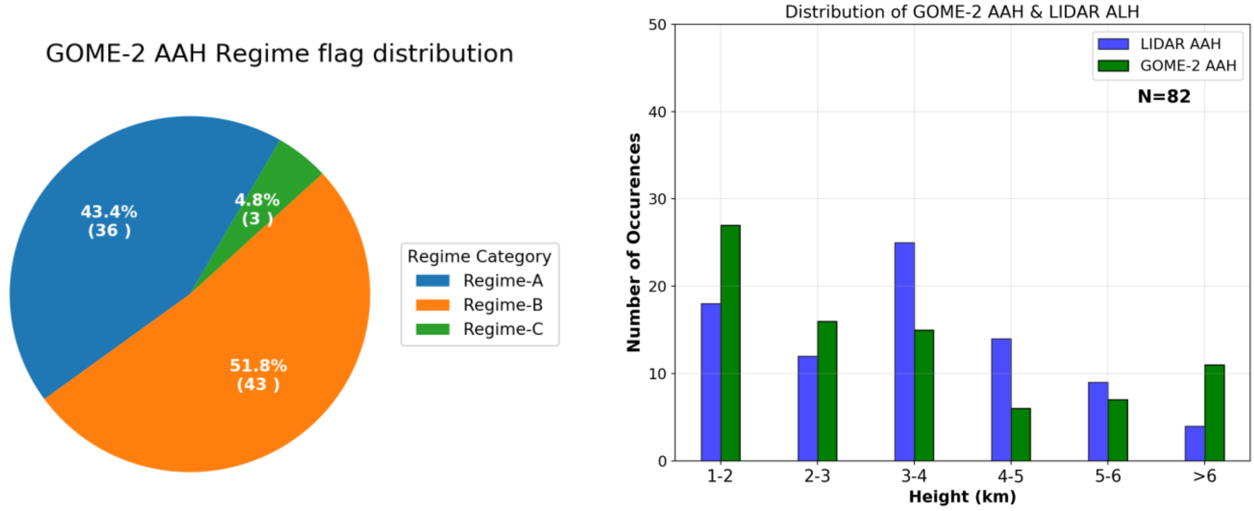

Figure 41. (left) Distribution of reliability category (GOME2 AAH Regime flag) of the selected collocated observations and (right) bar plot of GOME-2 AAH (green) and EARLINET ALH (blue) stations collocations after all criteria are applied. The height ranges of bins are between 1-2, 2-3, 3-4, 4-5, 5-6 and > 6 km.

Table 16. GOME-2 AAH and EARLINET comparison statistics.

EARLINET stations		**# Collocated observations**	**Mean bias (km)**	**Std (km)**
1.	Barcelona, Spain	32	-0.36	1.95
2.	Thessaloniki, Greece	24	-0.06	1.84
3.	Minsk, Belarus	5	0.56	0.61
4.	Bucharest, Romania	10	1.36	2.53
5.	Limassol, Cyprus	11	-0.07	1.65
6.	**All stations**	**82**	**-0.08**	**1.74**

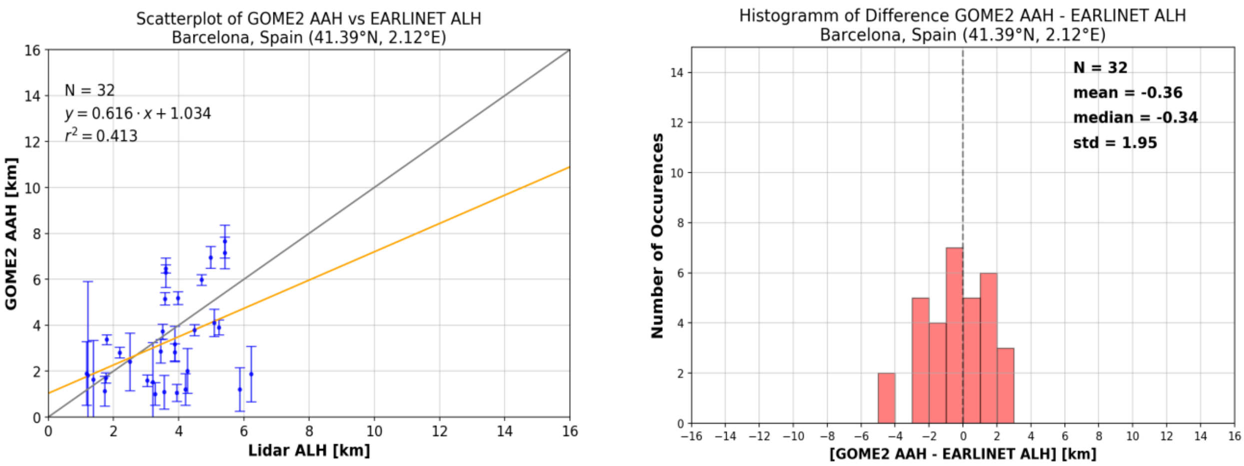

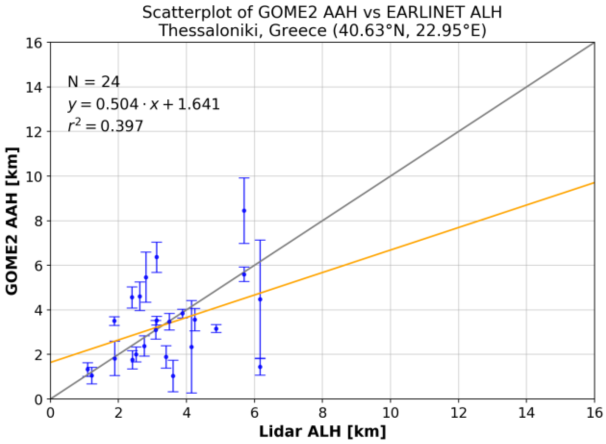
Scatterplot of GOME2 AAH vs EARLINET ALH
Thessaloniki, Greece (40.63°N, 22.95°E)
N = 24
$y = 0.504 \cdot x + 1.641$
$r^2 = 0.397$
GOME2 AAH [km]
Lidar ALH [km]

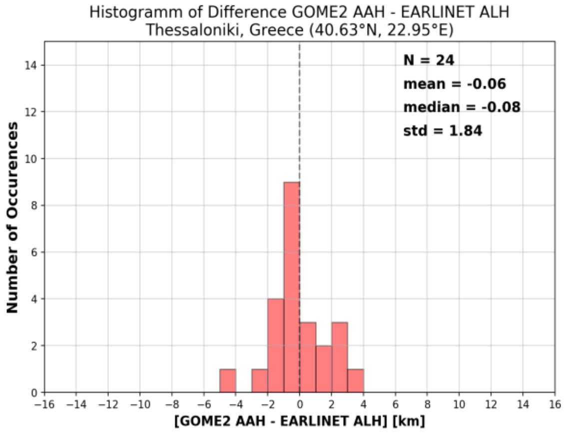
Histogramm of Difference GOME2 AAH - EARLINET ALH
Thessaloniki, Greece (40.63°N, 22.95°E)
N = 24
mean = -0.06
median = -0.08
std = 1.84
Number of Occurences
[GOME2 AAH - EARLINET ALH] [km]

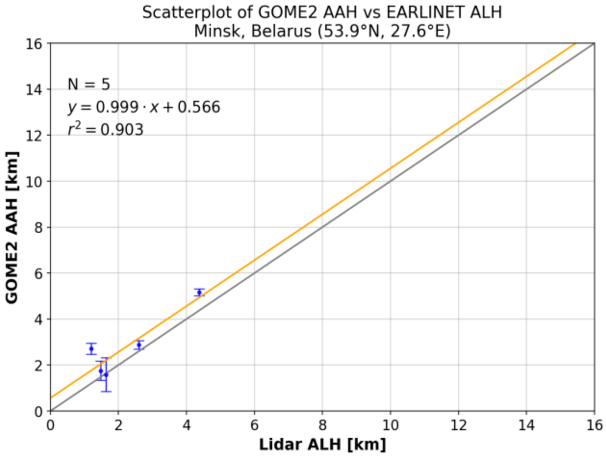
Scatterplot of GOME2 AAH vs EARLINET ALH
Minsk, Belarus (53.9°N, 27.6°E)
N = 5
$y = 0.999 \cdot x + 0.566$
$r^2 = 0.903$
GOME2 AAH [km]
Lidar ALH [km]

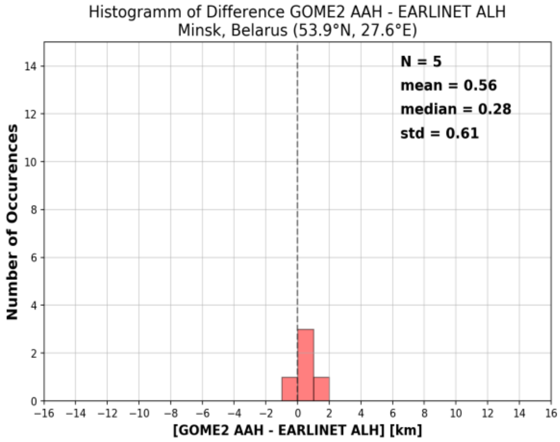
Histogramm of Difference GOME2 AAH - EARLINET ALH
Minsk, Belarus (53.9°N, 27.6°E)
N = 5
mean = 0.56
median = 0.28
std = 0.61
Number of Occurences
[GOME2 AAH - EARLINET ALH] [km]

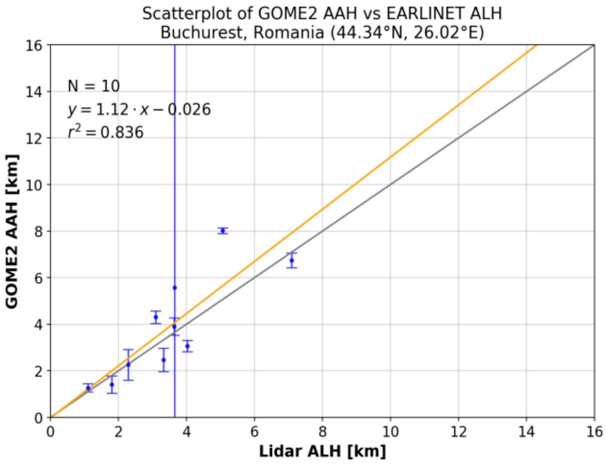
Scatterplot of GOME2 AAH vs EARLINET ALH
Bucharest, Romania (44.34°N, 26.02°E)
N = 10
$y = 1.12 \cdot x - 0.026$
$r^2 = 0.836$
GOME2 AAH [km]
Lidar ALH [km]

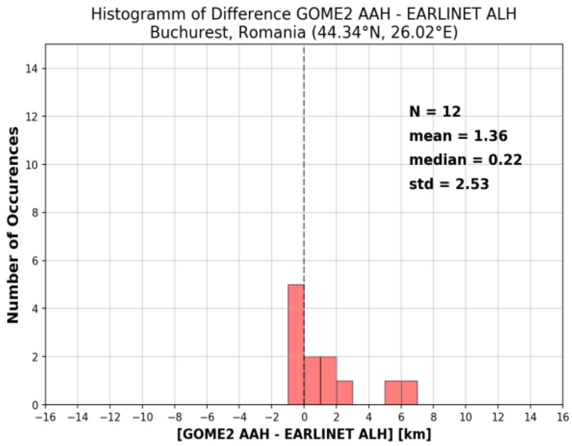
Histogramm of Difference GOME2 AAH - EARLINET ALH
Bucharest, Romania (44.34°N, 26.02°E)
N = 12
mean = 1.36
median = 0.22
std = 2.53
Number of Occurences
[GOME2 AAH - EARLINET ALH] [km]

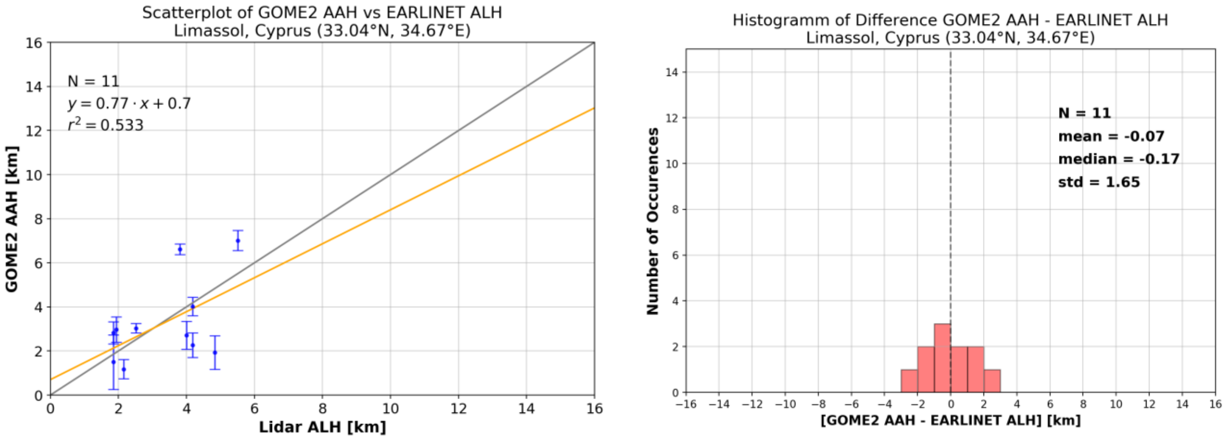

Figure 42. (Left panels) Scatter plots between GOME-2 AAH and ground-based lidar aerosol layer height and (right panels) histograms of the absolute bias, with further statistics in the legend for the five stations shown in Table 16 . The error bars in the left represent the associated AAH error of the GOME2 observations.

Figure 43 (upper) is a composite summary plot showing the distribution of GOME-2 AAH and EARLINET aerosol layer height differences for all EARLINET stations shown in this report (a total of 82 collocated cases). The different stations are color coded (Figure 43, upper left) as the lidar systems are not the same in all stations, which could further amplify the differences in the comparisons. The comparisons for all GOME-2 pixels against the simultaneous lidar observation color-coded by their associated AAI values is also shown in Figure 43 (upper right). Furthermore, in Figure 43 (lower panel) a summary of a histogram plot with the distribution of GOME-2 AAH and EARLINET aerosol layer height differences for all EARLINET stations is showing for a total of 82 collocated cases. The near Gaussian distribution of the absolute difference is centered slightly to the left, indicating lower GOME-2 AAH values on average with a mean bias of -0.08km and standard deviation of 1.74km, a very promising result considering all the individual uncertainties of both datasets as well as the collocation criteria. The related metrics are given in Table 16.

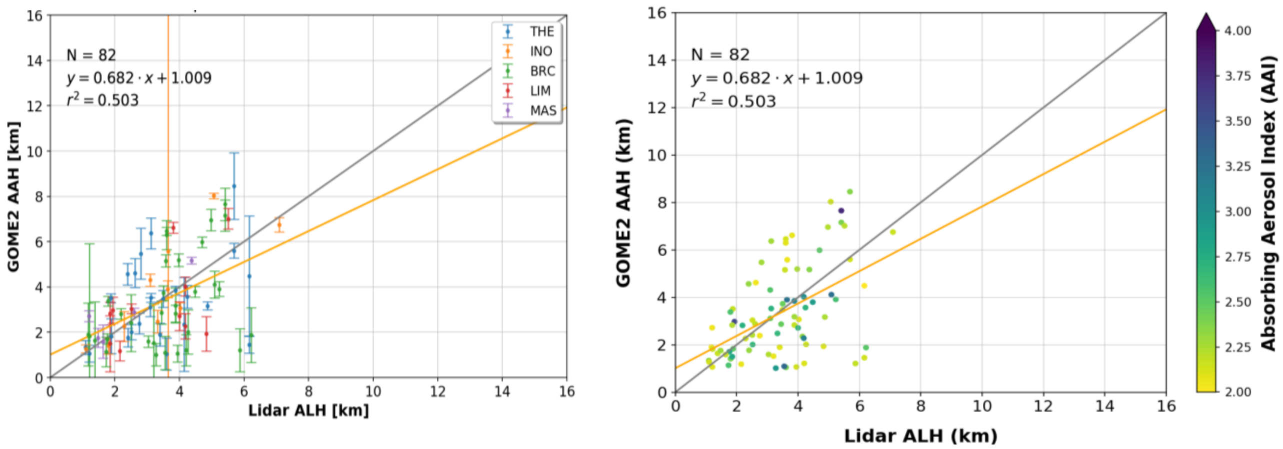

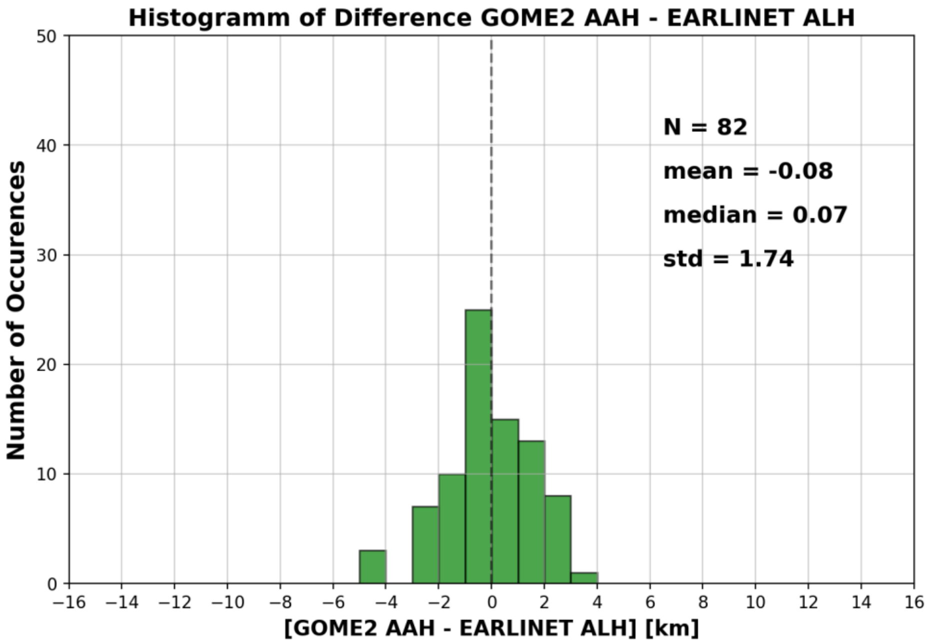

Figure 43. The upper panel shows a scatter plot between GOME-2 AAH and ground-based lidar aerosol layer height for the different lidar stations (THE: Thessaloniki, BRC: Barcelona, INO: Bucharest, LIM: Limassol, MAS: Minsk). (Upper left) The comparisons are colour-coded for the different stations and include the error bars represent the AAH error for the GOME2 observations. (Upper right) the colour-code indicates the associated AAI reported by GOME2. The lower panel shows the histogram of the absolute bias for all collocated study cases.

4.2.2 Case studies

Atmospheric particles, particularly the mineral dust particles greatly influence the Earth's radiation balance and climate. The Sahara desert is the world's primary source of dust aerosols and every year large quantities of dust are emitted into the atmosphere during the high wind periods. Strong winds can blow sand from desert regions into the free troposphere where it is advected over great distances (Prospero et al., 2002). The Mediterranean basin is a region influenced by a wide range of air masses originating mainly from Africa. In this section, we present validation results for a Sahara desert dust event in the Mediterranean basin using in synergy lidar and satellite measurements. Appendix B contains a second case study.

4.2.2.1 Saharan dust over Thessaloniki on July 10th, 2019

To determine the geometrical properties of dust aerosol layers we have used the vertical profile of the backscatter coefficient at 1064 nm (Figure 44, upper left). In addition, the wavelet covariance coefficient profile is shown (Figure 44, upper right), resulting in the backscatter signal for aerosol layer detection. Horizontal red dashed lines represent the top of each detected layer. The backscatter profile on the 10^{th} of July 2019 shows a well-defined dust layer between 1 and 4.5 km a.s.l. This aerosol layer was quite stable during the period of measurement. The RCS color map shows that on the 10^{th} of July 2019, a thick aerosol layer is detected from the ground up to 4.5 km and two thin aerosol layers are found at a height of about 5-6km (Figure 44, lower). To identify the origin of the observed aerosol layers, we used 5-day backward trajectories using the National Oceanic and Atmospheric Administration Hybrid Single-Particle Langrangian Integrated Trajectory (NOAA-HYSPLIT) model at several altitudes (Figure 45, left). During this Saharan dust event, Raman/lidar measurements were performed at Thessaloniki. An integrating modelling system, the Dust Regional Atmospheric

Modelling (DREAM) model (Nickovic et al.,2001) was also used for the accurate description of the dust load in the atmosphere (Figure 45**Error! Reference source not found.**, right).

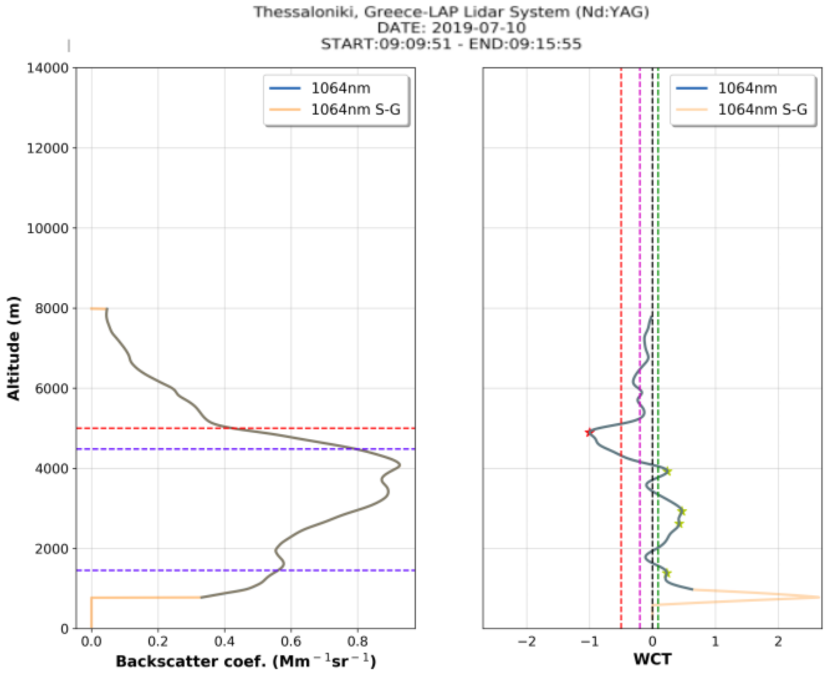

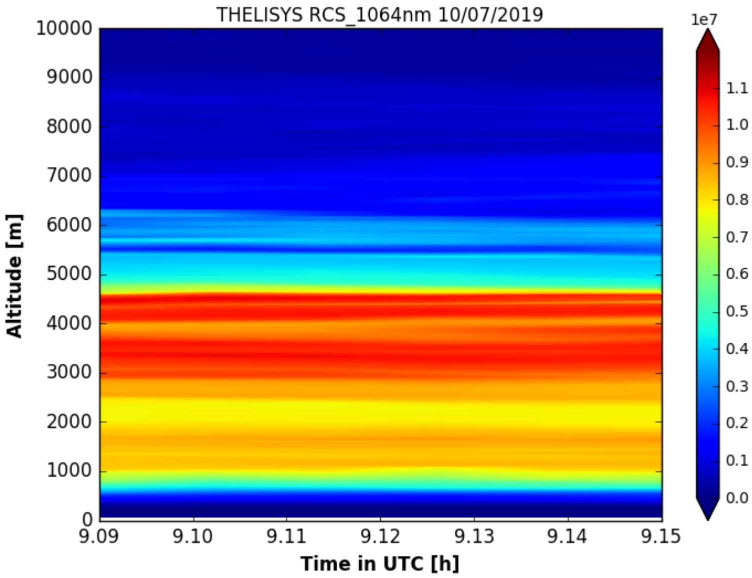

Figure 44. The upper left plot shows the lidar backscatter profile at 1064 nm. The horizontal blue lines represent the GOME-2 AAH and red lines represent the top of the dust layer. The upper right plot shows the resulting WCT profile and the bottom plot shows the temporal evolution of the range-corrected lidar signal (RCS) in arbitrary units from the Thessaloniki lidar station on July 10th, 2019.

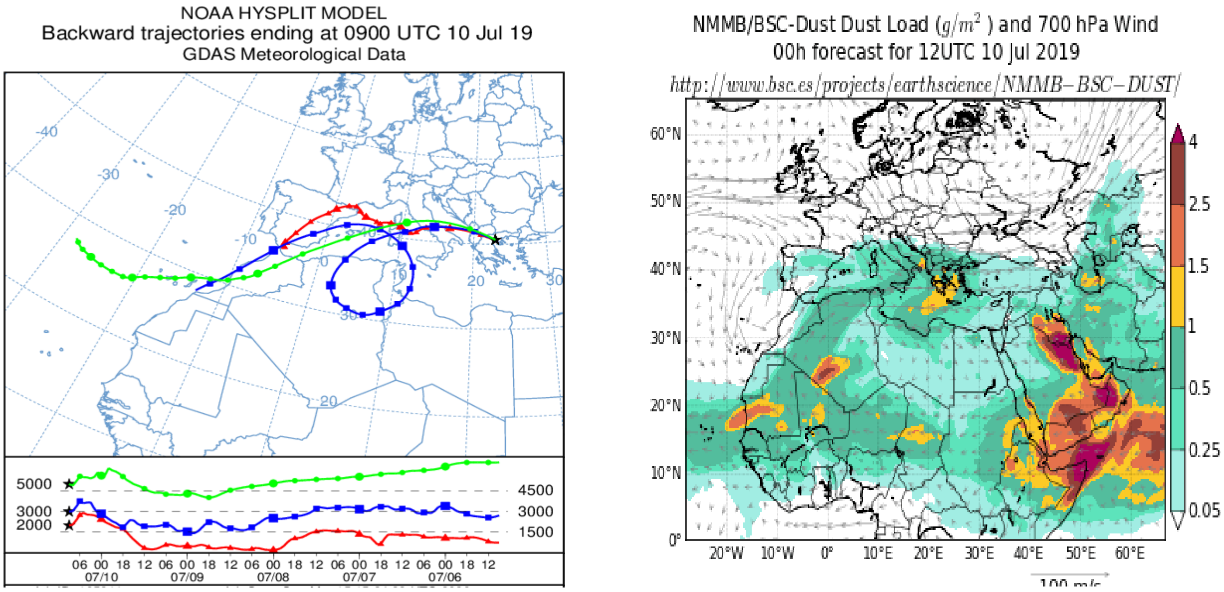

Figure 45: (Left) The 5-day NOAA HYSPLIT backward trajectories ending at the position of Thessaloniki 10 July 2019, 09:00 UTC (40.63°N, 22.95°E) and (right) dust loading map (g/m^2) calculated by the DREAM model

The satellite aerosol height information is available from GOME-2B and GOME-2C instruments for this day. All the necessary information about the GOME-2 pixels nearest to the Thessaloniki lidar station for the two satellites is shown in Table 17. In this case, the best agreement is found for the collocation to the GOME-2B pixel [first column] which is closest spatially, at 60 km, but probably most importantly is associated with completely clear skies as shown by the very low cloud fraction of 4%.

Table 17: Satellite products from MetOp-B & MetOp-C overpasses on July 10, 2019.

Satellite	**GOME-2B**	**GOME-2C**
Satellite Time	08:04:00 UT	08:38:12 UT
Lidar Time	0	0
Distance	60km	122km
AAI	2.1	2.2
AAH	4.48km	1.45km
CF	0.04	0.37

5 Issues encountered

Both teams encountered some issues during their validation exercise. They will be discussed in the following sections.

5.1 Issues encountered by RMI

A first issue was the difficulty to find collocations both in space and time between GOME-2 and CALIOP overpasses. CALIOP has far from a global coverage (due to its narrow footprint of 100m), whereas GOME-2 has a near global coverage. It was decided to set a threshold of 100 km for the maximum distance between the center of a GOME-2 pixel and the CALIOP coordinates. This was done to ensure that both satellites are looking at the 'same' location but strongly limits our study data set. Currently, no threshold is fixed for the time difference between overpasses as this would limit our data set even more. However, by accepting all time differences, it might be possible that GOME-

2 and CALIOP are not really looking at the same air mass. Apart from finding collocations, it was not always easy to find overpasses ‘near’ the eruption sites.
Another limiting factor was that only cases with AAI higher than 4 were taken into account to ensure that the amount of absorbing aerosols is high enough. Should cases with AAI between 2 and 4 also be allowed in order to increase the data set?
Difficulty also arose from the aerosol type classification used by CALIOP, which is partly based on the position of the layers in the atmosphere. CALIOP distinguishes between tropospheric (clean marine, dust, polluted continental, clean continental, dust, smoke and dusty marine types) and stratospheric (PSC aerosol, volcanic ash, sulfate and elevated smoke) aerosol layers. It is known that due to this distinction based on altitude, volcanic aerosol types in the troposphere are sometimes misclassified as dust or polluted dust.

5.2 Issues encountered by AUTH

The basic issue in the AUTH study was the difficulty to find good spatiotemporal collocations between EARLINET lidar stations observations and GOME-2/MetOp overpass. For the comparison of the GOME-2 AAH against aerosol height from EARLINET lidars, the coincidence criteria are set to a 150 km search radius between the satellite pixel center and the geolocation of the ground-based station. The LIDAR measurements nearest to the GOME-2 overpass time within a 5 hour temporal interval were selected for every available day of measurement, to ensure a sufficiently large collocation database. It should also be noted that the temporal criterion is enforced since most of the EARLINET lidar observations occur at night while the GOME-2/Metop orbits are in the morning. For each ground based measurement, only the spatially closest GOME-2 measurements were selected in the comparison study. Furthermore, certain criteria for ensuring the quality and representativeness of the satellite measurements, such as sun glint and AAI values greater than 2 were taken into account. Selecting these criteria, the total set of available satellite pixels is quite small. Most of the satellite measurements available from GOME-2 / MetOp refer to cases with AAI between 2 and 4.
EARLINET consists of quite different lidar systems regarding the number of measured wavelengths and different technical structures and for this reason EARLINET database required homogenization to ensure that all lidars are providing similar quality observations and hence can be included in the data pool.

6 Conclusions

Two teams validated the AAH product using a different approach.

RMI decided to focus its validation exercise on specific cases of volcanic eruptions for which, within the framework of aviation safety, it is important to know the height of the volcanic ash layers. A list of case studies was selected based on both information from the Global Volcanism Program of Smithsonian Institution and on clear signals found on GOME-2 AAI images. Important is that RMI only took into account cases where the AAI for the GOME-2 pixels was higher than 4 and that a maximum difference of 100 km between the GOME-2 center pixel and the CALIOP overpass was allowed.

Overall, GOME-2A, GOME-2B and GOME-2C are able to represent the minimum CALIOP layer height with a mean error of -2.5 ± 5 km, -1.2 ± 5.9 km and -2 ± 5.8 km respectively. For the maximum CALIOP layer height, the mean errors are -3.3 ± 5.1 km, -2.1 ± 5.9 km and -2.6 ± 5.9 km respectively. The high standard deviation is due to the inclusion of stratospheric aerosol species. If these stratospheric aerosol types are removed from the dataset, the errors become -0.2 ± 3.6 km, -0.1 ± 5.4 km and -0.8 ± 3.8 km for GOME-2A, GOME-2B and GOME-2C respectively for the minimum CALIOP layer height and -1.0 ± 3.6 km, -1.0 ± 5.4 km and -1.4 ± 3.9 km for GOME-2A, GOME-2B and GOME-2C respectively for the maximum CALIOP layer height. In the GOME-2 AAH product, reliability flags are used to define the confidence level of the AAH. It would be expected that the high confidence AAH pixels have a better agreement with the CALIOP layer height, however, but this was not the case.

For each AAH pixel, the error on the AAH (given by KNMI as part of the product) was studied. On average, the errors are quite small: 0.4 km, 0.4 km and 0.3 km for GOME-2A, -2B and -2C respectively.
The data set validated by RMI was analyzed further to check its agreement with the accuracy requirements defined in Table 1. For the investigated data sets for GOME-2A and GOME-2B, less than 60% of the points are within the threshold limits. Only taking into account tropospheric aerosol species improves the results. Analyzing boxplots of differences between GOME-2 AAH and CALIOP layer height for different aerosol types supports the fact that the performance of the product is better for tropospheric aerosol types. This is not optimal as the product is intended to be used to monitor volcanic aerosol layers, which are often located higher up in the atmosphere.

Some more conclusions could be drawn from looking at the volcanic case studies individually. A first conclusion is that the AAH product from GOME-2 does not work for elevated volcanic ash layers at altitudes higher than 15 km, due to the fact that the FRESCO algorithm using the O2-A band is not sensitive for the signal at these altitudes. If volcanic layers are present at these altitudes, it is impossible for GOME-2 to pick up the signal from the absorbing aerosols.
Apart from that, it proved quite challenging to validate the GOME-2 AAH product for these specific case studies due to several reasons. First, not every volcanic eruption has GOME-2 and/or CALIOP overpasses within its plume and without trajectory modelling it is difficult to determine whether overpasses should observe volcanic species in their path. It was in some cases decided to look for overpasses a bit further away from the actual volcano site, but again, it was challenging to state with absolute certainty that volcanic species should be present at that location. The fact that it is known that CALIOP sometimes misclassifies tropospheric volcanic aerosol as dust or polluted dust further complicates the validation. In some cases, the AAH from a GOME-2 pixel agreed with the height of these dust or polluted dust layers, but it is difficult to be certain that they are actually misclassified volcanic layers. The fact that there are sometimes large time differences between the overpasses can create situations where both satellites might not be looking at the same air mass.

In some cases, GOME-2 was able to see, to some extent, the absorbing volcanic aerosol layer (such as from the Calbuco eruption). When different types of aerosol layers are present, the AAH often coincides with one of the CALIOP species, but in most cases not with the volcanic layers. GOME-2 is in some cases able to nicely capture the dust layer, but definitely not always.
First results from the comparison of the CALIOP smoke layer height with GOME-2C AAH for the some days during the Australian bush fires show better and promising results.

AUTH validated the GOME-2 AAH product by comparing it to the aerosol layer height observed by the European EARLINET lidar database. The entire 2007 to 2019 satellite time series has been investigated for valid AAH measurements after filtering appropriately for the corresponding AAI value, as well as the suggested filters such as those searching for Sun glint cases, Solar eclipse events and high cloud fractions. The EARLINET database was similarly rigorously examined to locate observations free of lingering cloud signals, as well as sufficient collocation per location, so that the validation results may be assumed statistically meaningful. The main comparisons, based on five European lidar dataset were included in the main validation analysis are:

- The Barcelona, Spain, lidar provided 32 collocations with a mean bias and standard deviation of -0.36 ± 1.95 km.
- The Thessaloniki, Greece, lidar provided 24 collocations with a difference to the GOME2 observations of -0.06 ± 1.84 km.
- The Minsk, Belarus, lidar with 5 collocation and mean bias of 0.79 ± 0.61 km.
- The Bucharest, Romania, lidar, with 10 collocations and mean bias of -0.03 ± 2.53 km
- The Limassol, Cyprus, lidar with 11 collocations and mean bias of -0.07 ± 1.65 km.

Overall, the statistics showed an extremely hopeful comparison with a mean bias of -0.08 ± 1.8km. Recall that the current requirements for the accuracy of the product, shown in the beginning of this report, are for layer heights < 10km: threshold accuracy, 3km; target accuracy, 2km and optimal accuracy 1km. In Table 18 the number of cases that fulfill each of these accuracy criteria are given, as a total statistics [final column] as well as for the three regimes in the GOME2A AAH database [first three columns]. Note that for the target accuracy of 2km is achieved in ~74% of the total individual comparisons and the threshold accuracy of 3km for ~82% of the collocations. We hence conclude that, for all the limitations in the comparisons with the lidar signals, the product meets the target accuracy both as mean bias and as standard deviation.

Table 18. Percentage of collocated Lidar & GOME2 AAH cases that fulfill the optimal accuracy criteria [first line], the target criteria [second line], the threshold criteria [third line] for Regime A in the first column, Regime B in the second, Regime C in the third and the totality of the collocations in the final column.

	Regime A | 36 cases	**Regime B | 43 cases**	**Regime C | 3 cases**	**Total cases | 82 cases**
Optimal | 1 km	55.81%	58.33%	33.33%	56.1%
Target | 2km	81.4%	66.67%	33.33%	73.17%
Threshold | 3km	88.37%	75%	66.67%	81.71%

Considering the differences mainly in the temporal collocation, as well as the difference between the satellite pixel size and the point view of the ground-based observations, these results are extremely promising in that the stable aerosol layers are well captured by the satellite sensors.

Furthermore, two extreme Saharan dust transport events were captured by both ground-based lidars and GOME-2 during February, 2017 and July, 2019. The merits of a *per case* analysis are hence demonstrated in the presented comparisons, showing the ability of both systems in observing such complex and dynamic events.

The recommendations of this validation analysis are that the GOME-2 AAH product is mature enough to be rendered operational and that it contains unique information on the height of the atmospheric aerosol load within 3km and on regional scales of 150 km that can be useful in numerous climate studies and even assimilation experiments in global forecast systems such as the ECMWF CAMS.

7 Future perspectives

Trajectory modelling could be used by RMI in the future to check the direction of the air mass to make sure that both GOME-2 and CALIOP are looking at the volcanic plume. Also, it might be useful to define a threshold for the maximum time difference between GOME-2 and CALIOP overpasses or to allow for larger differences in distance between the overpasses to track volcanic plumes further away from their source.

8 Acknowledgements

The data of the GOME-2 Absorbing Aerosol Height (AAH) product are provided by KNMI in the framework of the EUMETSAT Satellite Application Facility on Atmospheric Composition Monitoring (AC SAF). GOME-2 AAI browsed images are freely distributed via the TEMIS website at http://www.temis.nl/.
EARLINET aerosol profile data are reported in the EARLINET Data base: https://data.earlinet.org /, and are accessible from its repository and from the ACTRIS Data Portal (http://actris.nilu.no). The data policy of these data is harmonized with the ACTRIS data policy. The authors gratefully acknowledge the NOAA Air Resources Laboratory (ARL) for the provision of the HYSPLIT transport and dispersion model and/or READY website https://www.ready.noaa.gov used in this publication. data and/or images from the (NMMB/BSC-Dust or BSC-DREAM8b) model, operated by the Barcelona Supercomputing Center (http://www.bsc.es/ess/bsc-dust-daily-forecast/).
The CALIOP data were obtained from the NASA Langley Research Center Atmospheric Science Data Center. https://eosweb.larc.nasa.gov/project/calipso/cal_lid_l2_vfm_standard_v4_20

9 Acronyms and abbreviations

AAH	Absorbing Aerosol Height
AAI	Absorbing Aerosol Index
ACSAF	Atmospheric Composition Satellite Application Facility
ALH	Aerosol Layer Height
ARS	Aerosol Retrieval System
ATBD	Algorithm Theoretical Basis Document
AUTH	Aristotle University of Thessaloniki
CALIOP	Cloud–Aerosol Lidar with Orthogonal Polarization
CDF	Computable Document Format
CF	Cloud Fraction
CH	Cloud Height
DR	Data Record
DREAM	Dust Regional Atmospheric Modelling
EARLINET	European Lidar Network
ESA	European Space Agency
EUMETSAT	European Organization for the Exploitation of Meteorological Satellites
FRESCO	Fast Retrieval Scheme for Clouds from the Oxygen A band
GDP	GOME Data Processor
GOME	Global Ozone Monitoring Experiment
GTS	Global Telecommunication System
HDF	Hierarchical Data Format
KNMI	Koninklijk Nederlands Meteorologisch Instituut
LIDAR	Light Detection and Ranging
MetOp	Meteorological Operational Satellite
NASA	National Aeronautics and Space Administration
NOAA-HYSPLIT	National Oceanic and Atmospheric Administration Hybrid Single-Particle Lagrangian Integrated Trajectory
NRT	Near-Real Time
PBL	Planetary Boundary Layer
PDU	Product Dissemination Unit
PUM	Product User Manual
RMI	Royal Meteorological Institute of Belgium
SA	Scene Albedo

SAF	Satellite Application Facility
SH	Scene Height
TEMIS	Tropospheric Emission Monitoring Internet Service
UTC	Universal Time Coordinate
UV	UltraViolet
VAAC	Volcanic Ash Advisory Center
VIS	Visible
WCT	Wavelet Covariance Transform
WMO	World Meteorological Organization

10 References

10.1 Applicable ACSAF Documents

ATBD: SAF Algorithm Theoretical Basis Document, Absorbing Aerosol Height, Tilstra L.G, Tuinder O.N.E., Wang P., Stammes P., SAF/AC/KNMI/ATBD/005, issue 1.4/2019, 02-04-2019

PUM: SAF Product User Manual, GOME-2 Absorbing Aerosol Height, Tilstra L.G, Tuinder O.N.E., Wang P., Stammes P., SAF/AC/KNMI/PUM/006, issue 0.1/2019, 05-04-2019

10.2 Articles

Amiridis, V., Balis, D., Kazadzis, S., Bais, A., Giannakaki, E., Papayannis, A. and Zerefos, C.: Four years aerosol observations with a Raman lidar at Thessaloniki, Greece in the framework of EARLINET, J. Geophys. Res., 110, D21203, doi:10.1029/2005JD006190, 2005.

Amiridis, V., Balis, D. S., Giannakaki, E., Stohl, A., Kazadzis, S., Koukouli, M. E. and Zanis, P.: Optical characteristics of biomass burning aerosols over Southeastern Europe determined from UV-Raman lidar measurements, Atmos. Chem. Phys., 9, 2431–2440, doi:10.5194/acp-9-2431-2009, 2009.

Amiridis, V., Wandinger, U., Marinou, E., Giannakaki, E., Tsekeri,A., Basart, S., Kazadzis, S., Gkikas, A., Taylor, M., Baldaand Ansmann, A.: Optimizing CALIPSO Saharan dust retrievals, Atmos. Chem. Phys., 13, 12089–12106, doi:10.5194/acp-13-12089-2013, 2013.

Ansmann, A., Wandinger, U., Riebesell, M., Weitkamp, C. and Michaelis, W.: Independent measurement of extinction and backscatter profiles in cirrus clouds by using a combined Raman elastic-backscatter lidar, Appl. Opt., 31, 7113–7131,https://doi.org/10.1364/AO.31.007113, 1992.

Ansmann, A., Tesche, M., Gross, S., Freudenthaler, V., Seifert, P., Hiebsch, A., Schmidt, J., Wandinger, U., Mattis, I., Müller, D. and Wiegner, M. : The 16 April 2010 major volcanic ash plume over central Europe: EARLINET lidar and AERONET photometer observations at Leipzig and Munich, Germany, Geophys. Res. Lett.,37, L13810,doi:10.1029/2010GL043809, 2010.

Baars, H., Ansmann, A., Engelmann, R. and Althausen, D.: Continuous monitoring of the boundary-layer top with lidar, Atmos. Chem. Phys., 8, 7281–7296, https://doi.org/10.5194/acp-8-7281-2008 , 2008.

Baars, H., Kanitz, T., Engelmann, R., Althausen, D., Heese,B., Komppula, M., Preißler, J., Tesche, M., Ansmann, A.,Wandinger, U., Lim, J.-H., Ahn, J. Y., Stachlewska, I. S.,Amiridis, V., Marinou, E., Seifert, P., Hofer, J., Skupin, A.,Schneider, F., Bohlmann, S., Foth, A., Bley, S., Pfüller, A., Giannakaki, E., Lihavainen, H., Viisanen, Y., Hooda, R. K., Pereira,S. N., Bortoli, D., Wagner, F., Mattis, I., Janicka, L., Markowicz,K. M., Achtert, P., Artaxo, P., Pauliquevis, T., Souza, R. A. F.,Sharma, V. P., van Zyl, P. G., Beukes, J. P., Sun, J., Rohwer, E. G.,Deng, R., Mamouri, R.-E. and Zamorano, F.: An overview of the first decade of PollyNET: an emerging network of automated Raman-polarization lidars for continuous aerosol profiling, At-mos. Chem. Phys., 16, 5111–5137, https://doi.org/10.5194/acp-16-5111-2016 , 2016.

Balis, D., Koukouli, M.-E., Siomos, N., Dimopoulos, S., Mona,L., Pappalardo, G., Marenco, F., Clarisse, L., Ventress, L. J.,Carboni, E., Grainger, R. G., Wang, P., Tilstra, G., van der A,R., Theys, N. and Zehner, C.: Validation of ash optical depth and layer height retrieved from passive satellite sensors using EARLINET and airborne lidar data: the case of the Eyjafjallajökull eruption, Atmos. Chem. Phys., 16, 5705–5720,https://doi.org/10.5194/acp-16-5705-2016 , 2016.

Brooks, I. M.: Finding boundary layer top: Application of a wavelet covariance transform to lidar backscatter profiles. J. Atmos. Oceanic Technol., 20, 1092–1105, 2003.

de Graaf, M., Stammes, P., Torres, O. and Koelemeijer, R. B. A.: Absorbing Aerosol Index: Sensitivity analysis, application to GOME and comparison with TOMS,J. Geophys. Res.,110, D01201,doi:10.1029/2004JD005178, 2005.

de Graaf, M., Tuinder, O. N. E. and Tilstra, L. G.: O3MSAF Algorithm Theoretical Basis Document for ARS,O3MSAF/KNMI/ATBD/002, Issue 1.0, KNMI, 2010.

Fernández, A. J., Sicard, M., Costa, M. J., Guerrero-Rascado, J. L., Gómez-Amo, J. L., Molero, F., Barragán, R., Bortoli, D., Bedoya-Velásquez, A. E., Utrillas, M. P., Salvador, P., Granados-Muñoz, M. J., Potes, M., Ortiz-Amezcua, P., Martínez-Lozano, J. A., Artíñano, B., Muñoz-Porcar, C., Salgado, R., Román, R., Rocadenbosch, F., Salgueiro, V., Benavent-Oltra, J. A., Rodríguez-Gómez, A., Alados-Arboledas, L., Comerón, A. and Pujadas, M.: February 2017 extreme Saharan dust outbreak in the Iberian Peninsula: from lidar-derived optical properties to evaluation of forecast models, Atmos. Chem. Phys. Discuss., https://doi.org/10.5194/acp-2018-370, 2018.

Flamant, C., Pelon, J., Flamant, P. H. and Durand, P.: Lidar determination of the entrainment zone thickness at the top of the unstable marine atmospheric boundary layer. Bound. Layer Meteor., 83, 247–28, 1997.

Freudenthaler, V., Linne, H., Chaikovski, A., Groß, S. and Rabus, D.: EARLINET lidar quality assurance tools, Atmos. Meas. Tech. Discuss., in preparation, 2014.

Giannakaki, E., Balis, D. S., Amiridis, V. and Zerefos, C.: Optical properties of different aerosol types: seven years of combined Raman-elastic backscatter lidar measurements in Thessaloniki, Greece, Atmos. Meas. Tech., 3, 569–578, https://doi.org/10.5194/amt-3-569-2010, 2010.

Klett, J.D.: Stable analytical inversion solution for processing lidar returns, Appl. Opt., 20, 211–220, https://doi.org/10.1364/AO.20.000211, 1981.

Mamouri, R. E., Papayannis, A., Amiridis, V., M ̈uller, D., Kokkalis,P., Rapsomanikis, S., Karageorgos, E. T., Tsaknakis, G., Nenes,A., Kazadzis, S. and Remoundaki, E.: Multi-wavelength Raman lidar, sun photometric and aircraft measurements in combination with inversion models for the estimation of the aerosol optical and physico-chemical properties over Athens, Greece, At-mos. Meas. Tech., 5, 1793–1808, doi:10.5194/amt-5-1793-2012, 2012.

Matthias, V., Freudenthaler, V., Amodeo, A., Balin, I., Balis, D., Bösenberg, J., Chaikovsky, A., Chourdakis, G., Comeron, A.,Delaval, A., Tomasi, F. D., Eixmann, R., Hågård, A., Komguem,L., Kreipl, S., Matthey, R., Rizi, V., Rodrigues, J. A., Wandinger,U. and Wang, X.: Aerosol lidar intercomparison in the frame-work of the EARLINET project. 1.Instruments, Appl. Opt., 43,961–976, https://doi.org/10.1364/AO.43.000961, 2004.

Munro, R., and Eisinger, M.: GOME-2 Level 1 Product Generation Specification, PGS v6.1, EU-METSAT, 2006.

Pappalardo, G., Mona, L., D'Amico, G., Wandinger, U., Adam, M.,Amodeo, A., Ansmann, A., Apituley, A., Alados Arboledas, L.,Balis, D., Boselli, A., Bravo-Aranda, J. A., Chaikovsky, A., Comeron, A., Cuesta, J., De Tomasi, F., Freudenthaler, V., Gausa,M., Giannakaki, E., Giehl, H., Giunta, A., Grigorov, I., Groß,S., Haeffelin, M., Hiebsch, A., Iarlori, M., Lange, D., Linné, H.,Madonna, F., Mattis, I., Mamouri, R.-E., McAuliffe, M. A. P.,Mitev, V., Molero, F., Navas-Guzman, F., Nicolae, D., Papayan-nis, A., Perrone, M. R., Pietras, C., Pietruczuk, A., Pisani, G.,Preißler, J., Pujadas, M., Rizi, V., Ruth, A. A., Schmidt, J.,Schnell, F., Seifert, P., Serikov, I., Sicard, M., Simeonov, V.,Spinelli, N., Stebel, K., Tesche, M., Trickl, T., Wang, X., Wagner, F., Wiegner, M. and Wilson, K. M.: Four-dimensional distribution of the 2010 Eyjafjallajökull volcanic cloud over Europe observed by EARLINET, Atmos. Chem. Phys., 13, 4429–4450, https://doi.org/10.5194/acp-13-4429-2013, 2013.

Pappalardo, G., Amodeo, A., Apituley, A., Comeron, A., Freuden-thaler, V., Linné, H., Ansmann, A., Bösenberg, J., D'Amico,G., Mattis, I., Mona, L., Wandinger, U., Amiridis, V., Alados-Arboledas, L., Nicolae, D. and Wiegner, M.: EARLINET: towards an advanced sustainable European aerosol lidar network, Atmos. Meas. Tech., 7, 2389–2409, https://doi.org/10.5194/amt-7-2389-2014, 2014.

Papayannis, A., Nicolae, D., Kokkalis, P., Binietoglou, I., Talianu, C., Belegante, L., Tsaknakis, G., Cazacu, M., Vetres, I. and Ilic, L.: Optical, size and mass properties of mixed type aerosols in Greece and Romania as observed by synergy of lidar and sunphotometers in combination with model simulations: A case study, Sci. Total Environ., 500–501, 277–294, https://doi.org/10.1016/j.scitotenv.2014.08.101, 2014.

Siomos, N., Balis, D. S., Voudouri, K. A., Giannakaki, E., Filioglou, M., Amiridis, V., Papayannis, A, and Fragkos, K.: Are EARLINET and AERONET climatologies consistent? The case of Thessaloniki, Greece, Atmos. Chem. Phys., 18, 11885–11903, https://doi.org/10.5194/acp-18-11885-2018, 2018.

Siomos, N., Balis, D. S., Poupkou, A., Liora, N., Dimopoulos, S., Melas, D., Giannakaki, E., Filioglou, M., Basart, S. and Chaikovsky, A.: Investigating the quality of modeled aerosol profiles based on combined lidar and sunphotometer data, Atmos. Chem. Phys., 17, 7003–7023, https://doi.org/10.5194/acp-17-7003-2017, 2017.

Siomos, N.: Climatology and classification of the optical and microphysical properties of aerosols using ground-based remote sensing techniques, Doctoral Dissertation, Aristotle University of Thessaloniki, Greece, GRI-2019-23387, http://ikee.lib.auth.gr/record/302303/, 2018.

Stammes, P., Sneep, M., de Haan, J. F., Veefkind, J. P., Wang, P. and Levelt, P. F.: Effective cloud fractions from the Ozone Monitoring Instrument: Theoretical framework and validation, J. Geophys. Res., 113, D16S38, doi:10.1029/2007JD008820, 2008.

Tilstra, L. G., de Graaf, M., Aben, I. and Stammes, P.: Analysis of 5 years SCIAMACHY Absorbing Aerosol Index data, in Proceedings of the 2007 Envisat Symposium, ESA Special Publication SP-636, European Space Agency, ESA/ESTEC, Noordwijk, The Netherlands, 2007.

Tilstra, L. G., Tuinder, O. N. E. and Stammes, P.: GOME-2 Absorbing Aerosol Index: Statistical analysis, comparison to GOME-1 and impact of instrument degradation, in Proceedings of the 2010 EUMETSAT Meteorological Satellite Conference, EUMETSAT P.57, 2010.

Tilstra, L. G., de Graaf, M., Tuinder, O. N. E., van der A, R. J. and Stammes, P.: Studying trends in aerosol presence using the Absorbing Aerosol Index derived from GOME-1, SCIAMACHY, and GOME-2, in Proceedings of the 2011 EUMETSAT Meteorological Satellite Conference, EUMETSAT P.59, 2011a.

Tilstra, L. G., de Graaf, M., Aben, I. and Stammes, P.: In-flight degradation correction of SCIAMACHY UV reflectances and Absorbing Aerosol Index, J. Geophys. Res., 117, D06209, doi: 10.1029/2011JD016957, 2012.

Tilstra, L. G., O. N. E. Tuinder, P. Wang, and P. Stammes, Surface reflectivity climatologies from UV to NIR determined from Earth observations by GOME-2 and SCIAMACHY, J. Geophys. Res. Atmos., 122, doi:10.1002/2016JD025940, 2017.

Tuinder, O. N. E. and Tilstra, L. G.: Near Real-Time, Offline and Data Set Aerosol Products – Product User Manual, Doc. No. O3MSAF/KNMI/PUM/002, Issue 1.61, 11 January 2016, KNMI, De Bilt, The Netherlands, 2016.

Tuinder, O., de Graaf, M., Tilstra, G., de Vries, M.P. and Kooreman, M.: ATBD for the NRT, Offline and Data Record Absorbing Aerosol Index Products, Doc. No. ACSAF/LNMI/ATBD/002, Issue 2.61, 5 September 2019, KNMI, De Bilt, The Netherlands, 2019.

Wang, P., Stammes, P., van der A, R., Pinardi, G. and van Roozendael, M.: FRESCO+: an improved O 2 A-band cloud retrieval algorithm for tropospheric trace gas retrievals, Atmos. Chem. Phys., 8 (21), 6565–6576, doi:10.5194/acp-8-6565-2008, 2008.

Wang, P., Tuinder, O. N. E., Tilstra, L. G., de Graaf, M. and Stammes, P.: Interpretation of FRESCO cloud retrievals in case of absorbing aerosol events, Atmos. Chem. Phys., 12(19), 9057–9077, doi:10.5194/acp-12-9057-2012, 2012.

11 Appendix A

This appendix contains the results from different case studies performed by RMI but not discussed in the main document.

11.1 Barren island eruption

According to officials from the Geological Survey of India, the eruption was first recorded on the 25th of September 2018 by satellite images[3]. For this case study, only data from GOME-2B were available. Data from two consecutive days are studied: 25 and 26 September 2018.

11.1.1 GOME-2B

The location of the volcano and the studied GOME-2B and CALIOP overpasses on the 25th of September 2018 are shown in Figure 46. Figure 47 shows the extended CALIOP overpass vertical profile where the pixels within 100 km of GOME-2B are highlighted by the red box and Figure 48 shows the observed aerosol layer height from CALIOP and the AAH detected by GOME-2B in function of latitude.

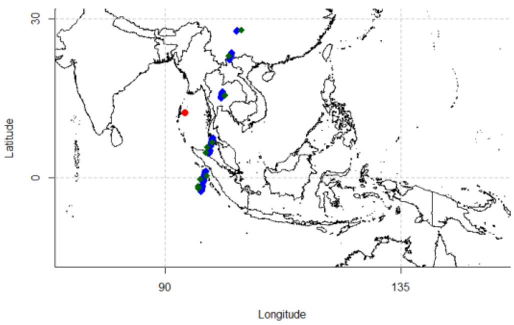

Figure 46: The location of the volcano is shown in red. The location of the CALIOP and GOME-2B overpasses on the 25th of September 2018 are shown in blue and green respectively.

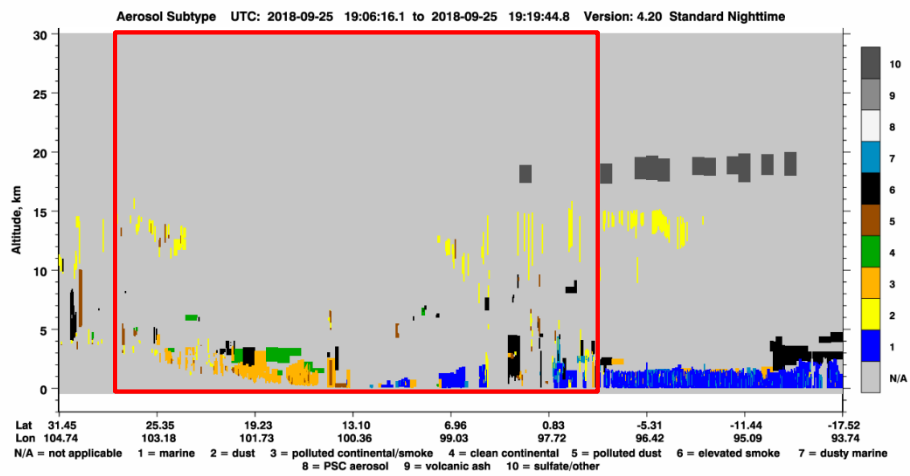

---

3 http://timesofindia.indiatimes.com/articleshow/66112494.cms?utm_source=twitter.com&utm_source=contentofinterest&utm_medium=text&utm_campaign=cppst; 8/11/2019

Figure 47: CALIOP overpass on the 25th of September 2018 from 19:06:16 to 19:19:44. The approximate part of the overpass within 100 km of GOME-2B overpasses is highlighted by the red box.

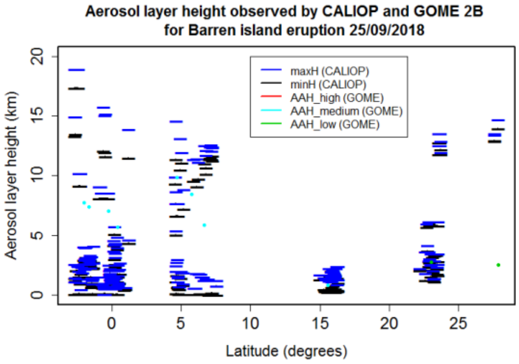

Figure 48: The aerosol layer height detected by CALIOP is shown in blue (maximum layer height) and black (minimum layer height) as a function of latitude for the 25th of September 2018. The GOME-2B AAH pixels located within 100 km of a CALIOP overpass pixel are presented in red (high reliability), cyan (medium reliability) and green (low reliability).

CALIOP detected clean marine, dust, clean continental, polluted continental, polluted dust, smoke, dusty marine and sulfate layers (Figure 47 and Table 19). The only volcanic species observed by CALIOP (sulfate) was found between 2°S and 3°S at an altitude between 17.3 and 19 km. The closest GOME-2B pixel (medium reliability) was located 85 km away and the time difference between overpasses was 15 h. Its AAH is equal to 7.7 km. It is known that volcanic aerosols in the troposphere are often misclassified by CALIOP as dust or polluted dust. These species were detected by CALIOP at altitudes between 0.1-15.8 km and between 0.4-13.6 km respectively. The closest GOME-2B pixels are located at respectively 14 km and 11 km. Again the time difference was 15 h. Due to the large time difference between both overpasses, it is likely that the two satellites are not looking at the same air mass. Trajectory modelling can be used in the future to confirm this.

Table 19: Height of the aerosol layer detected by CALIOP for the different aerosol species compared to the AAH detected by GOME-2B for pixels located within 100 km distance for the 25th of September 2018.

Aerosol type	CALIOP	AAH
Clean marine	0-2.1 km	5.7-9.8 km
Dust	0.1-15.8 km	2.5-9.8 km
Clean continental	0.0-3.5 km	0.8-7.7 km
Polluted continental	1.3-6.2 km	0.8-2.8 km
Polluted dust	0.4-13.6 km	0.8-7.7 km
Smoke	0.1-9.1 km	2.8-9.8 km
Dusty marine	0.1-4.4 km	5.7-9.8 km
Sulfate	17.3-19 km	7.7 km

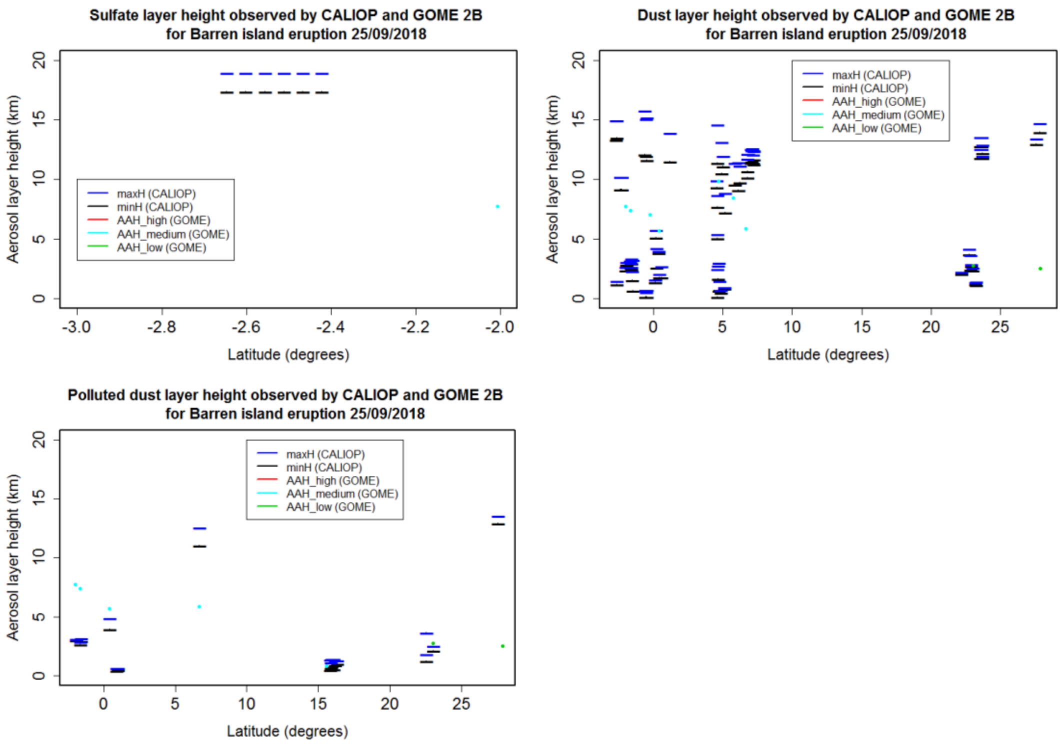

Figure 49: Detail of the sulfate (upper left), dust (upper right) and polluted dust layer (lower left) heights as detected by CALIOP in function of latitude for the 25th of September 2018. The GOME-2B AAH pixels located within 100 km of a CALIOP overpass pixel are presented in red (high reliability), cyan (medium reliability) and green (low reliability).

The studied CALIOP and GOME-2B overpasses from the 26th September 2018, located 'near' the volcano, are shown in Figure 50. Figure 51 shows the extended CALIOP overpass vertical profiles where the pixels within 100 km of GOME-2B are highlighted by the red box and Figure 52 shows the observed aerosol layer height from CALIOP and the AAH detected by GOME-2B in function of latitude.

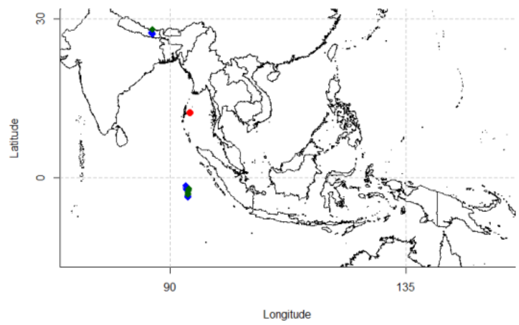

Figure 50: The location of the volcano is shown in red. The location of the CALIOP and GOME-2B overpasses on the 26th of September 2018 are shown in blue and green respectively.

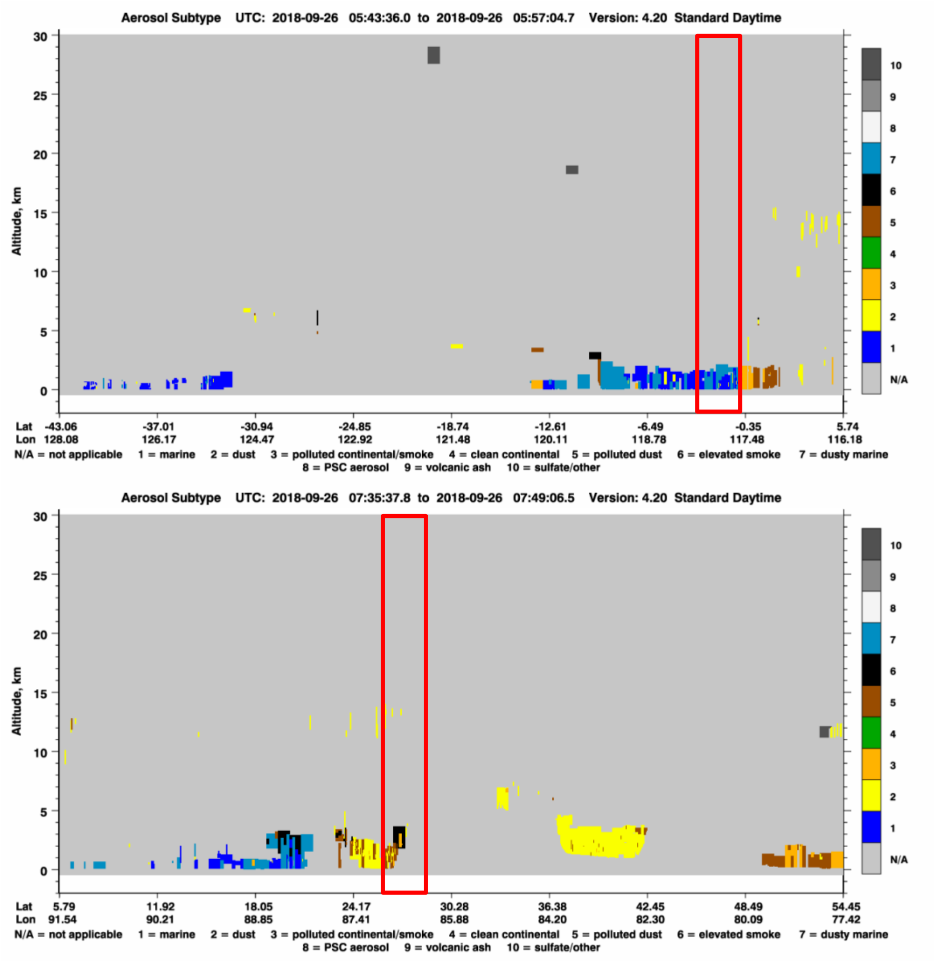

Figure 51: CALIOP overpasses on the 26th of September 2018 from 5:43:36 to 5:57:04 and from 07:35:37 to 07:49:06. The approximate parts of the overpasses within 100 km of GOME-2B overpasses are highlighted by the red box.

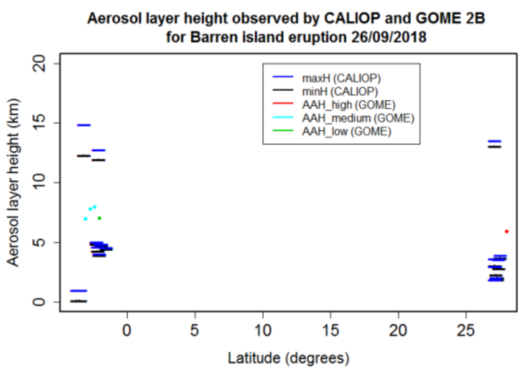

Figure 52: The aerosol layer height detected by CALIOP is shown in blue (maximum layer height) and black (minimum layer height) as a function of latitude for the 26th of September 2018. The GOME-2B AAH pixels located within 100 km of a CALIOP overpass pixel are presented in red (high reliability), cyan (medium reliability) and green (low reliability).

As can be seen in Figure 52, the AAH from GOME-2B have either high, medium or low reliability. CALIOP detected clean marine, dust, clean continental, polluted dust and smoke aerosol layers (Figure 51 and Table 20). No volcanic species were observed on this day. Dust and polluted dust layers were detected by CALIOP at altitudes between 2.8-14.9 km and between 4.5-5.0 km respectively. The closest GOME-2B pixels are located at respectively 10 km and 40 km. The time difference between overpasses was 4.4 h.

Table 20: Height of the aerosol layer detected by CALIOP for the different aerosol species compared to the AAH detected by GOME-2B for pixels located within 100 km distance for the 26th of September 2018.

	CALIOP	AAH
Clean marine	0.1-1.0 km	7.0-7.8 km
Dust	2.8-14.9 km	5.9-8.0 km
Clean continental	1.9-3.0 km	5.9 km
Polluted dust	4.5-5.0 km	7.0-8.0 km
Smoke	1.8-4.9 km	5.9-8.0 km

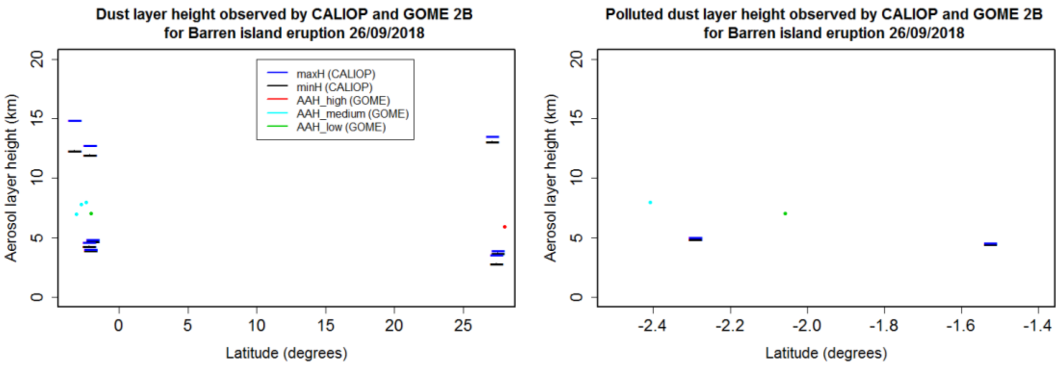

Figure 53: Detail of the dust and polluted dust layer heights as detected by CALIOP in function of latitude for the 26th of September 2018. The GOME-2B AAH pixels located within 100 km of a CALIOP overpass pixel are presented in red (high reliability), cyan (medium reliability) and green (low reliability).

11.2 Bulusan eruption

The Philippine Institute of Volcanology and Seismology reported that on the 1st of May 2015, a steam-and-ash explosion from Bulusan was detected for five minutes by the seismic network[4]. Based on the AAI images, it was decided to look at data for the period from 1-3 May 2015.

11.2.1 GOME-2A

Sadly, there were no CALIOP/GOME-2A overpasses within 100 km of each other close to the volcano on the three days of study.

11.2.2 GOME-2B

On the 3rd of May 2015, CALIOP and GOME-2B pixels were found around the SE border of Russia and China (Figure 54). CALIOP detected clean marine, dust, polluted continental, polluted dust, smoke and sulfate aerosol layers (Figure 55 and Table 21). A sulfate layer was detected by CALIOP at an altitude from 26.9-28 km. The closest GOME-2B pixel has an AAH of 1.4 km, is located 10 km away from the closest CALIOP pixel and the time difference between these overpasses is ~2.5 h. GOME-2B does not capture the height of this sulfate layer nor the height of the dust or polluted dust layers (Figure 57). It agrees more with the polluted continental and clean marine layers.
In this case, the dust/polluted dust layer are probably not misclassified volcanic layers, as it seems that these pixels are most probably not in the plume of the erupted volcano.

[4] https://volcano.si.edu/volcano.cfm?vn=273010#May2015

Table 21: Height of the aerosol layer detected by CALIOP for the different aerosol species compared to the AAH detected by GOME-2B for pixels located within 100 km distance for the 3rd of May 2015.

	CALIOP	AAH
Clean marine	0.4-2.2 km	1.4 km
Dust	1.3-15.8 km	1.4 km
Polluted continental	1.3-2.0 km	1.4 km
Polluted dust	0.4-3.7 km	1.4 km
Smoke	3.1-3.6 km	1.4 km
Sulfate	26.9-28.0 km	1.4 km

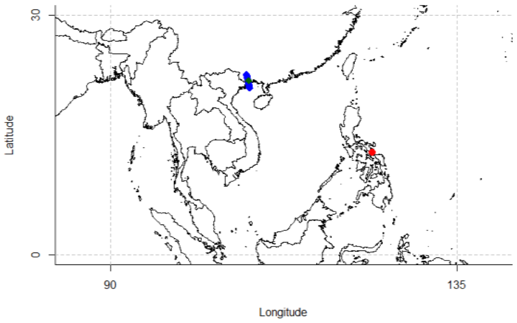

Figure 54: The location of the volcano is shown in red. The location of the CALIOP and GOME-2B overpasses on the 3rd of May 2013 are shown in blue and green respectively.

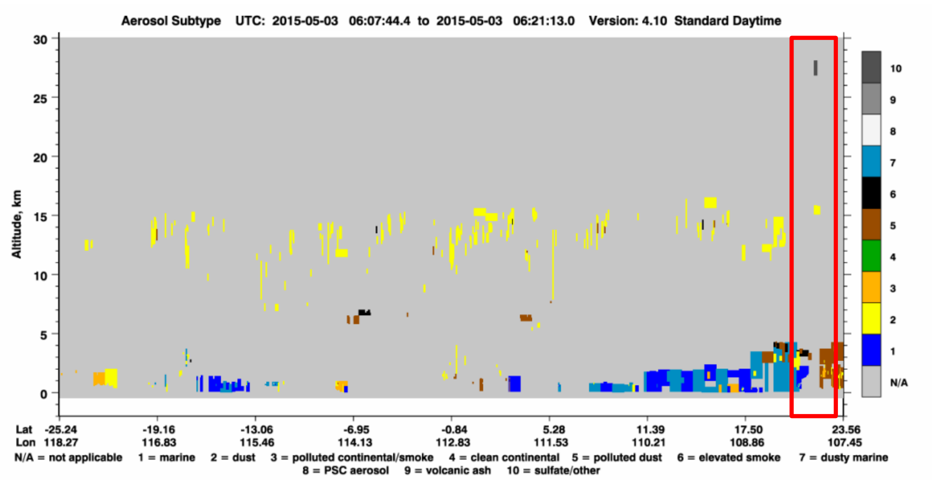

Figure 55: CALIOP overpass on the 3rd of May 2015 from 06:07:44 to 06:21:13. The approximate part of the overpass within 100 km of GOME-2B overpasses is highlighted by the red box.

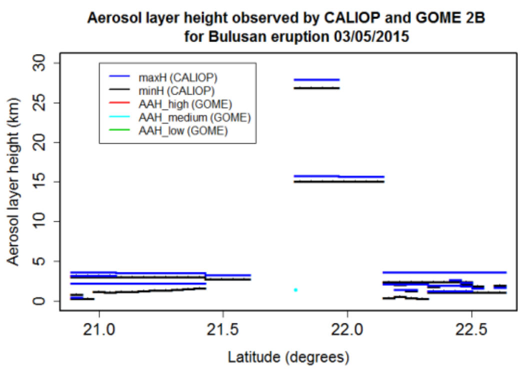

Figure 56: The aerosol layer height detected by CALIOP is shown in blue (maximum layer height) and black (minimum layer height) as a function of latitude for the 3rd of May 2015. The GOME-2B AAH pixels located within 100 km of a CALIOP overpass pixel are presented in red (high reliability), cyan (medium reliability) and green (low reliability).

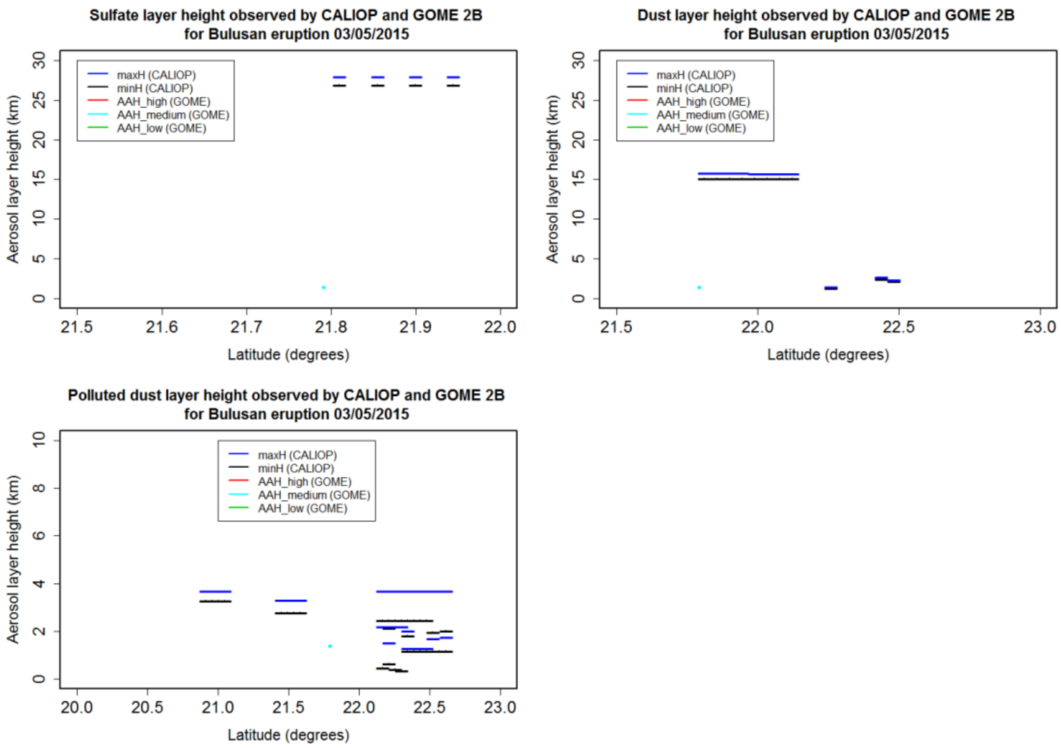

Figure 57: Detail of the sulfate (upper left), dust (upper right) and polluted dust layer (lower left) heights as detected by CALIOP in function of latitude for the 3rd of May 2015. The GOME-2B AAH pixels located within 100 km of a CALIOP overpass pixel are presented in red (high reliability), cyan (medium reliability) and green (low reliability).

11.3 Eyjafjallojökull eruption

The Institute of Earth Sciences at the Nordic Volcanological Center reported that a new set of craters opened in the early morning of 14 April 2010 under the ice-covered central summit caldera of Eyjafjallajökull. An ash plume rose to more than 8 km altitude, and was deflected to the E by winds[5]. On the 15th of April, the eruption plume reached mainland Europe, causing the closure of large areas of airspace. Activity continued during the 16th of April at a similar level as the previous day. It was decided to look at data from GOME-2A for 14-17 April 2010.

11.3.1 GOME-2A

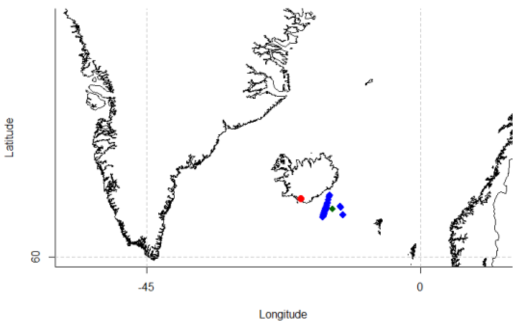

Figure 58: The location of the volcano is shown in red. The location of the CALIOP and GOME-2A overpasses on the 15th of April 2010 are shown in blue and green respectively.

[5] https://volcano.si.edu/volcano.cfm?vn=372020#April2010

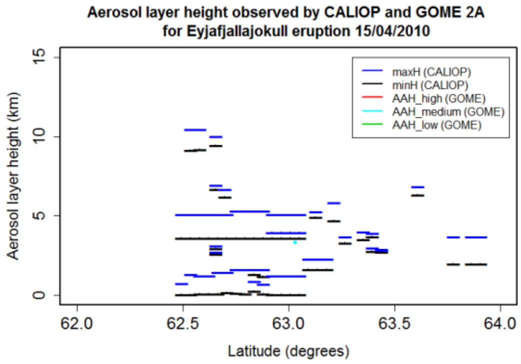

Figure 59: The aerosol layer height detected by CALIOP is shown in blue (maximum layer height) and black (minimum layer height) as a function of latitude for the 15th of April 2010. The GOME-2A AAH pixels located within 100 km of a CALIOP overpass pixel are presented in red (high reliability), cyan (medium reliability) and green (low reliability).

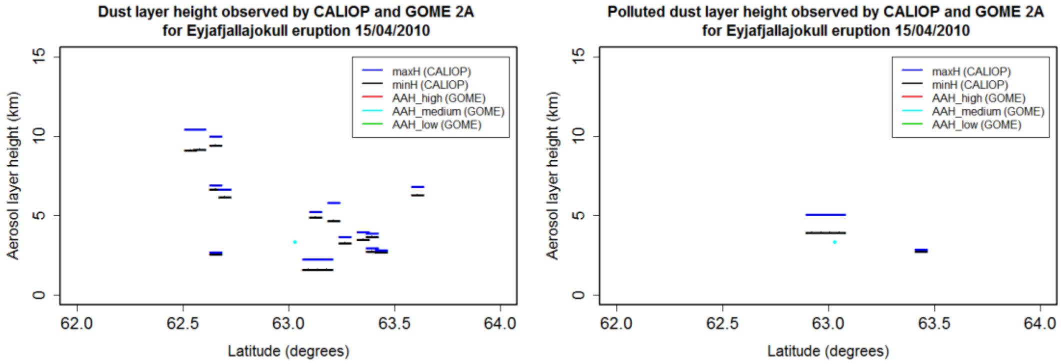

Figure 60: Detail of the dust (left) and polluted dust (right) layer detected by CALIOP. The maximum and minimum layer heights are shown in blue and black respectively as a function of latitude for the 15th of April 2010. The GOME-2A AAH pixels located within 100 km of a CALIOP overpass pixel are presented in red (high reliability), cyan (medium reliability) and green (low reliability).

Table 22: Height of the aerosol layer detected by CALIOP for the different aerosol species compared to the AAH detected by GOME-2A for pixels located within 100 km distance for the 15th of April 2010.

	CALIOP	**AAH**
Clean marine	0.1-1.6 km	3.4 km
Dust	1.6-10.5 km	3.4 km
Polluted dust	2.7-5.1 km	3.4 km
Smoke	2.0-5.3 km	3.4 km

On the 14th and 17th of April 2010, no GOME-2A and CALIOP overpasses within 100 km of each other were close to the volcano. On the 15th of April 2010, CALIOP and GOME-2A overpasses were ‘near’ the volcano (as shown in Figure 58). Figure 59 and Figure 60 show the observed aerosol layer height from CALIOP and the AAH detected by GOME-2A in function of latitude. CALIOP detected clean marine, dust, polluted dust and smoke but no specific volcanic aerosol species (Figure 61 and Table 22). However, as it is known that below the tropopause, volcanic ash is often ‘misclassified’ as dust or polluted dust and volcanic sulfate is often ‘misclassified’ as elevated smoke, these subtypes are taken into account in the analysis. GOME-2A has only 1 pixel (with medium reliability) in the region and its AAH is equal to 3.4 km. It is located ~50 km away from the closest CALIOP pixel. Dust is observed up to 10.5 km by CALIOP. Smoke and polluted dust are observed up to ~5 km. The time difference between CALIOP and GOME-2A overpasses is ~8 h.

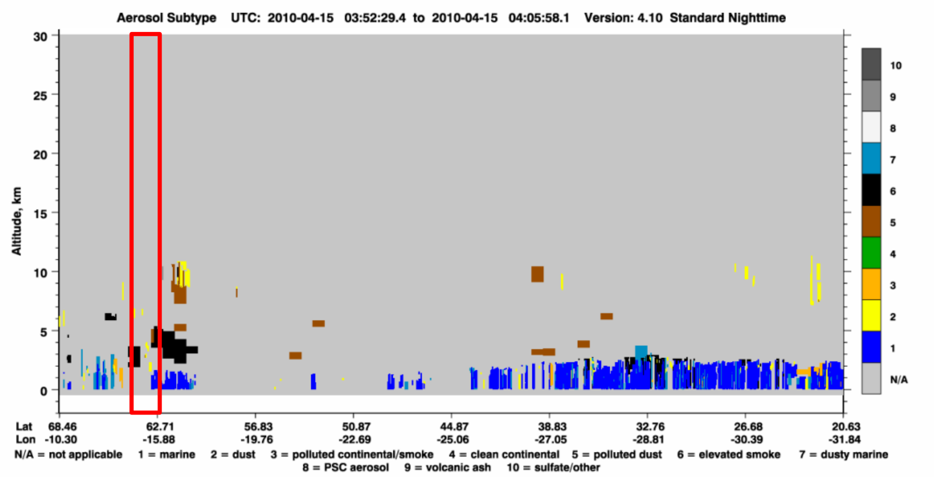

Figure 61: CALIOP overpass on the 15th of April 2010 from 03:52:29 to 04:05:58. The approximate part of the overpass within 100 km of GOME-2A overpasses is highlighted by the red box.

For the 16th of April 2010, CALIOP and GOME-2A overpasses were located over the European mainland where volcanic ash was detected (as discussed in several papers (e.g. Ansmann et al. 2010) (shown in Figure 62). Figure 63 shows the observed aerosol layer height from CALIOP and the AAH detected by GOME-2A in function of latitude.

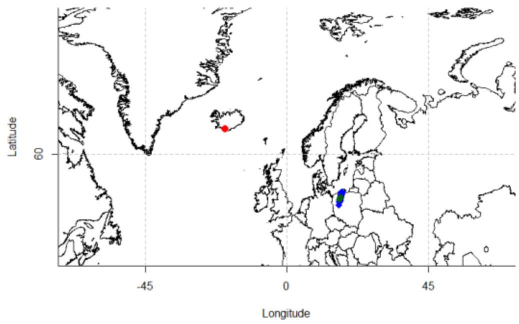

Figure 62: The location of the volcano is shown in red. The location of the CALIOP and GOME-2A overpasses on the 16th of April 2010 are shown in blue and green respectively.

CALIOP only observes aerosols from the polluted continental type (Figure 64). The maximum height of these CALIOP pixels varies between ~1 and ~2 km whereas the 'corresponding' GOME-2A pixels have an AAH around 1 km (Figure 63). In this case, the height difference is rather small and GOME-2A seems to agree with CALIOP. The time difference between GOME and CALIOP is around 7 h and the GOME-2A pixel closest to a CALIOP pixel can be found at a distance of 14 km.

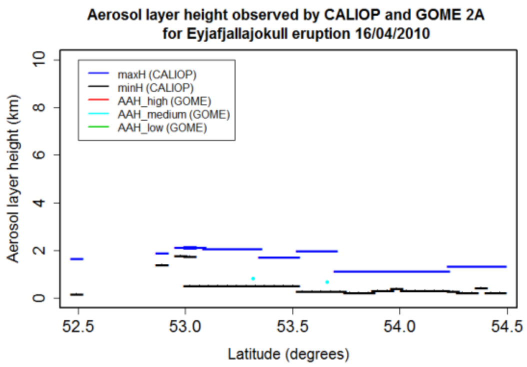

Figure 63: The aerosol layer height detected by CALIOP is shown in blue (maximum layer height) and black (minimum layer height) as a function of latitude for the 16th of April 2010. The GOME-2A AAH pixels located within 100 km of a CALIOP overpass pixel are presented in red (high reliability), cyan (medium reliability) and green (low reliability).

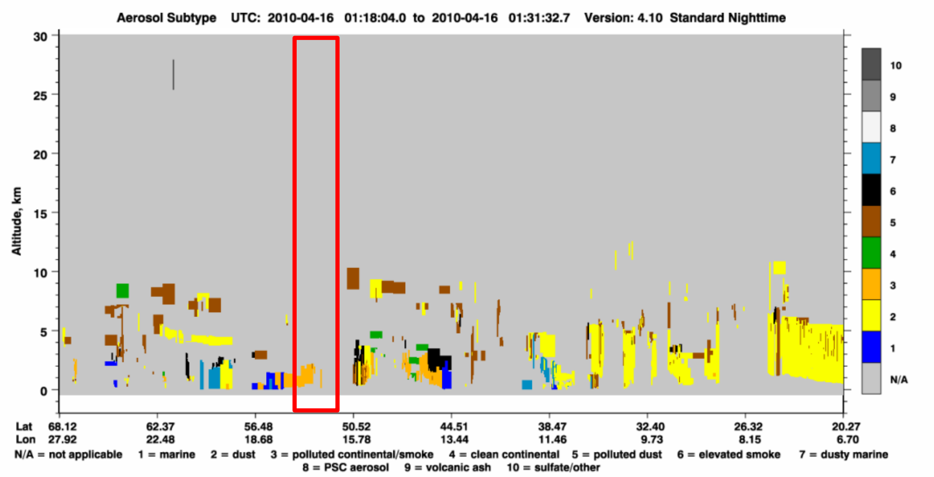

Figure 64: CALIOP overpass on the 16th of April 2010 from 01:18:04 to 01:31:32. The approximate part of the overpass within 100 km of GOME-2A overpasses is highlighted by the red box.

11.4 Grimsvotn

The eruption of the Grimsvotn volcano began at 16h30 on 21 May 2011 and at 20 h the eruption plume rose to an altitude over 20 km a.s.l[6]. The plume altitude fell to 15 km a.s.l. during the night but occasionally still rose to 20 a.s.l. Ash from the lower part of the eruption plume drifted S and at higher altitudes drifted E. During the morning of 22 May 2011 the plume rose to an altitude of 10-15 km a.s.l. Most of the plume drifted S, but lower parts traveled SW. During 22-23 May 2011 the ash plume rose to altitudes of 5-10 km a.s.l. and drifted S at lower altitudes and W at altitudes 8 km a.s.l. and higher. On 24 May 2011 the ash plume was estimated to be mostly below 5 km a.s.l. Satellite images showed the plume extending over 800 km from the eruption site towards the S and SE. Based on the AAI images, it was decided to study data from the 22nd until the 24th of May 2011.

11.4.1 GOME-2A

For the 22nd and 24th of May 2011, no GOME-2A and CALIOP data located within 100 km of each other were found near the volcano.

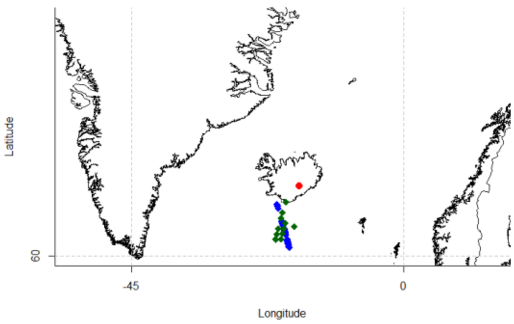

Figure 65: The location of the volcano is shown in red. The location of the CALIOP and GOME-2A overpasses on the 23rd of May 2011 are shown in blue and green respectively.

[6] https://volcano.si.edu/volcano.cfm?vn=373010#May2011

The GOME-2A and CALIOP overpasses near the volcano on the 23rd of May 2011 are shown in Figure 65. CALIOP detects clean marine, dust, polluted dust, smoke and sulfate aerosol layers (see Figure 66 and Table 23). All GOME-2A pixels have high or medium reliability. The AAH of GOME-2A agrees quite well with the height of the dust layer observed by CALIOP. The distance between the closest GOME-2A and CALIOP pixels is about 5 km and the difference in overpass time is ~1 h.

Table 23: Height of the aerosol layer detected by CALIOP for the different aerosol species compared to the AAH detected by GOME-2A for pixels located within 100 km distance for the 23rd of May 2011.

	CALIOP	**AAH**
Clean marine	0.1-0.3 km	1.0-1.4 km
Dust	0.1-7.2 km	1.0-3.7 km
Polluted dust	3.6-4.4 km	1.0-1.5 km
Smoke	3.2-3.3 km	1.3 km
Sulfate	8.8-9.3 km	1.2-1.3 km

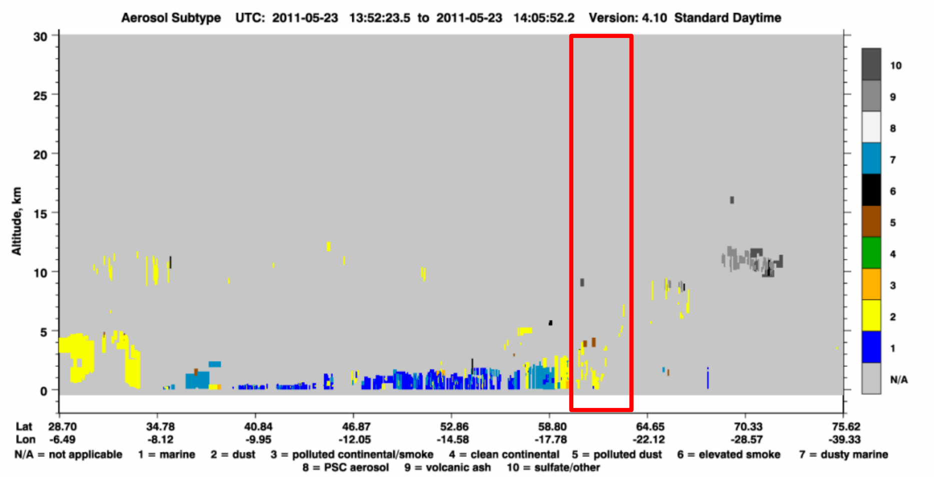

Figure 66: CALIOP overpass on the 23rd of April 2011 from 13:52:23 to 14:05:52. The approximate part of the overpass within 100 km of GOME-2A overpasses is highlighted by the red box.

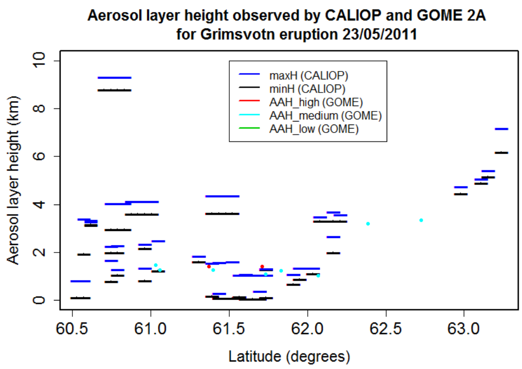

Figure 67: The aerosol layer height detected by CALIOP is shown in blue (maximum layer height) and black (minimum layer height) as a function of latitude for the 23rd of May 2011. The GOME-2A AAH pixels located within 100 km of a CALIOP overpass pixel are presented in red (high reliability), cyan (medium reliability) and green (low reliability).

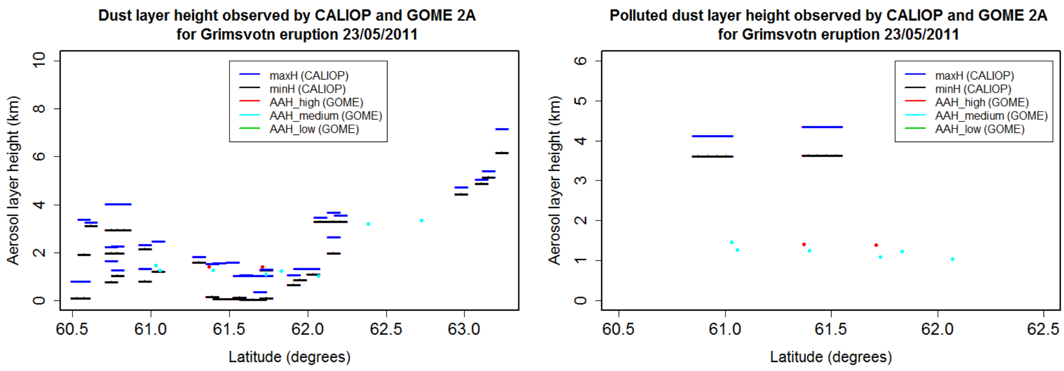

Figure 68: Detail of the dust (left) and polluted dust (right) layer detected by CALIOP. The maximum and minimum layer heights are shown in blue and black respectively as a function of latitude for the 23rd of May 2011. The GOME-2A AAH pixels located within 100 km of a CALIOP overpass pixel are presented in red (high reliability), cyan (medium reliability) and green (low reliability).

11.5 Kasatochi

On the 7th of August 2008, an ash plume at an altitude of at least 10.7 km a.s.l. was detected on satellite imagery drifting SSW[7]. Three major explosive eruptions produced ash plumes that rose to an altitude of 13.7 km a.s.l. Ash emissions became continuous on the 8th of August and an ash plume drifted for more than 950 km in a counterclockwise spiral at altitudes of about 9.1-13.7 km a.s.l. On the 9th of August ash plumes were detected on satellite imagery early in the day; clouds prevented views during the rest of the day. The ash plume from the third eruption on the 7th of August was seen on satellite imagery 1850 km ESE of the volcano and was elongated NE-SW over 1200 km. Data from GOME-2A from 7 to 9 August 2008 was studied.

11.5.1 GOME-2A

Only on the 8th of August, CALIOP and GOME-2A pixels were found near the location of the volcano (Figure 69).

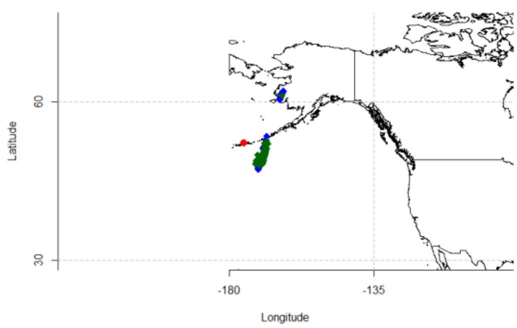

Figure 69: The location of the volcano is shown in red. The location of the CALIOP and GOME-2A overpasses for the 8th of August 2008 are shown in blue and green respectively.

CALIOP detected clean marine, dust, clean continental, polluted continental, polluted dust, smoke, dusty marine, volcanic ash and sulfate aerosol layers (Figure 70 and Table 24). The volcanic ash and sulfate layers were not detected by GOME-2A (Figure 72). The GOME-2A AAH values are

[7] http://volcano.si.edu/volcano.cfm?vn=311130#August2008

somewhere in between the lower and higher dust layers detected by CALIOP. The distance between the closest GOME-2A and CALIOP pixels is ~8 km and the difference in overpass time is around 8.5 h.

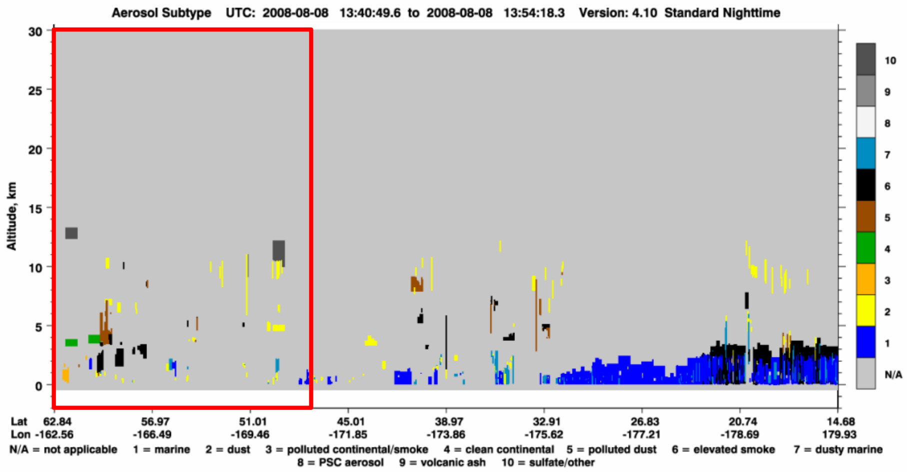

Figure 70: CALIOP overpass on the 8th of August 2008 from 13:40:49 to 13:54:18. The approximate part of the overpass within 100 km of GOME-2A overpasses is highlighted by the red box.

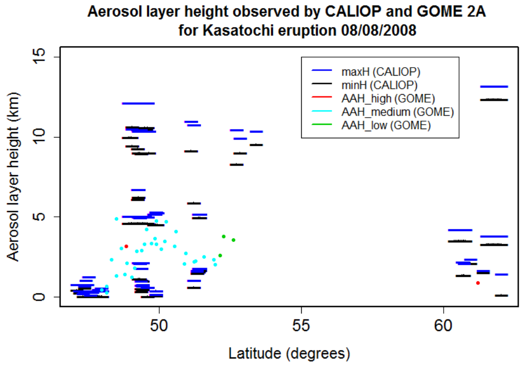

Figure 71: The aerosol layer height detected by CALIOP is shown in blue (maximum layer height) and black (minimum layer height) as a function of latitude for the 8th of August 2008. The GOME-2A AAH pixels located within 100 km of a CALIOP overpass pixel are presented in red (high reliability), cyan (medium reliability) and green (low reliability).

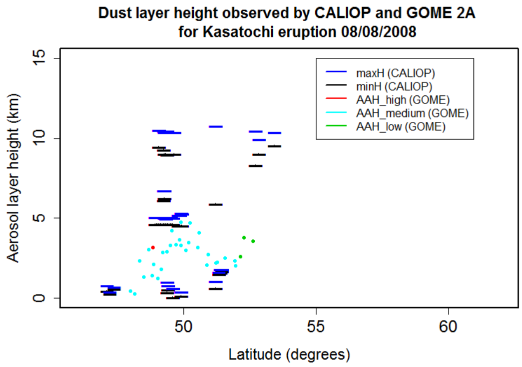

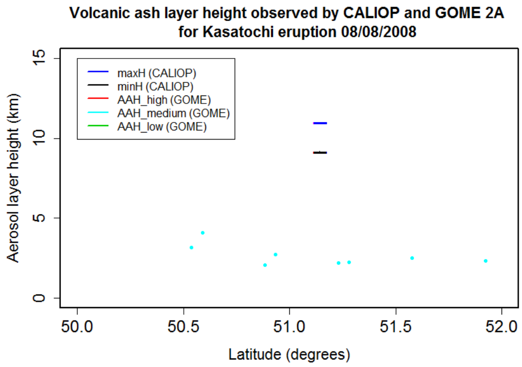

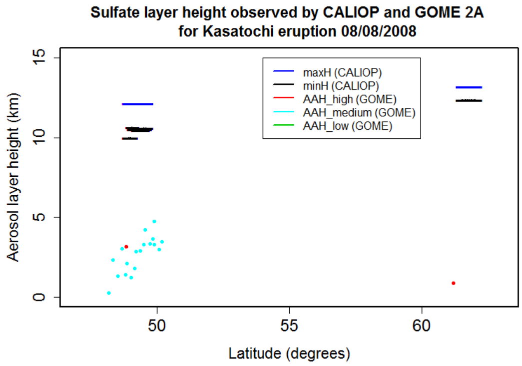

Figure 72: Detail of the dust (upper left),volcanic ash (upper right) and sulfate (lower left) layer detected by CALIOP. The maximum and minimum layer heights are shown in blue and black respectively as a function of latitude for the 23rd of May 2011. The GOME-2A AAH pixels located within 100 km of a CALIOP overpass pixel are presented in red (high reliability), cyan (medium reliability) and green (low reliability).

Table 24: Height of the aerosol layer detected by CALIOP for the different aerosol species compared to the AAH detected by GOME-2A for pixels located within 100 km distance for the 8th of August 2008.

	CALIOP	AAH
Clean marine	0.0-2.2 km	0.3-4.9 km
Dust	0.0-10.8 km	0.3-4.7 km
Clean continental	0.1-2.4 km	0.9 km
Polluted continental	3.3-4.2 km	0.9 km
Polluted dust	1.5-1.7 km	0.9 km
Smoke	5.0-5.2 km	2.1-3.2 km
Dusty marine	0.1-2.1 km	1.2-4.7 km
Volcanic ash	9.1-11 km	2.1-4.1 km
Sulfate	10.0-13.2 km	0.3-4.7 km

11.6 Krakatau

It was reported that seismicity at Anak Krakatau increased on the 17th of February 2017, with earthquakes indicating emissions slowing transforming into continuous tremor[8]. At 19h04, Strombolian explosions ejected incandescent material 200 m high. Data from the 19th to 24th of February 2017 were studied.

11.6.1 GOME-2A

GOME-2A did not have any overpasses within 100 km of CALIOP near the volcano for the period from 19-24 February 2017.

11.6.2 GOME-2B

GOME-2B and CALIOP have overpasses within 100 km near the volcano on the 22nd of February 2017 (Figure 73). CALIOP observed clean marine, dust, clean continental, polluted continental and smoke aerosol layers (Figure 74 and Table 25) but no specific volcanic aerosol types. All GOME-2B AAH pixels have either medium or low reliability level and the AAH is between 0 and 5.6 km (Figure 75). The distance between the closest GOME-2A and CALIOP pixels is ~3 km and the difference in

[8] http://volcano.si.edu/volcano.cfm?vn=262000&vtab=Weekly#February2017

overpass time is either ~8.5 h or ~14.5 h. The height of the dust layer (which might actually be volcanic ash) is shown in Figure 76. Based on the results, we assume that the GOME-2B and CALIOP overpasses are not within the plume of the volcano.

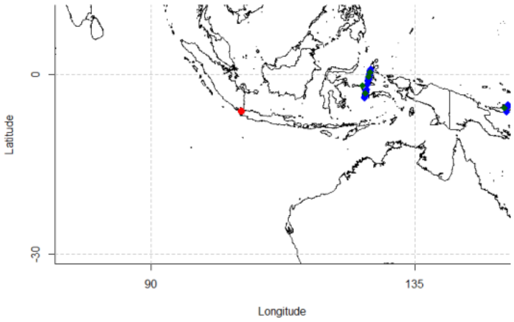

Figure 73: The location of the volcano is shown in red. The location of the CALIOP and GOME-2B overpasses for the 22nd of February 2017 are shown in blue and green respectively.

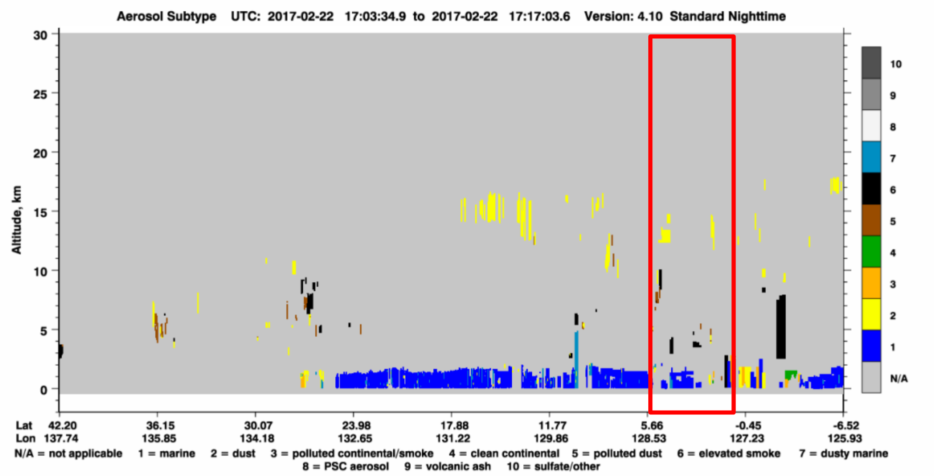

Figure 74: CALIOP overpass on the 22nd of February 2017 from 17:03:34 to 17:17:03. The approximate part of the overpass within 100 km of GOME-2B overpasses is highlighted by the red box.

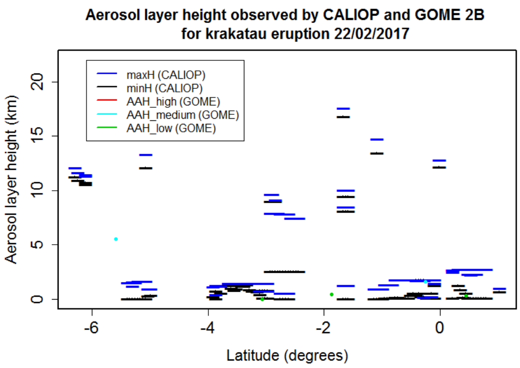

Figure 75: The aerosol layer height detected by CALIOP is shown in blue (maximum layer height) and black (minimum layer height) as a function of latitude for the 22nd of February 2017. The GOME-2B AAH pixels located within 100 km of a CALIOP overpass pixel are presented in red (high reliability), cyan (medium reliability) and green (low reliability).

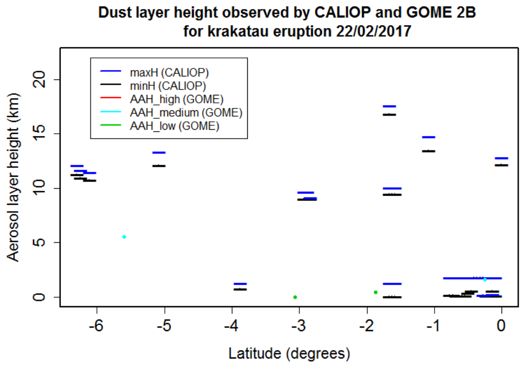

Figure 76: Detail of the dust layer detected by CALIOP. The maximum and minimum layer heights are shown in blue and black respectively as a function of latitude for the 22nd of February 2017. The GOME-2B AAH pixels located within 100 km of a CALIOP overpass pixel are presented in red (high reliability), cyan (medium reliability) and green (low reliability).

Table 25: Height of the aerosol layer detected by CALIOP for the different aerosol species compared to the AAH detected by GOME-2B for pixels located within 100 km distance for the 23nd of February 2017.

	CALIOP	AAH
Clean marine	0.1-2.3 km	0.0-5.6 km
Dust	0.1-17.6 km	0.0-5.6 km
Clean continental	0.1-2.8 km	0.0-1.6 km
Polluted continental	0.7-1.5 km	0.0 km
Polluted dust	0.7-11.4 km	0.3-5.6 km
Smoke	0.1-8.5 km	0.0-1.6 km

11.7 Nishinoshima

The Japan Coast Guard reported that visual observations of Nishinoshima from an aircraft during the afternoon of 11 July confirmed that the eruption was ongoing. Based on a pilot observation the Tokyo Volcanic Ash Advisory Center (VAAC) reported that on 18 July an ash plume rose to 3 km a.s.l.[9] Data from 13 and 14 July 2018 have been studied for both GOME-2A and GOME-2B.

11.7.1 GOME-2A

On the 13th of July 2018, overpasses from both GOME-2A and CALIOP were found near the volcano (

Figure 77).

[9] http://volcano.si.edu/volcano.cfm?vn=284096#June2018

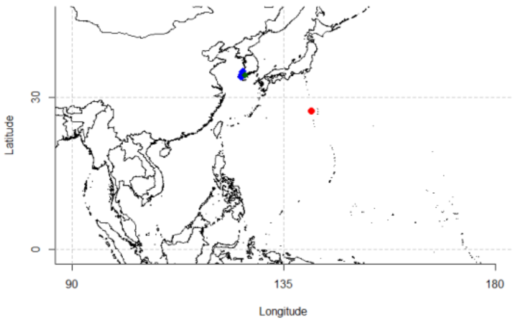

Figure 77: The location of the volcano is shown in red. The location of the CALIOP and GOME-2A overpasses for the 13th of July 2018 are shown in blue and green respectively.

CALIOP detected clean marine, clean continental, polluted continental and polluted dust (Figure 78 and Table 26). No specific volcanic species were detected and it seems as if the CALIOP and GOME-2A overpasses are not in the plume of the volcano. The observed AAH agrees with the height of the aerosol layers detected by CALIOP (Figure 79). The distance between the closest GOME-2A and CALIOP pixels is ~65 km and the difference in overpass time is ~15 h.

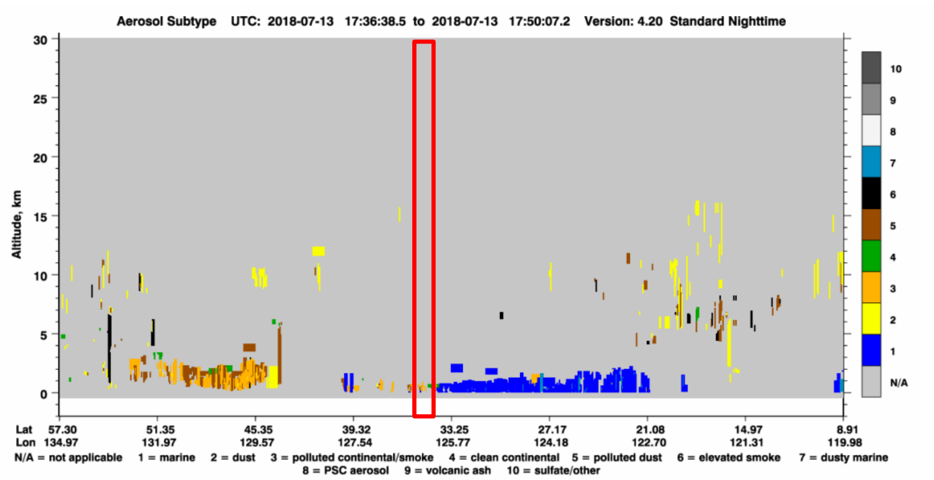

Figure 78: CALIOP overpass on the 13th of July 2018 from 17:36:38 to 17:50:07. The approximate part of the overpass within 100 km of GOME-2A overpasses is highlighted by the red box.

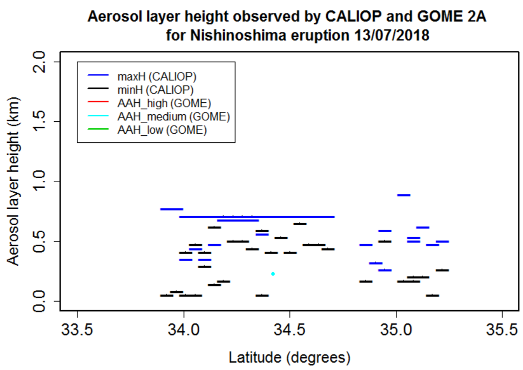

Figure 79: The aerosol layer height detected by CALIOP is shown in blue (maximum layer height) and black (minimum layer height) as a function of latitude for the 13th of July 2018. The GOME-2A AAH pixels located within 100 km of a CALIOP overpass pixel are presented in red (high reliability), cyan (medium reliability) and green (low reliability).

Table 26: Height of the aerosol layer detected by CALIOP for the different aerosol species compared to the AAH detected by GOME-2A for pixels located within 100 km distance for the 13th of July 2018.

	CALIOP	**AAH**

Clean marine	0.1-0.8 km	0.2 km
Polluted continental	0.2-0.9 km	0.2 km
Clean continental	0.4-0.7 km	0.2 km
Polluted dust	0.2-0.5 km	0.2 km

On the 14th of July 2018, overpasses from both GOME-2A and CALIOP were found further away from the volcano (Figure 80). CALIOP detected dust, polluted dust and smoke (Figure 81 and Table 27). No specific volcanic species were detected and it seems as if the CALIOP and GOME-2A overpasses are not in the plume of the volcano. The observed AAH agrees with the height of the aerosol layers detected by CALIOP (Figure 82). The distance between the closest GOME-2A and CALIOP pixels is ~82 km and the difference in overpass time is 2 h.

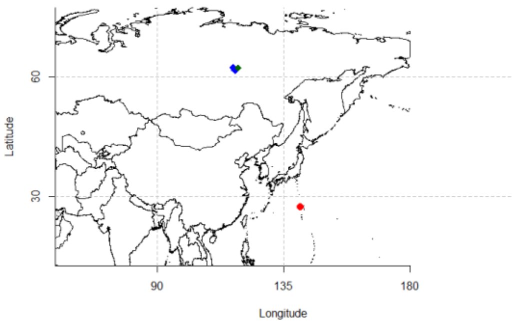

Figure 80: The location of the volcano is shown in red. The location of the CALIOP and GOME-2A overpasses for the 14th of July 2018 are shown in blue and green respectively.

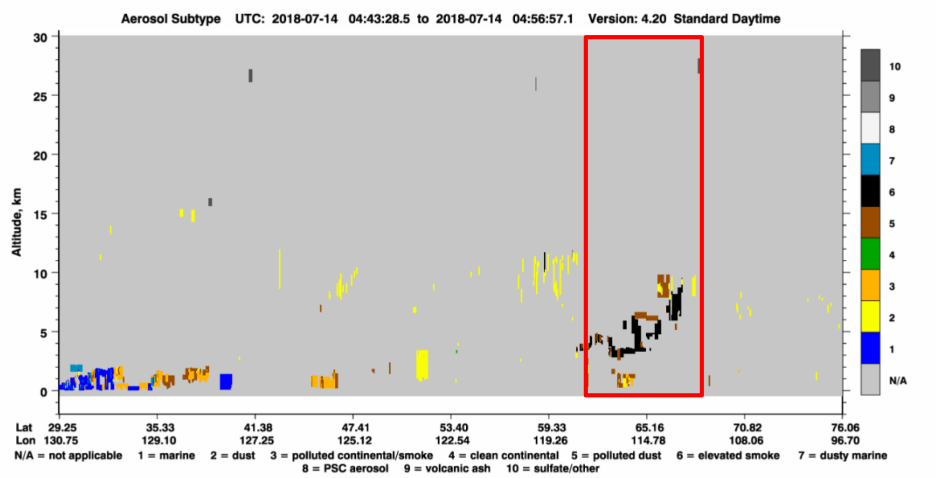

Figure 81: CALIOP overpass on the 14th of July 2018 from 04:43:28 to 04:56:57. The approximate part of the overpass within 100 km of GOME-2A overpasses is highlighted by the red box.

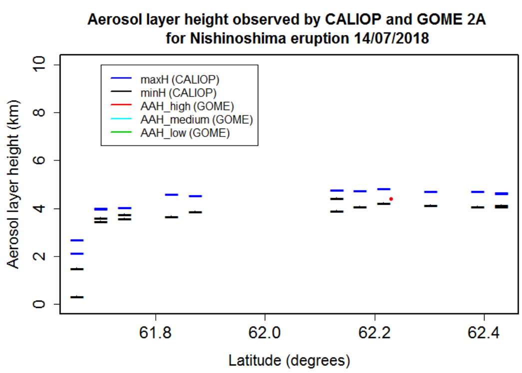

Figure 82: The aerosol layer height detected by CALIOP is shown in blue (maximum layer height) and black (minimum layer height) as a function of latitude for the 14th of July 2018. The GOME-2A AAH pixels located within 100 km of a CALIOP overpass pixel are presented in red (high reliability), cyan (medium reliability) and green (low reliability).

Table 27: Height of the aerosol layer detected by CALIOP for the different aerosol species compared to the AAH detected by GOME-2A for pixels located within 100 km distance for the 14th of July 2018.

	CALIOP	**AAH**
Dust	1.5-4 km	4.4 km
Polluted dust	0.3-4.8 km	4.4 km
Smoke	3.6-4.8 km	4.4 km

11.7.2 GOME-2B

On the 13th of July 2018, overpasses from both GOME-2B and CALIOP were found near the volcano (Figure 83). CALIOP detected clean marine, clean continental, polluted continental and polluted dust (Figure 78). No specific volcanic species were detected and it seems as if the CALIOP and GOME-2B overpasses are not in the plume of the volcano. The observed AAH agrees with the height of the aerosol layers detected by CALIOP (Figure 84 and Table 28). The distance between the closest GOME-2B and CALIOP pixels is ~65 km and the difference in overpass time is 15 h.

Table 28: Height of the aerosol layer detected by CALIOP for the different aerosol species compared to the AAH detected by GOME-2A for pixels located within 100 km distance for the 13th of July 2018.

	CALIOP	**AAH**
Clean marine	0.1-0.8 km	0.2 km
Polluted continental	0.2-0.9 km	0.2 km
Clean continental	0.4-0.7 km	0.2 km
Polluted dust	0.2-0.5 km	0.2 km

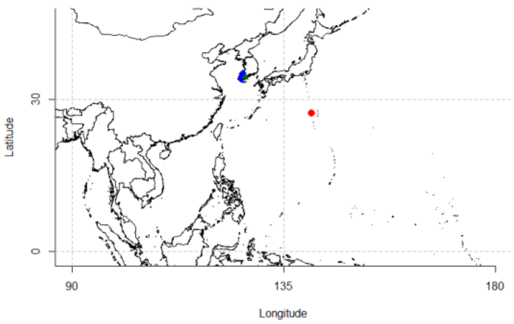

Figure 83: The location of the volcano is shown in red. The location of the CALIOP and GOME-2B overpasses for the 13th of July 2018 are shown in blue and green respectively.

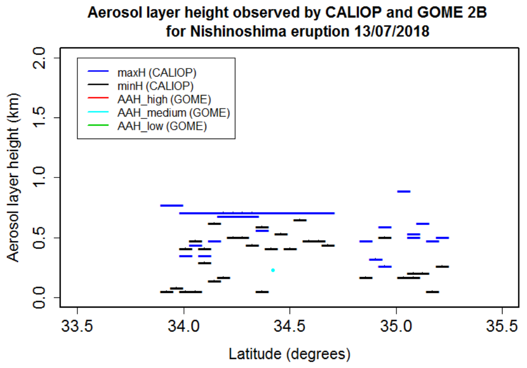

Figure 84: The aerosol layer height detected by CALIOP is shown in blue (maximum layer height) and black (minimum layer height) as a function of latitude for the 13th of July 2018. The GOME-2B AAH pixels located within 100 km of a CALIOP overpass pixel are presented in red (high reliability), cyan (medium reliability) and green (low reliability).

On the 14th of July 2018, overpasses from both GOME-2B and CALIOP were found further away from the volcano (Figure 85). CALIOP detected dust, polluted continental, polluted dust and smoke (Figure 81 and

The aerosol layer height detected by CALIOP is shown in blue (maximum layer height) and black (minimum layer height) as a function of latitude for the 14th of July 2018. The GOME-2B AAH pixels located within 100 km of a CALIOP overpass pixel are presented in red (high reliability), cyan (medium reliability) and green (low reliability).

Table 29). The satellite overpasses are most likely not in the plume of the volcano which explains why no volcanic aerosol layers are observed. According to Figure 86, the AAH agrees quite well with the layer height detected by CALIOP. The distance between the closest GOME-2B and CALIOP pixels is ~12 km and the difference in overpass time is 1 or 7 h.

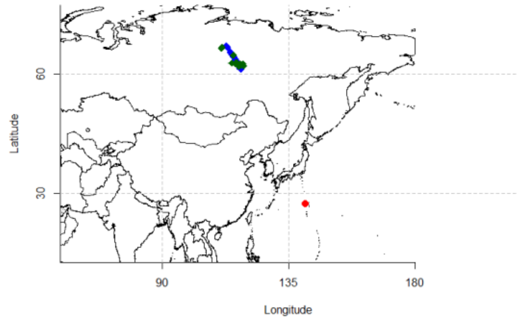

Figure 85: The location of the volcano is shown in red. The location of the CALIOP and GOME-2B overpasses for the 14th of July 2018 are shown in blue and green respectively.

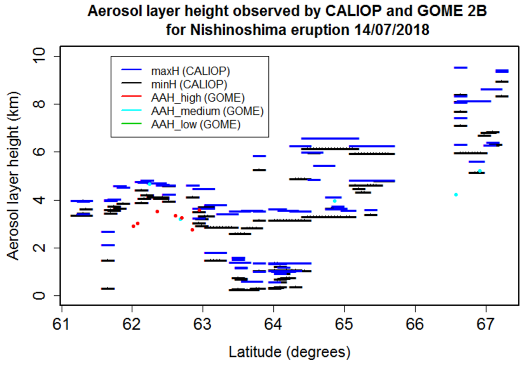

Figure 86: The aerosol layer height detected by CALIOP is shown in blue (maximum layer height) and black (minimum layer height) as a function of latitude for the 14th of July 2018. The GOME-2B AAH pixels located within 100 km of a CALIOP overpass pixel are presented in red (high reliability), cyan (medium reliability) and green (low reliability).

Table 29: Height of the aerosol layer detected by CALIOP for the different aerosol species compared to the AAH detected by GOME-2B for pixels located within 100 km distance for the 14th of July 2018.

	CALIOP	AAH
Dust	0.3-9.6 km	2.9-5.2 km
Polluted continental	0.3-1.5 km	3.3-4.0 km
Polluted dust	0.3-6.6 km	2.7-5.2 km
Smoke	2.8-9.4 km	2.7-5.2 km

11.8 Paluweh

According to news articles, an explosion from Paluweh occurred at 23h00 on the 2nd of February 2013[10] and ashfall was reported during 2-3 February. Based on analyses of satellite imagery, wind data, and pilot reports, the Darwin VAAC reported that on 3 February 2013 ash plumes from Paluweh rose to altitudes of 13.1-13.7 km a.s.l. and drifted 325-590 km SE, S, and SW. Elevated levels of sulfur dioxide were also detected. The next day ash plumes at an altitude of 7.6 km a.s.l. were observed. Based on analyses of satellite imagery and wind data, the Darwin VAAC reported that during 8-12 February ash plumes from Paluweh rose to altitudes of 2.1-3.7 km a.s.l. and drifted 35-110 km NW, NNW, and N. Data from GOME-2A and GOME-2B were studied from the 2nd until the 11th of February 2013.

11.8.1 GOME-2A

On the 3rd of February 2013, GOME-2A and CALIOP detected pixels 'near' the volcano (Figure 87). CALIOP detected clean marine, dust, polluted dust and smoke (Figure 88 and Table 30). Only one GOME-2A pixel was within 100 km of the CALIOP overpass. The AAH of this pixel was equal to 0.7 km and it only has a medium reliability level. The height does agree with the surrounding CALIOP clean marine layer (Figure 89). The time difference between overpasses is ~9 h.

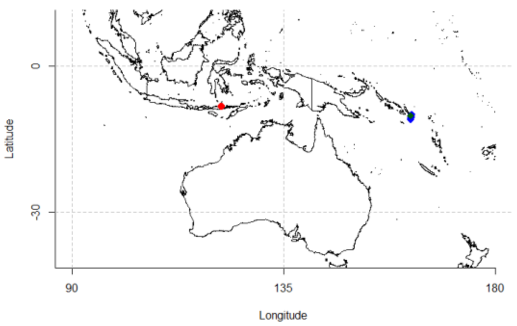

Figure 87: The location of the volcano is shown in red. The location of the CALIOP and GOME-2A overpasses for the 3rd of February 2013 are shown in blue and green respectively.

Table 30: Height of the aerosol layer detected by CALIOP for the different aerosol species compared to the AAH detected by GOME-2A for pixels located within 100 km distance for the 3rd of February 2013.

[10] https://volcano.si.edu/volcano.cfm?vn=264150#February2013

	CALIOP	AAH
Clean marine	0.1-2.6 km	0.7 km
Dust	6.9-17.0 km	0.7 km
Polluted dust	6.4-9.5 km	0.7 km
Smoke	7.6-9.5 km	0.7 km

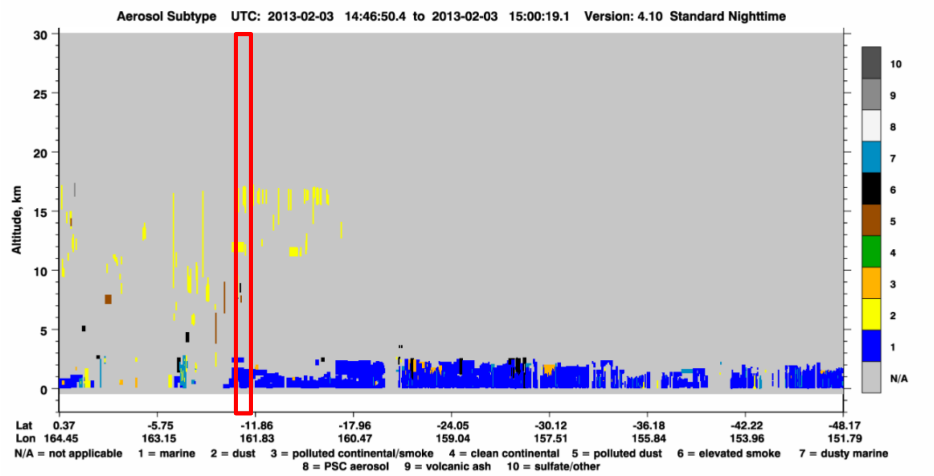

Figure 88: CALIOP overpass on the 3rd of February 2013 from 14:46:50 to 15:00:19. The approximate part of the overpass within 100 km of GOME-2A overpasses is highlighted by the red box.

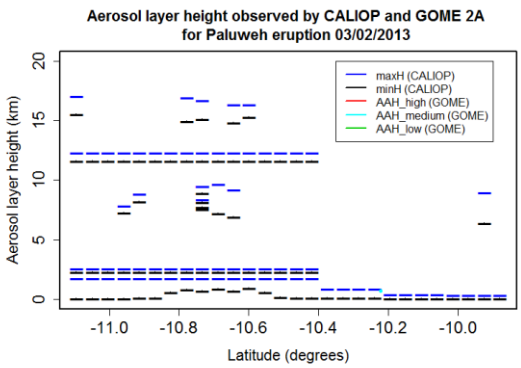

Figure 89: The aerosol layer height detected by CALIOP is shown in blue (maximum layer height) and black (minimum layer height) as a function of latitude for the 3rd of February 2013. The GOME-2A AAH pixels located within 100 km of a CALIOP overpass pixel are presented in red (high reliability), cyan (medium reliability) and green (low reliability).

On the 4th of February 2013, GOME-2A and CALIOP also detected pixels 'near' the volcano (Figure 90). CALIOP detected polluted continental and dusty marine (Figure 91 and Table 31). Again, there is only one GOME-2A pixel within 100 km of the CALIOP overpass. The low reliability AAH is equal to 0.2 km and agrees with the layer heights detected by CALIOP (Figure 92). The time difference between overpasses is ~3.5 h.

Table 31: Height of the aerosol layer detected by CALIOP for the different aerosol species compared to the AAH detected by GOME-2A for pixels located within 100 km distance for the 4th of February 2013.

	CALIOP	AAH
Polluted continental	0.1-0.4 km	0.2 km
Dusty marine	0.1-0.4 km	0.2 km

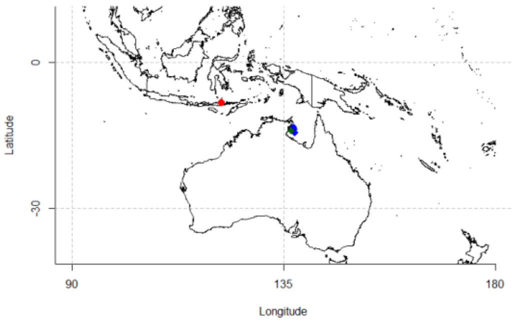

Figure 90: The location of the volcano is shown in red. The location of the CALIOP and GOME-2A overpasses for the 4th of February 2013 are shown in blue and green respectively.

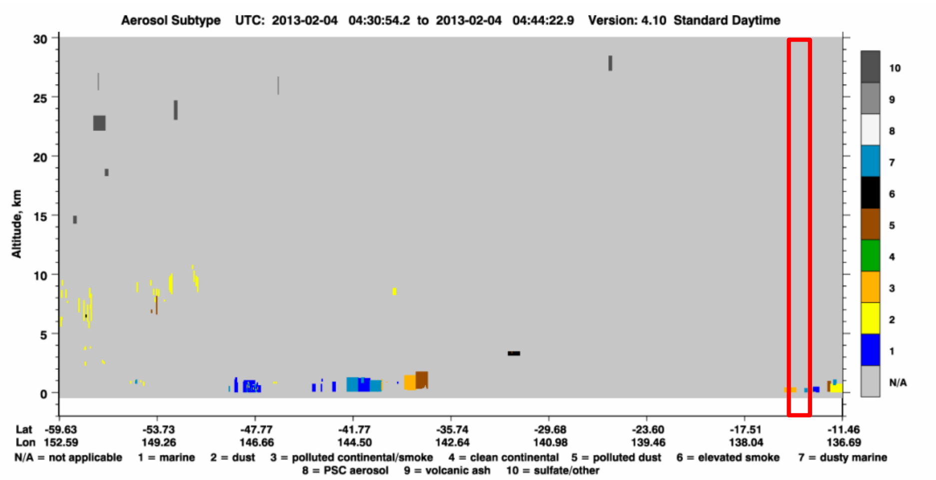

Figure 91: CALIOP overpass on the 4th of February 2013 from 04:30:54 to 04:44:22. The approximate part of the overpass within 100 km of GOME-2A overpasses is highlighted by the red box.

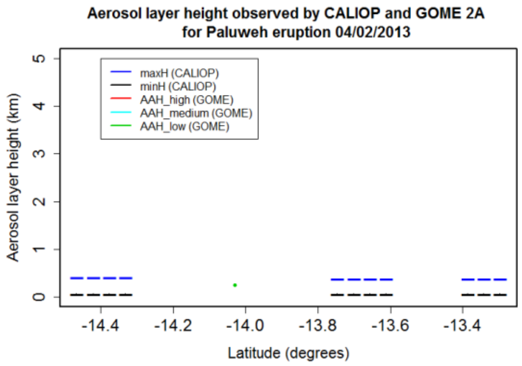

Figure 92: The aerosol layer height detected by CALIOP is shown in blue (maximum layer height) and black (minimum layer height) as a function of latitude for the 4th of February 2013. The GOME-2A AAH pixels located within 100 km of a CALIOP overpass pixel are presented in red (high reliability), cyan (medium reliability) and green (low reliability).

On the 8th of February 2013, GOME-2A and CALIOP also detected pixels 'near' the volcano (Figure 93). CALIOP detected clean marine, dust, clean and polluted continental and smoke (Figure 94 and Table 32). Only two GOME-2A pixels are located within 100 km of the CALIOP overpasses. Their AAH is 0.2 and 0.4 km and their reliability level is low and medium respectively (Figure 95). The AAH of both GOME-2A pixels agrees with the height of the clean marine layer detected by CALIOP (Figure 96). The time difference between overpasses is ~15 h.

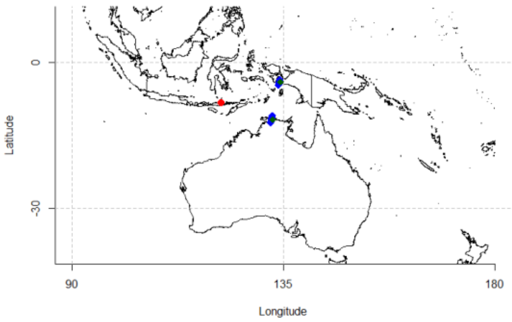

Figure 93: The location of the volcano is shown in red. The location of the CALIOP and GOME-2A overpasses for the 8th of February 2013 are shown in blue and green respectively.

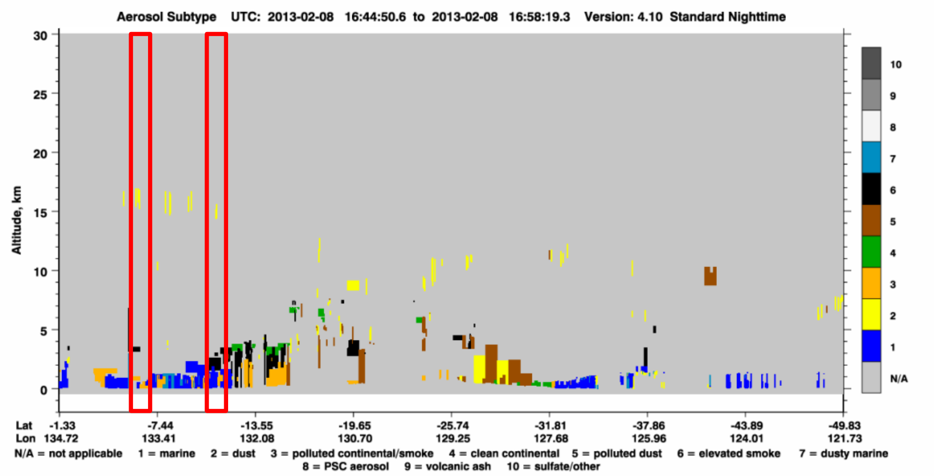

Figure 94: CALIOP overpass on the 8th of February 2013 from 16:44:50 to 16:58:19. The approximate part of the overpass within 100 km of GOME-2A overpasses is highlighted by the red box.

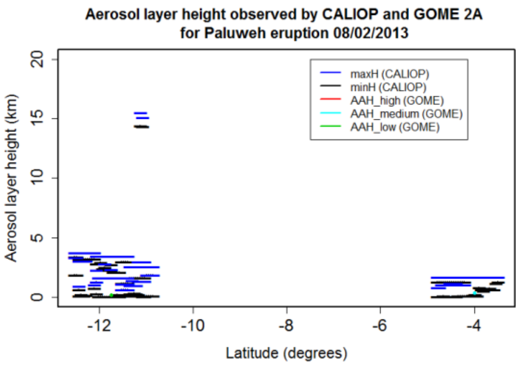

Figure 95: The aerosol layer height detected by CALIOP is shown in blue (maximum layer height) and black (minimum layer height) as a function of latitude for the 8th of February 2013. The GOME-2A AAH pixels located within 100 km of a CALIOP overpass pixel are presented in red (high reliability), cyan (medium reliability) and green (low reliability).

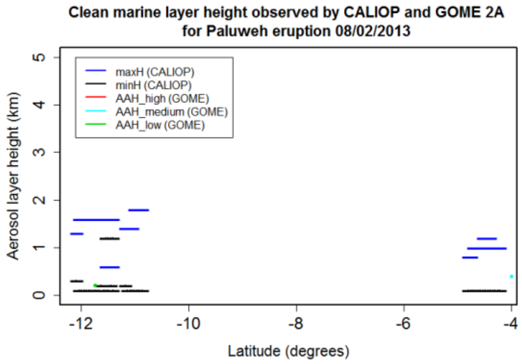

Figure 96: Detail of the clean marine layer detected by CALIOP. The maximum and minimum layer heights are shown in blue and black respectively as a function of latitude for the 8th of February 2013. The GOME-2A AAH pixels located within 100 km of a CALIOP overpass pixel are presented in red (high reliability), cyan (medium reliability) and green (low reliability).

Table 32: Height of the aerosol layer detected by CALIOP for the different aerosol species compared to the AAH detected by GOME-2A for pixels located within 100 km distance for the 8th of February 2013.

	CALIOP	AAH
Clean marine	0.1-1.8 km	0.2-0.4 km
Dust	0.8-15.5 km	0.2 km
Polluted continental	0.1-1.7 km	0.2-0.4 km
Clean continental	3.2-3.8 km	0.2 km
Smoke	0.1-3.5 km	0.2 km

On the 11th of February 2013, GOME-2A and CALIOP also detected pixels 'near' the volcano (Figure 97). CALIOP detected clean marine, dust, polluted continental, smoke and dusty marine aerosols (Figure 98 and Table 33). Only two GOME-2A pixels are located within 100 km of the CALIOP overpasses. Their AAH is 0.8 and 0.9 km and their reliability level is low (Figure 99). The AAH of both GOME-2A pixels agrees with the height of the clean marine layer detected by CALIOP (Figure 100). The time difference between overpasses is ~14.5 h.

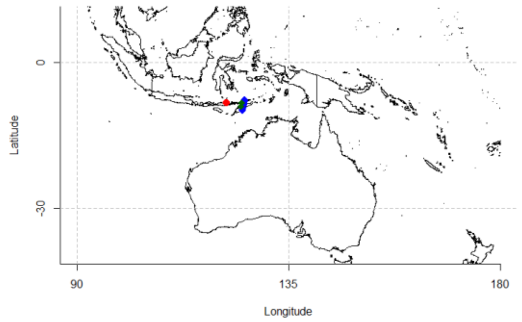

Figure 97: The location of the volcano is shown in red. The location of the CALIOP and GOME-2A overpasses for the 11th of February 2013 are shown in blue and green respectively.

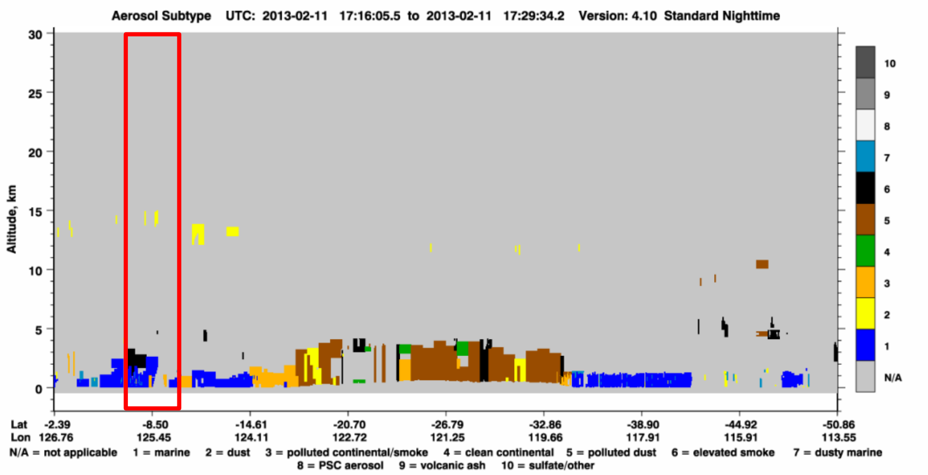

Figure 98: CALIOP overpass on the 11th of February 2013 from 17:16:05 to 17:29:34. The approximate part of the overpass within 100 km of GOME-2A overpasses is highlighted by the red box.

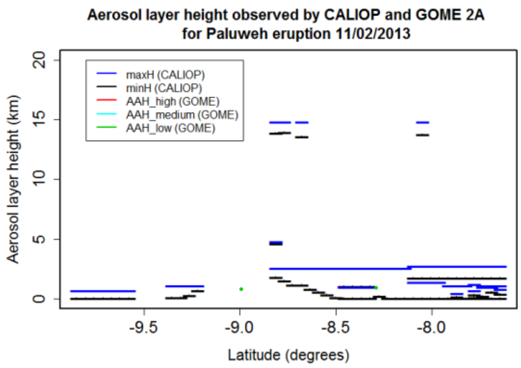

Figure 99: The aerosol layer height detected by CALIOP is shown in blue (maximum layer height) and black (minimum layer height) as a function of latitude for the 11th of February 2013. The GOME-2A AAH pixels located within 100 km of a CALIOP overpass pixel are presented in red (high reliability), cyan (medium reliability) and green (low reliability).

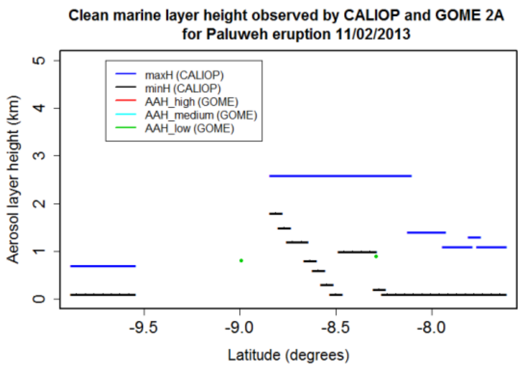

Figure 100: Detail of the clean marine layer detected by CALIOP. The maximum and minimum layer heights are shown in blue and black respectively as a function of latitude for the 11th of February 2013. The GOME-2A AAH pixels located within 100 km of a CALIOP overpass pixel are presented in red (high reliability), cyan (medium reliability) and green (low reliability).

Table 33: Height of the aerosol layer detected by CALIOP for the different aerosol species compared to the AAH detected by GOME-2A for pixels located within 100 km distance for the 11th of February 2013.

	CALIOP	**AAH**
Clean marine	0.1-2.6 km	0.8-0.9 km
Dust	13.6-14.8 km	0.8-0.9 km
Polluted continental	0.1-1.1 km	0.8-0.9 km
Smoke	1.7-4.8 km	0.8-0.9 km

Dusty marine	0.1-1.3 km	0.9 km

11.8.2 GOME-2B

On the 9th of February 2013, GOME-2B and CALIOP detected pixels ‘near’ the volcano (*Figure 101*). CALIOP detected clean marine, dust, polluted continental, polluted dust and smoke (*Figure 102* and *Table 34*). Several GOME-2B pixels are located within 100 km of the CALIOP overpass (*Figure 103*). The AAH of the pixels locally agrees with the height of either the clean marine, dust or smoke layers (*Figure 104*). The time difference between overpasses is either 15 (for the pixels around 100°E) or 21 h (for the pixels around 155°E).

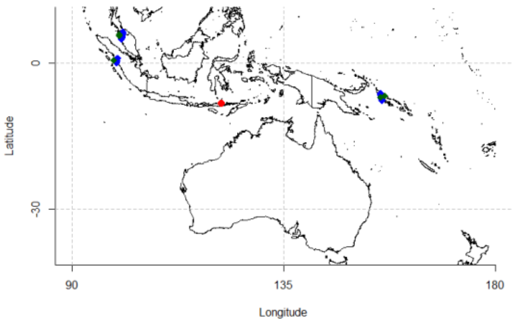

Figure 101: The location of the volcano is shown in red. The location of the CALIOP and GOME-2B overpasses for the 9th of February 2013 are shown in blue and green respectively.

Table 34: Height of the aerosol layer detected by CALIOP for the different aerosol species compared to the AAH detected by GOME-2B for pixels located within 100 km distance for the 9th of February 2013.

	CALIOP	**AAH**
Clean marine	0.1-1.0 km	0.3-0.4 km
Dust	1.4-14.6 km	0.3-5.8 km
Polluted continental	0.1-1.8 km	0.4-8.7 km
Polluted dust	0.2-12.5 km	0.3-8.7 km
Smoke	6.1-14.7 km	0.4-5.8 km

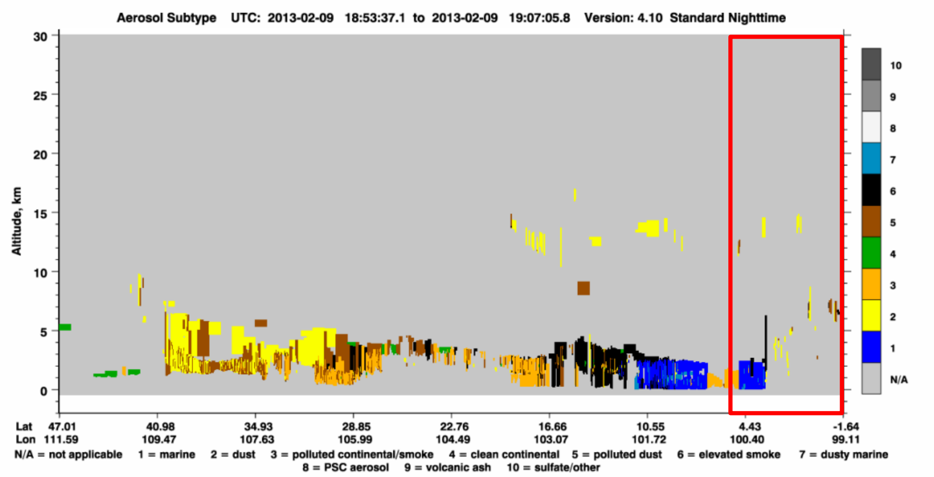

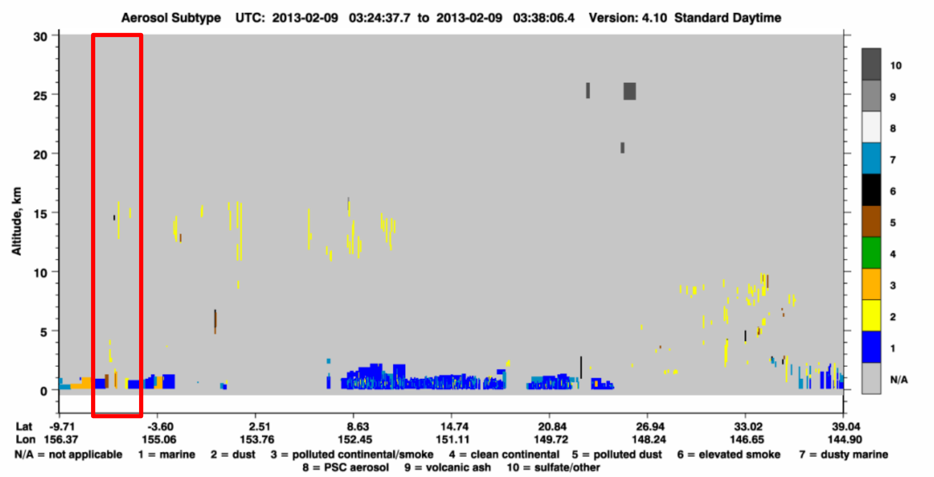

Figure 102: CALIOP overpass on the 9th of February 2013 from 18:53:37 to 19:07:05 (upper panel) and from 03:24:37 to 03:38:06 (lower panel). The approximate part of the overpasses within 100 km of GOME-2B overpasses are highlighted by the red boxes.

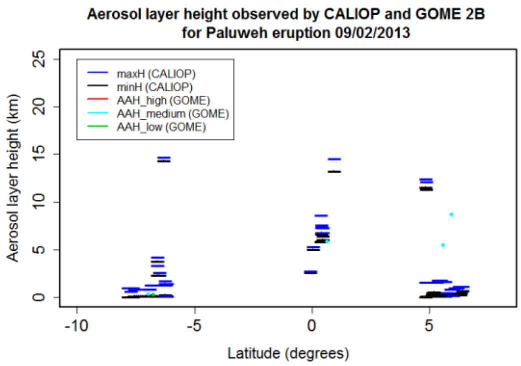

Figure 103: The aerosol layer height detected by CALIOP is shown in blue (maximum layer height) and black (minimum layer height) as a function of latitude for the 9th of February 2013. The GOME-2B AAH pixels located within 100 km of a CALIOP overpass pixel are presented in red (high reliability), cyan (medium reliability) and green (low reliability).

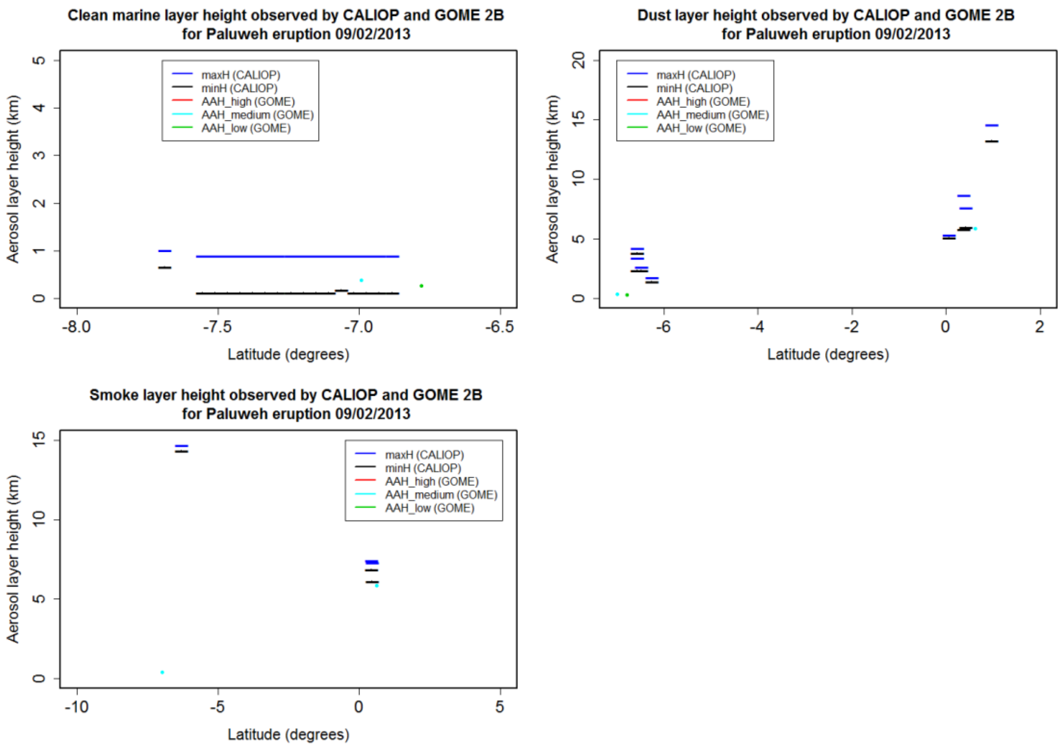

Figure 104: Detail of the clean marine (upper left), dust (upper right) and smoke (lower left) layer detected by CALIOP. The maximum and minimum layer heights are shown in blue and black respectively as a function of latitude for the 9th of February 2013. The GOME-2B AAH pixels located within 100 km of a CALIOP overpass pixel are presented in red (high reliability), cyan (medium reliability) and green (low reliability).

On the 10th of February 2013, GOME-2B and CALIOP detected pixels ‘near’ the volcano (*Figure 105*). CALIOP detected clean marine, dust, polluted continental and dusty marine (*Figure 106* and *Table 35*). Several GOME-2B pixels are located within 100 km of the CALIOP overpass (*Figure 107*). The AAH of the pixels locally agrees with the height of either the clean marine or dust layers (*Figure 108*). There is a time difference of 3 (for the pixels around 95°E) or 8 h (for the pixels around 160°E) between GOME-2A and CALIOP overpasses.

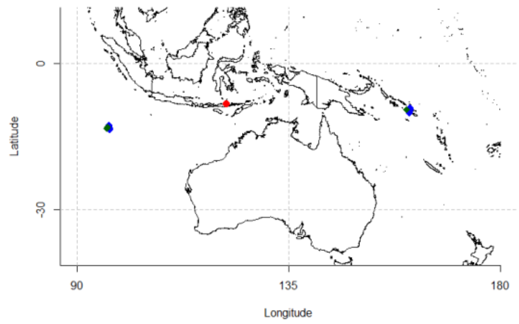

Figure 105: The location of the volcano is shown in red. The location of the CALIOP and GOME-2B overpasses for the 10th of February 2013 are shown in blue and green respectively.

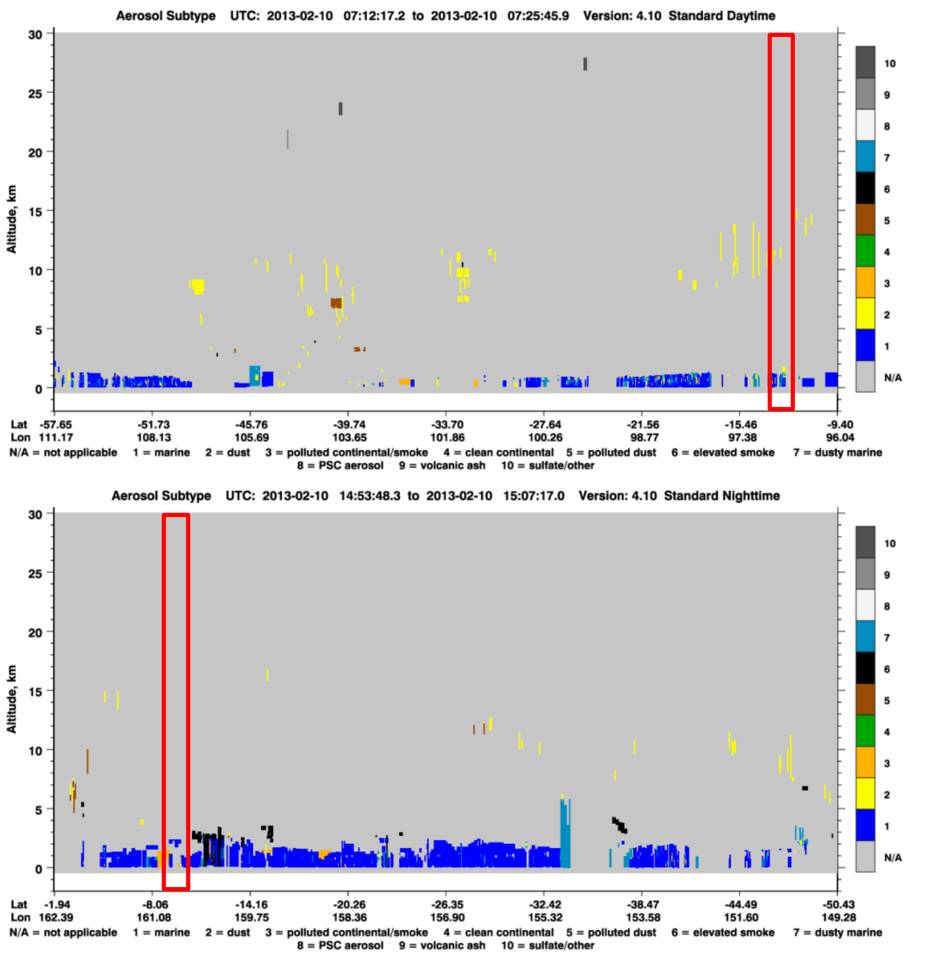

Figure 106: CALIOP overpass on the 10th of February 2013 from 07:12:17 to 07:25:45 (upper panel) and from 14:53:48 to 15:07:17 (lower panel). The approximate part of the overpasses within 100 km of GOME-2B overpasses are highlighted by the red boxes.

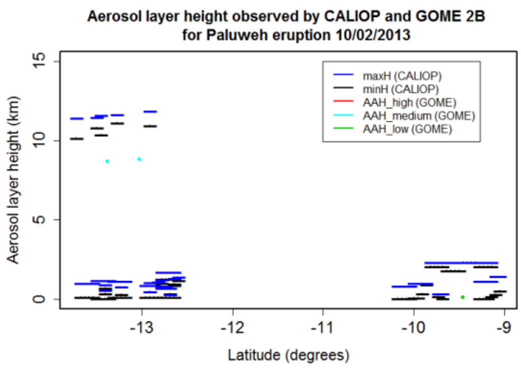

Figure 107: The aerosol layer height detected by CALIOP is shown in blue (maximum layer height) and black (minimum layer height) as a function of latitude for the 10th of February 2013. The GOME-2B AAH pixels located within 100 km of a CALIOP overpass pixel are presented in red (high reliability), cyan (medium reliability) and green (low reliability).

Table 35: Height of the aerosol layer detected by CALIOP for the different aerosol species compared to the AAH detected by GOME-2B for pixels located within 100 km distance for the 10th of February 2013.

	CALIOP	**AAH**
Clean marine	0.1-2.3 km	0.1-8.8 km
Dust	0.3-11.9 km	8.7-8.8 km
Polluted continental	0.1-1.4 km	0.1 km
Dusty marine	0.1-1.3 km	8.7-8.8 km

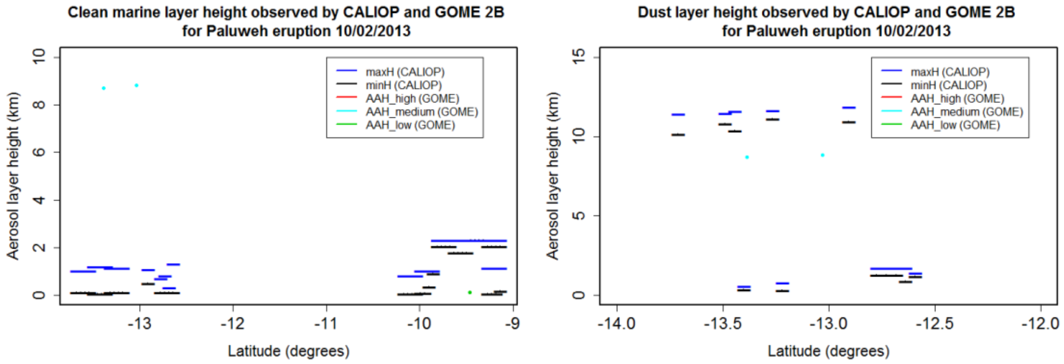

Figure 108: Detail of the clean marine (left) and dust (right) layer detected by CALIOP. The maximum and minimum layer heights are shown in blue and black respectively as a function of latitude for the 10th of February 2013. The GOME-2B AAH pixels located within 100 km of a CALIOP overpass pixel are presented in red (high reliability), cyan (medium reliability) and green (low reliability).

11.9 Puyehue-Cordon Caulle

The Buenos Aires VAAC reported that on 4 June 2011 ash plumes rose to altitudes of 10.7-13.7 km a.s.l. and drifted 870 km ESE[11]. The next day an ash plume continued to rise to altitudes of 10.7-12.2 km a.s.l. and had drifted as far as 1778 km ESE, over the coast of Argentina, and out into the Atlantic Ocean. A portion of the plume drifted WSW. Only data from the 5th of June 2011 was available from CALIOP.

11.9.1 GOME-2A

On the 5th of June 2011, GOME-2A and CALIOP detected pixels ‘near’ the volcano (Figure 109). CALIOP detected dust, polluted dust and volcanic ash (Figure 110 and Table 36). The AAH of GOME-2A agrees with the surrounding dust CALIOP layer instead of with the volcanic ash layer (Figure 111 and Figure 112). The time difference between overpasses is ~4 h.

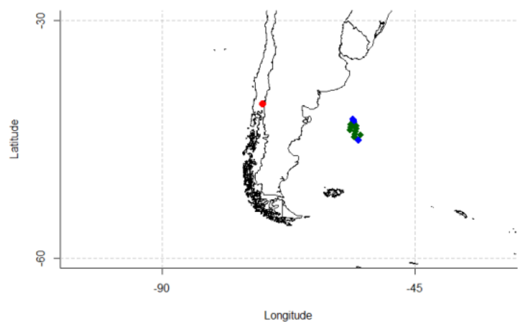

Figure 109: The location of the volcano is shown in red. The location of the CALIOP and GOME-2A overpasses for the 5th of June 2011 are shown in blue and green respectively.

[11] https://volcano.si.edu/volcano.cfm?vn=357150#June2011

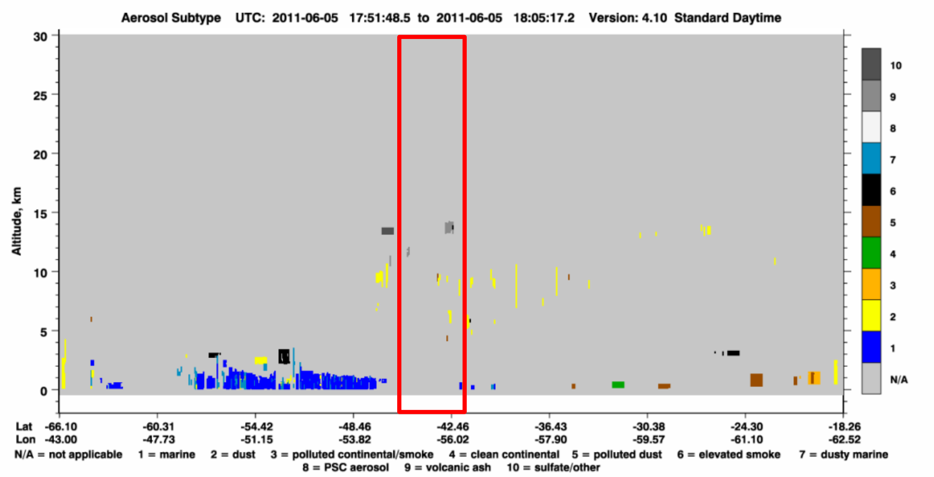

Figure 110: CALIOP overpass on the 5th of June 2011 from 17:51:48 to 18:05:17. The approximate part of the overpass within 100 km of GOME-2A overpasses is highlighted by the red box.

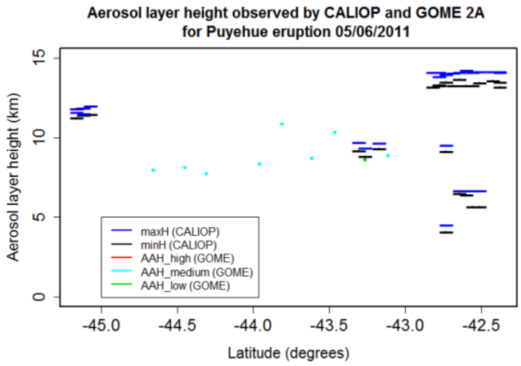

Figure 111: The aerosol layer height detected by CALIOP is shown in blue (maximum layer height) and black (minimum layer height) as a function of latitude for the 5th of June 2011. The GOME-2A AAH pixels located within 100 km of a CALIOP overpass pixel are presented in red (high reliability), cyan (medium reliability) and green (low reliability).

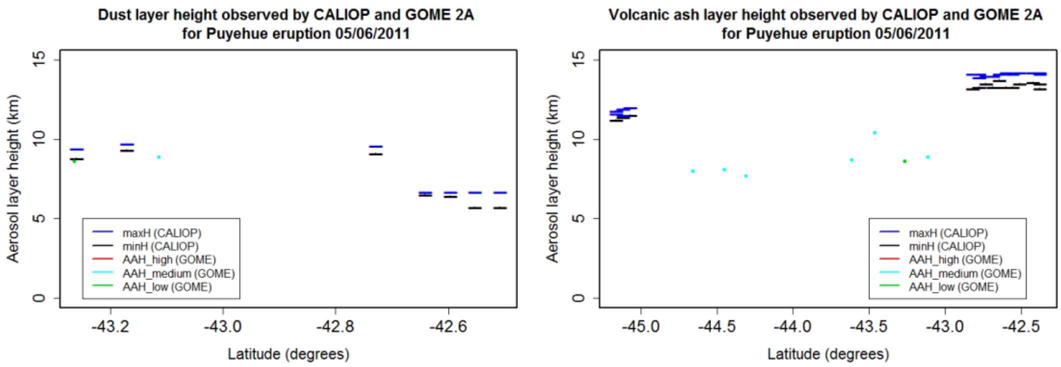

Figure 112: Detail of the dust (left) and volcanic ash (right) layer detected by CALIOP. The maximum and minimum layer heights are shown in blue and black respectively as a function of latitude for the 5th of June 2011. The GOME-2A AAH pixels located within 100 km of a CALIOP overpass pixel are presented in red (high reliability), cyan (medium reliability) and green (low reliability).

Table 36: Height of the aerosol layer detected by CALIOP for the different aerosol species compared to the AAH detected by GOME-2A for pixels located within 100 km distance for the 5th of June 2011.

	CALIOP	AAH
Dust	5.7-9.7 km	8.3-10.9 km
Polluted dust	4.1-9.7 km	8.3-10.9 km
Volcanic ash	11.2-14.2 km	7.7-10.4 km

11.10 Raikoke

A powerful eruption that began on the 22nd of June 2019 was identified based on satellite observations[12]. A series of at least nine explosions beginning at 05h05 and continuing to about 19h00 produced ash plumes, with a significant sulfur dioxide component, that rose 10-13 km a.s.l. and drifted E and NE. Strong explosions at 16h40 on 22 June generated ash plumes that rose to 10-11 km a.s.l. By 23 June the leading edge of the plume had drifted 2000 km ENE. On 23 June ash plumes continued to be visible, rising to 4.5 km and drifting NE. On 25 June ash plumes continued to be produced, rising as high as 2 km a.s.l. and drifting NW. Data from the 22nd and 23rd of June 2019 from GOME-2B and GOME-2C were analyzed.

11.10.1 GOME-2B

On the 22nd of June 2019, GOME-2B and CALIOP have several overpasses within 100 km of each other in the region around the volcano (Figure 113). CALIOP detects clean and dusty marine, dust and polluted dust, clean and polluted continental, smoke and volcanic ash layers (Table 37). GOME-2B is not able to capture the height of the volcanic ash layer as it located at an altitude higher than 15 km (which is higher than the detection limit of GOME-2) (Figure 115). However, the AAH of the GOME-2B pixels follows the height of the dust and polluted dust layers quite nicely (also seen in Figure 115) and it is known that CALIOP often misclassifies volcanic aerosol layers as dust or polluted dust. The time difference between overpasses ranges from 1 to 22 h.

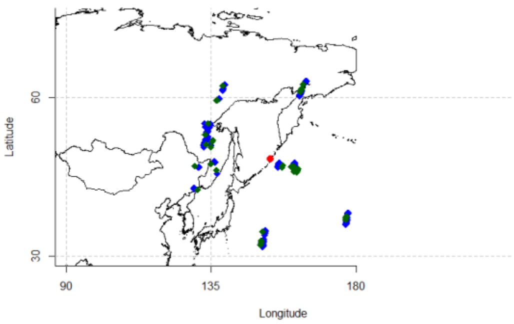

Figure 113: The location of the volcano is shown in red. The location of the CALIOP and GOME-2B overpasses for the 22nd of June 2019 are shown in blue and green respectively.

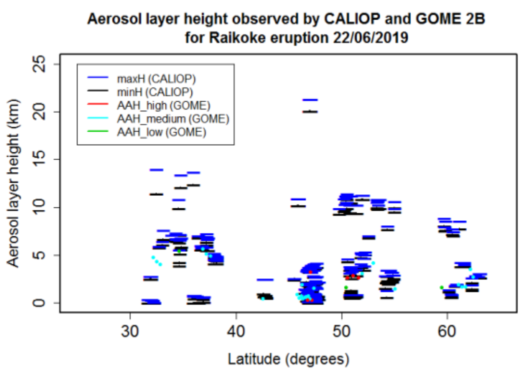

[12] https://volcano.si.edu/volcano.cfm?vn=290250#June2019

Figure 114: The aerosol layer height detected by CALIOP is shown in blue (maximum layer height) and black (minimum layer height) as a function of latitude for the 22nd of June 2019. The GOME-2B AAH pixels located within 100 km of a CALIOP overpass pixel are presented in red (high reliability), cyan (medium reliability) and green (low reliability).

Table 37: Height of the aerosol layer detected by CALIOP for the different aerosol species compared to the AAH detected by GOME-2B for pixels located within 100 km distance for the 22nd of June 2019.

	CALIOP	**AAH**
Clean marine	0.0-2.0 km	0.3-5.6 km
Dust	0.0-14.0 km	0.3-5.6 km
Polluted continental	0.5-2.5 km	0.3-0.9 km
Clean continental	1.1-5.4 km	2.6-4.2 km
Polluted dust	0.2-10.8 km	0.3-5.6 km
Smoke	1.5-7.3 km	0.3-5.6 km
Dusty marine	0.0-3.7 km	0.3-5.6 km
Volcanic ash	10.0-21.4 km	0.4-1.5 km

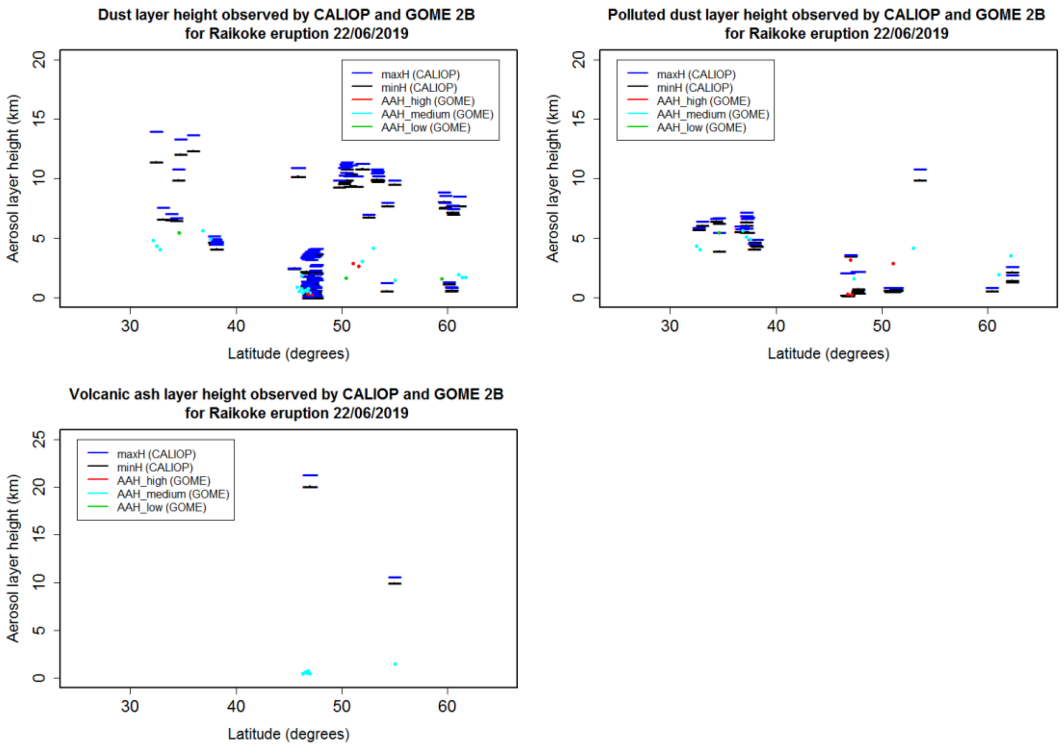

Figure 115: Detail of the dust (upper left), polluted dust (upper right) and volcanic ash (lower left) layer detected by CALIOP. The maximum and minimum layer heights are shown in blue and black respectively as a function of latitude for the 22nd of June 2019. The GOME-2B AAH pixels located within 100 km of a CALIOP overpass pixel are presented in red (high reliability), cyan (medium reliability) and green (low reliability).

On the 23rd of June 2019, GOME-2B and CALIOP have several overpasses within 100 km of each other in the region around the volcano (Figure 116). CALIOP detects clean and dusty marine, dust and polluted dust, polluted continental, smoke and sulfate layers (Table 38). GOME-2B is not able to capture the height of the sulfate layer as it located at an altitude higher than 15 km (which is higher than the detection limit of GOME-2) (Figure 118). However, the AAH of the GOME-2B pixels tends to follow height of the (polluted) dust and (clean and polluted) marine (also seen in Figure 118) CALIOP layers. The time difference between overpasses ranges from 0.5 to 21.5 h.

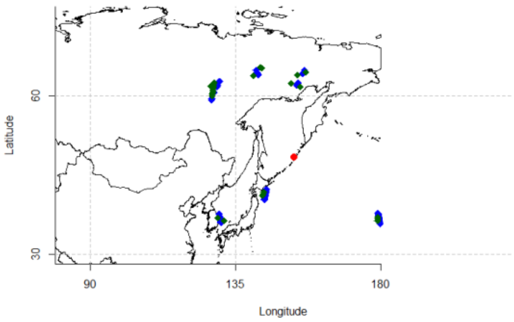

Figure 116: The location of the volcano is shown in red. The location of the CALIOP and GOME-2B overpasses for the 23rd of June 2019 are shown in blue and green respectively.

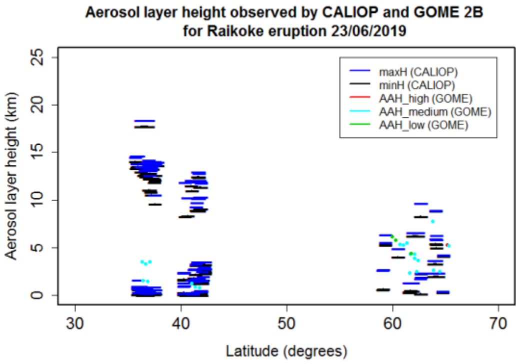

Figure 117: The aerosol layer height detected by CALIOP is shown in blue (maximum layer height) and black (minimum layer height) as a function of latitude for the 23rd of June 2019. The GOME-2B AAH pixels located within 100 km of a CALIOP overpass pixel are presented in red (high reliability), cyan (medium reliability) and green (low reliability).

Table 38: Height of the aerosol layer detected by CALIOP for the different aerosol species compared to the AAH detected by GOME-2B for pixels located within 100 km distance for the 23rd of June 2019.

	CALIOP	**AAH**
Clean marine	0.1-2.4 km	0.8-1.5 km
Dust	0.0-14.6 km	0.8-7.7 km
Polluted continental	2.0-2.4 km	7.7 km
Polluted dust	0.3-13.7 km	0.8-6.2 km
Smoke	1.8-13.8 km	0.8-6.2 km
Dusty marine	0.0-2.5 km	0.8-3.5 km
Sulfate	17.8-18.4 km	3.3-3.5 km

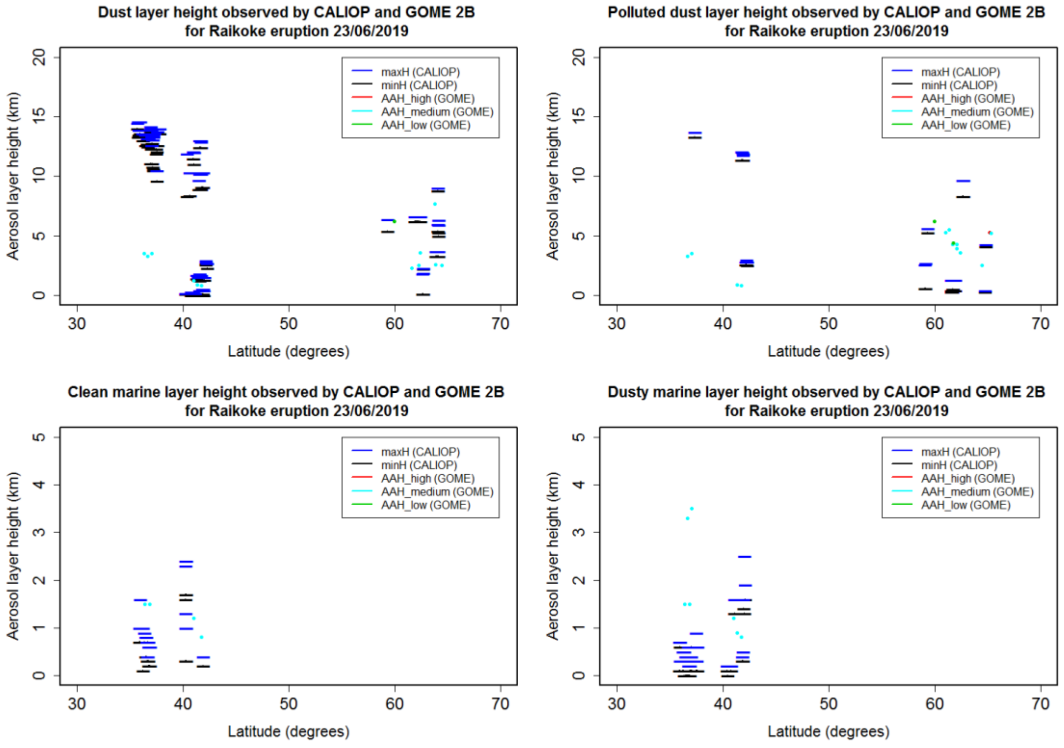

Figure 118: Detail of the dust (upper left), polluted dust (upper right), clean marine (lower left) and dusty marine (lower right) layer detected by CALIOP. The maximum and minimum layer heights are shown in blue and black respectively as a function of latitude for the 23rd of June 2019. The GOME-2B AAH pixels located within 100 km of a CALIOP overpass pixel are presented in red (high reliability), cyan (medium reliability) and green (low reliability).

11.10.2GOME-2C

On the 22nd of June 2019, GOME-2C and CALIOP have several overpasses within 100 km of each other in the region around the volcano (Figure 119). CALIOP detects clean and dusty marine, dust and polluted dust, clean and polluted continental, smoke and volcanic ash layers (Table 39). GOME-2C is not able to capture the height of the volcanic ash layer as it located at an altitude higher than 15 km (which is higher than the detection limit of GOME-2) (Figure 120 and Figure 121). However, the AAH of the GOME-2C pixels tends to follow the height of the dust layer (Figure 121). The time difference between overpasses ranges from 2 to 22 h.

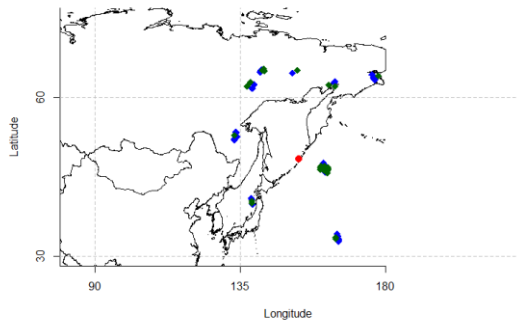

Figure 119: The location of the volcano is shown in red. The location of the CALIOP and GOME-2C overpasses for the 22nd of June 2019 are shown in blue and green respectively.

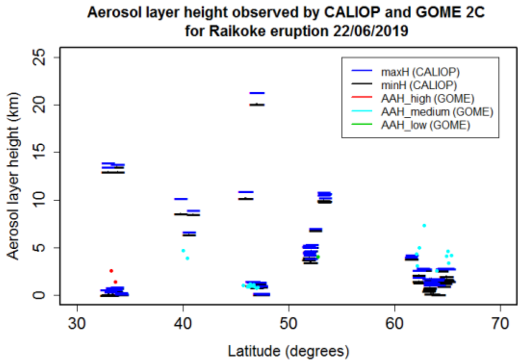

Figure 120: The aerosol layer height detected by CALIOP is shown in blue (maximum layer height) and black (minimum layer height) as a function of latitude for the 22nd of June 2019. The GOME-2C AAH pixels located within 100 km of a CALIOP overpass pixel are presented in red (high reliability), cyan (medium reliability) and green (low reliability).

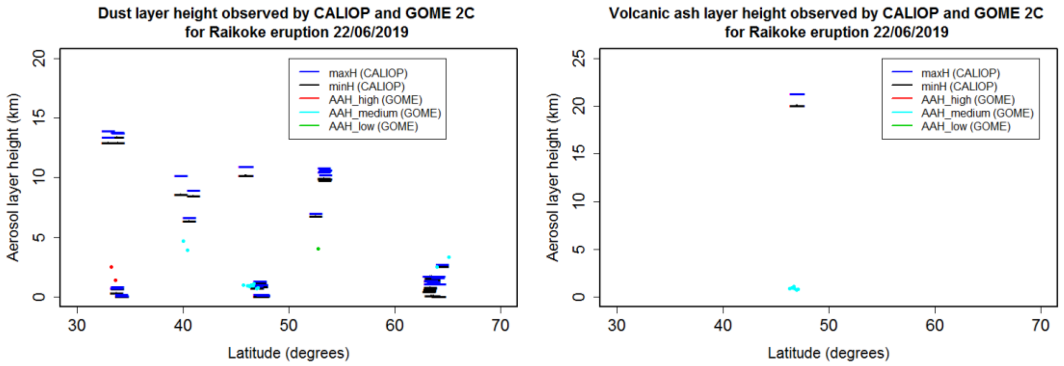

Figure 121: Detail of the dust (left) and volcanic ash (right) layer detected by CALIOP. The maximum and minimum layer heights are shown in blue and black respectively as a function of latitude for the 22nd of June 2019. The GOME-2C AAH pixels located within 100 km of a CALIOP overpass pixel are presented in red (high reliability), cyan (medium reliability) and green (low reliability).

Table 39: Height of the aerosol layer detected by CALIOP for the different aerosol species compared to the AAH detected by GOME-2C for pixels located within 100 km distance for the 22nd of June 2019.

	CALIOP	**AAH**
Clean marine	0.0-0.8 km	1.4-2.5 km
Dust	0.1-13.9 km	0.7-4.7 km
Polluted continental	0.9-2.8 km	0.7-4.6 km
Clean continental	3.8-5.4 km	3.1-4.0 km
Polluted dust	1.3-2.6 km	7.3 km
Smoke	2.7-5.3 km	4.0-5.0 km
Dusty marine	0.1-1.0 km	0.7-1.4 km
Volcanic ash	20.1-21.4 km	0.7-1.1 km

On the 23rd of June 2019, GOME-2C and CALIOP have several overpasses within 100 km of each other in the region around the volcano (Figure 122). CALIOP detects clean and dusty marine, dust and polluted dust, smoke and sulfate layers (Table 40). GOME-2C is not able to capture the height of this sulfate layer as it located at an altitude higher than 15 km (which is higher than the detection limit of GOME-2) (Figure 123 and Figure 124). However, the AAH of the GOME-2C pixels tends to follow the height of the dust layer (Figure 124). The time difference between overpasses ranges from 2 to 22 h.

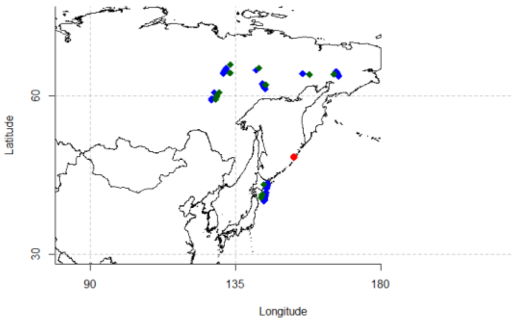

Figure 122: The location of the volcano is shown in red. The location of the CALIOP and GOME-2C overpasses for the 23rd of June 2019 are shown in blue and green respectively.

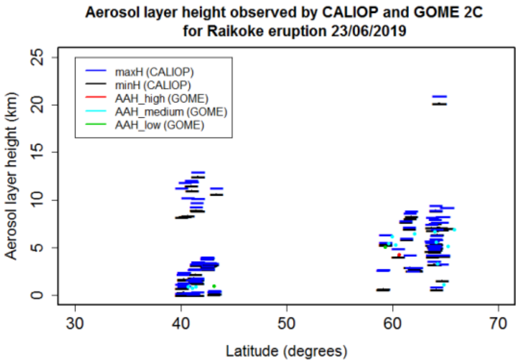

Figure 123: The aerosol layer height detected by CALIOP is shown in blue (maximum layer height) and black (minimum layer height) as a function of latitude for the 23rd of June 2019. The GOME-2C AAH pixels located within 100 km of a CALIOP overpass pixel are presented in red (high reliability), cyan (medium reliability) and green (low reliability).

Table 40: Height of the aerosol layer detected by CALIOP for the different aerosol species compared to the AAH detected by GOME-2B for pixels located within 100 km distance for the 23rd of June 2019.

	CALIOP	**AAH**
Clean marine	0.3-2.4 km	0.9 km
Dust	0.0-13.0 km	0.7-6.7 km
Polluted dust	0.6-9.2 km	1.0-6.9 km
Smoke	1.8-9.3 km	0.7-6.1 km
Dusty marine	0.0-1.6 km	0.7-0.9 km
Sulfate	5.6 km	20.2-21 km

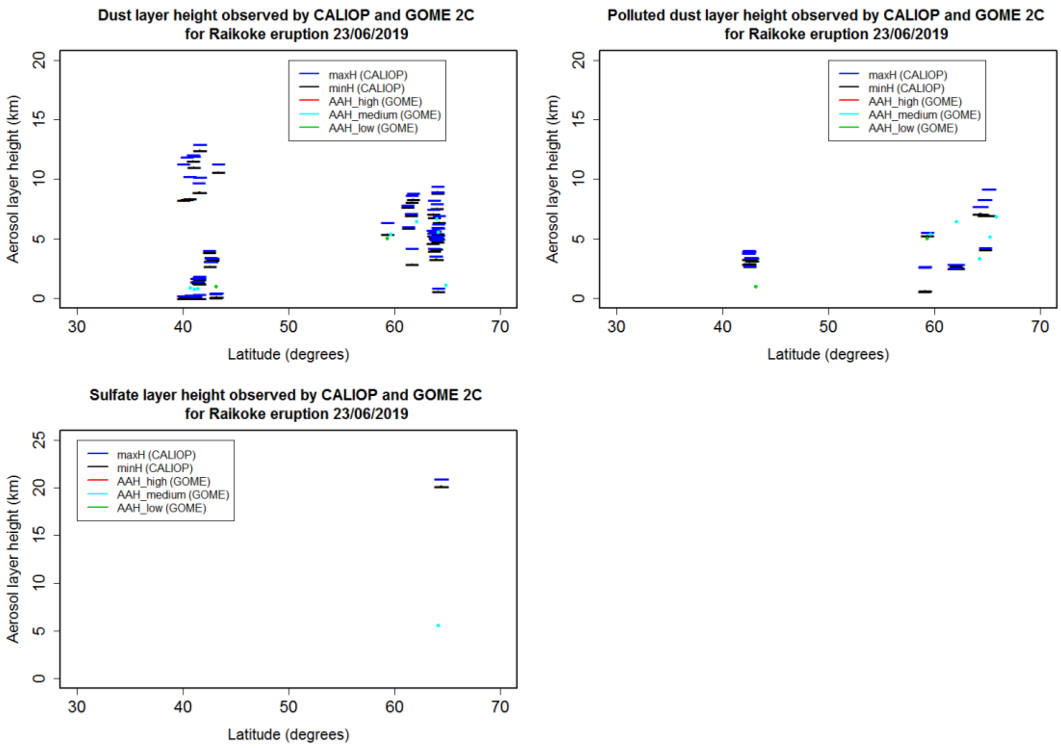

Figure 124: Detail of the dust (upper left) and polluted dust (upper right) and sulfate (lower left) layer detected by CALIOP. The maximum and minimum layer heights are shown in blue and black respectively as a function of latitude for the 23rd of June 2019. The GOME-2C AAH pixels located within 100 km of a CALIOP overpass pixel are presented in red (high reliability), cyan (medium reliability) and green (low reliability).

11.11 Rinjani

Based on satellite observations, the Darwin VAAC reported that on the 26th and 28th of October 2015 ash plumes rose to altitudes of 3-4 km a.s.l. and drifted 45-75 km SW and WSW[13].
Data from GOME-2A and GOME-2B were studied for the period from the 26th to 27th of October 2015.

11.11.1 GOME-2A

On the 27th of October 2015, GOME-2A and CALIOP have overpasses within 100 km of each other close to the volcano (Figure 125). CALIOP detects dust, clean and polluted continental, polluted dust and smoke layers (Figure 126 and Table 41). No volcanic species are detected but it is possible that CALIOP misclassified volcanic layers as dust or polluted dust. However, the AAH of the GOME-2A pixels only agrees with the height of the lower dust layers and not with the altitude of dust layers higher than 15 km as it cannot detect these layers (Figure 127 and Figure 128).

[13] https://volcano.si.edu/volcano.cfm?vn=264030#October2015

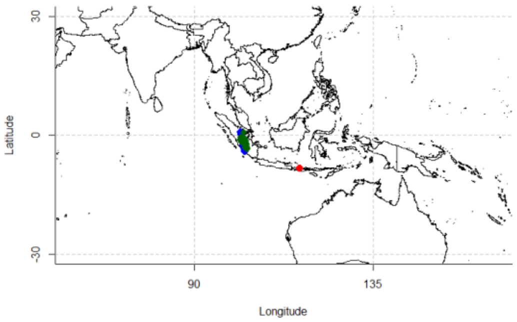

Figure 125: The location of the volcano is shown in red. The location of the CALIOP and GOME-2A overpasses for the 27th of October 2015 are shown in blue and green respectively.

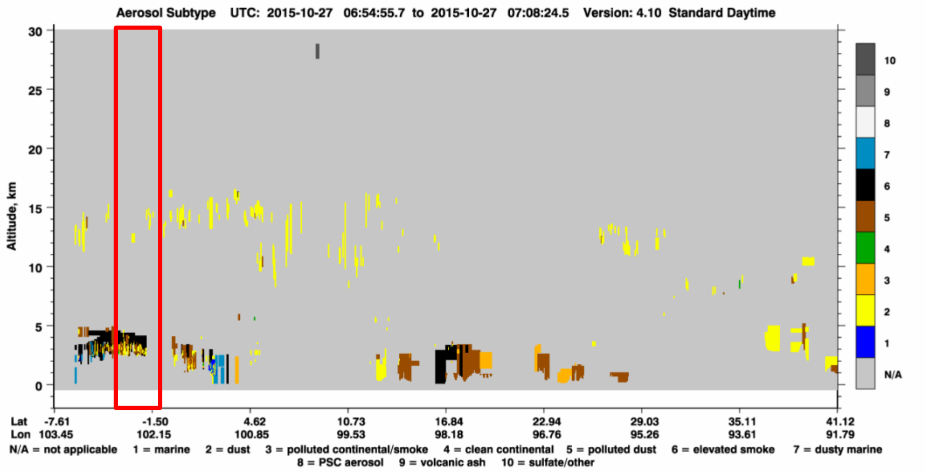

Figure 126: CALIOP overpass on the 27th of October 2015 from 06:54:55 to 07:08:24. The approximate part of the overpass within 100 km of GOME-2A overpasses is highlighted by the red box.

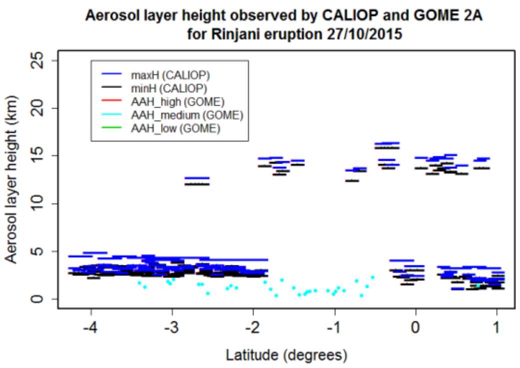

Figure 127: The aerosol layer height detected by CALIOP is shown in blue (maximum layer height) and black (minimum layer height) as a function of latitude for the 27th of October 2015. The GOME-2A AAH pixels located within 100 km of a CALIOP overpass pixel are presented in red (high reliability), cyan (medium reliability) and green (low reliability).

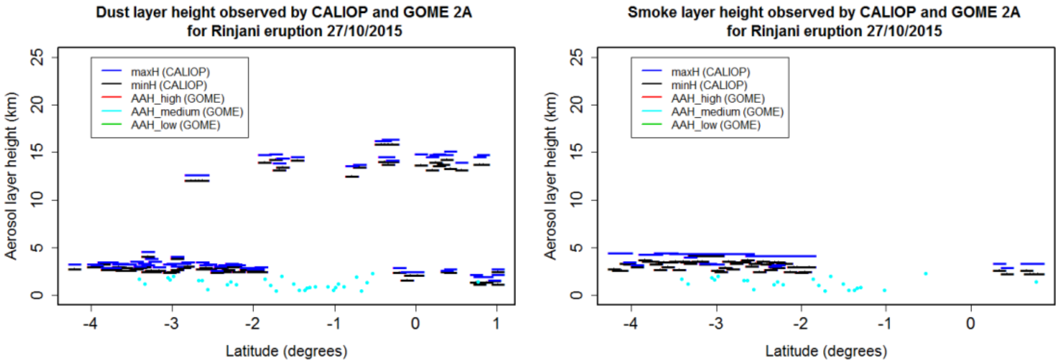

Figure 128: Detail of the dust (left) and smoke (right) layer detected by CALIOP. The maximum and minimum layer heights are shown in blue and black respectively as a function of latitude for the 27th of October 2015. The GOME-2A AAH pixels located within 100 km of a CALIOP overpass pixel are presented in red (high reliability), cyan (medium reliability) and green (low reliability).

Table 41: Height of the aerosol layer detected by CALIOP for the different aerosol species compared to the AAH detected by GOME-2B for pixels located within 100 km distance for the 23rd of June 2019.

	CALIOP	**AAH**
Dust	1.2-16.4 km	0.4-2.3 km
Polluted continental	1.4-3.3 km	0.6-2.0 km
Clean continental	2.6-2.8 km	1.2-2.0 km
Polluted dust	1.1-13.9 km	0.4-2.3 km
Smoke	2.3-4.5 km	0.4-2.3 km

11.11.2GOME-2B

On the 26th of October 2015, GOME-2B and CALIOP have overpasses within 100 km of each other close to the volcano (Figure 129). CALIOP detects clean and dusty marine, dust, clean and polluted continental, polluted dust and smoke layers (Figure 130 and Table 42). No volcanic species are detected but it is possible that CALIOP misclassified volcanic layers as dust or polluted dust. The AAH of the GOME-2A pixels partly agrees with the lower dust layer, the dusty marine and the smoke layer but fails the capture the higher dust layers (Figure 131 and Figure 132).

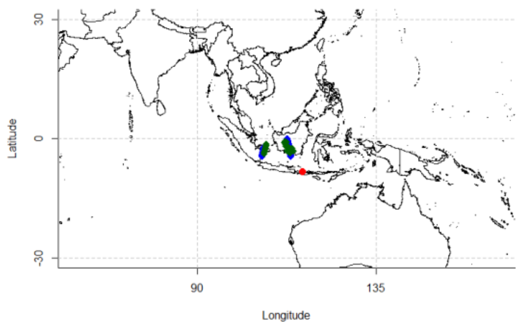

Figure 129: The location of the volcano is shown in red. The location of the CALIOP and GOME-2B overpasses for the 26th of October 2015 are shown in blue and green respectively.

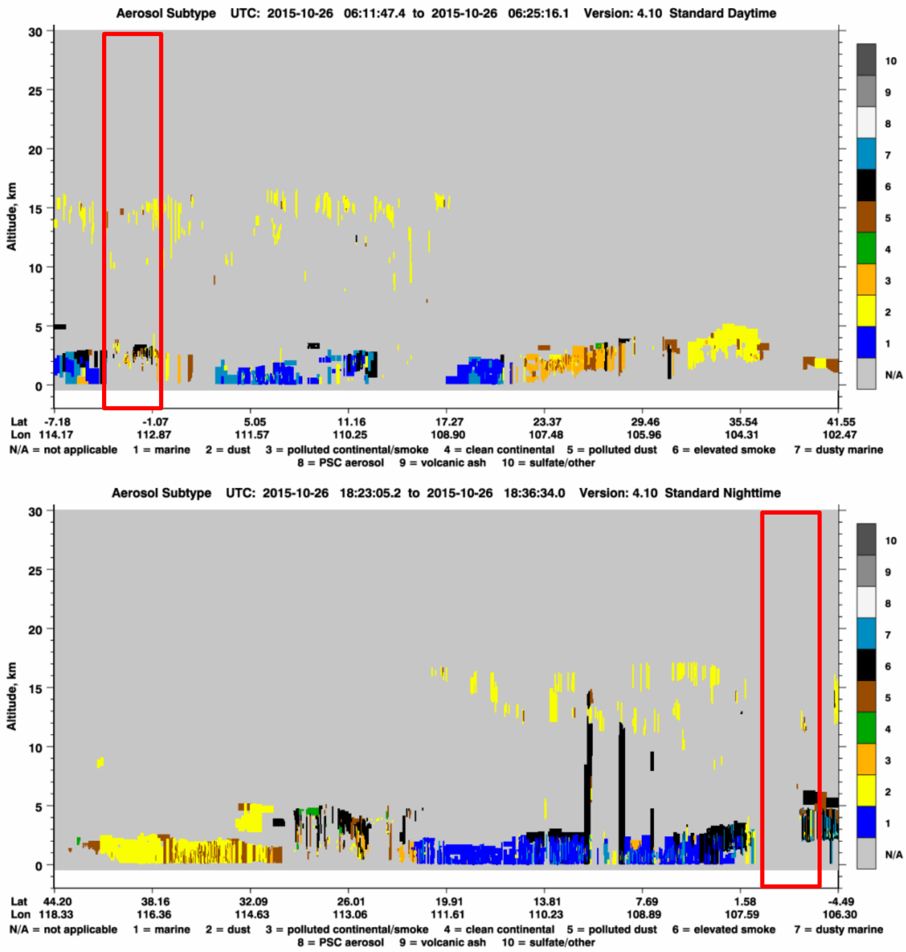

Figure 130: CALIOP overpass on the 26th of October 2015 from 06:11:26 to 06:25:16. The approximate part of the overpass within 100 km of GOME-2B overpasses is highlighted by the red box.

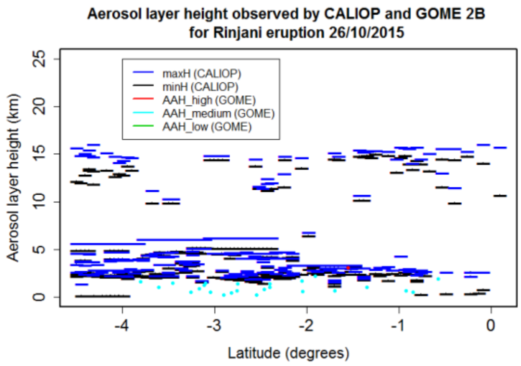

Figure 131: The aerosol layer height detected by CALIOP is shown in blue (maximum layer height) and black (minimum layer height) as a function of latitude for the 26th of October 2015. The GOME-2B AAH pixels located within 100 km of a CALIOP overpass pixel are presented in red (high reliability), cyan (medium reliability) and green (low reliability).

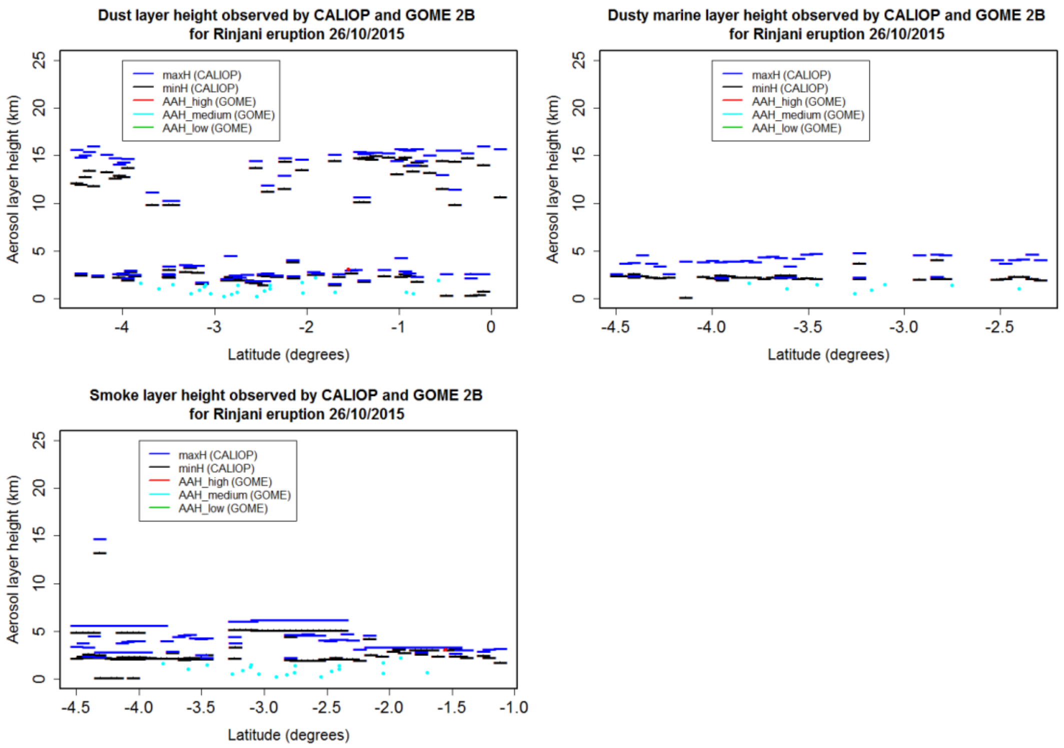

Figure 132: Detail of the dust (upper left) and dusty marine (upper right) and smoke (lower left) layer detected by CALIOP. The maximum and minimum layer heights are shown in blue and black respectively as a function of latitude for the 26th of October 2015. The GOME-2B AAH pixels located within 100 km of a CALIOP overpass pixel are presented in red (high reliability), cyan (medium reliability) and green (low reliability).

Table 42: Height of the aerosol layer detected by CALIOP for the different aerosol species compared to the AAH detected by GOME-2B for pixels located within 100 km distance for the 23rd of June 2019.

	CALIOP	**AAH**
Clean marine	0.1-2.3 km	0.5-1.0 km
Dust	0.4-16.0 km	0.2-3.0 km
Polluted continental	0.3-2.6 km	0.2-1.9 km
Clean continental	2.0-2.2 km	0.6-1.4 km
Polluted dust	1.2-14.9 km	0.2-3.0 km
Smoke	0.1-14.7 km	0.2-3.0 km
Dusty marine	0.1-4.8 km	0.5-1.6 km

11.12 Sarychev Peak

On the 13th of June 2009, ash plumes rose to an altitude of 7.5 km a.s.l. and drifted 200 km SW and 105 km SE[14]. On the 14th of June 2009, a large eruption produced an ash plume that rose to an altitude of 12 km a.s.l. A large explosion the next day sent an ash plume to an altitude of 8 km a.s.l.

Data from the 14th until the 16th of June 2009 from GOME-2A were studied.

11.12.1 GOME-2A

[14] https://volcano.si.edu/volcano.cfm?vn=290240#June2009

On the 14th of June 2009, GOME-2A and CALIOP have overpasses within 100 km of each other close to the volcano (Figure 133). CALIOP detects clean marine, dust, polluted dust and dusty marine aerosol layers (Figure 134 and Table 43). No volcanic species have been observed, however dust and polluted dust might be misclassified volcanic aerosols. It seems that the AAH from GOME-2A agrees slightly with the dust and dusty marine layers (Figure 135 and Figure 136). The time difference between GOME-2A and CALIOP overpasses is 15 h.

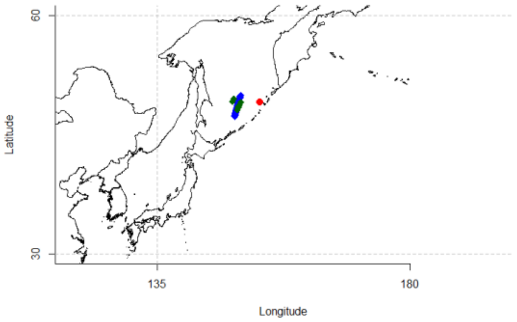

Figure 133: The location of the volcano is shown in red. The location of the CALIOP and GOME-2A overpasses for the 14th of June 2009 are shown in blue and green respectively.

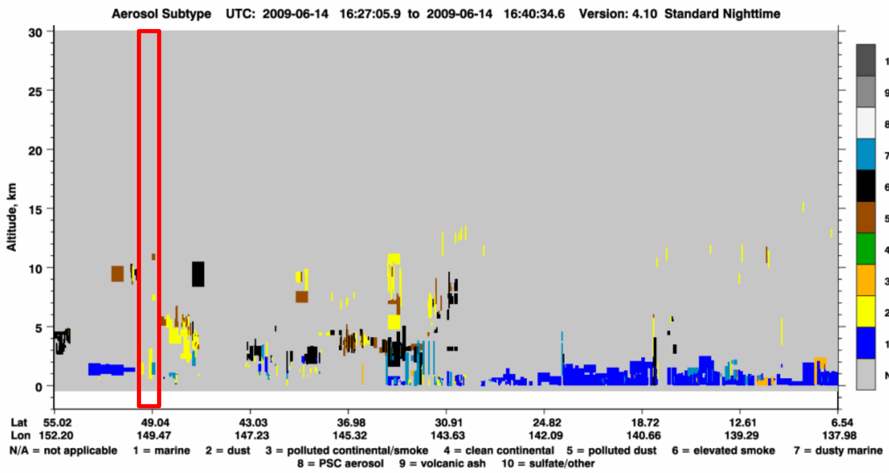

Figure 134: CALIOP overpass on the 14th of June 2009 from 16:27:05 to 16:40:34. The approximate part of the overpass within 100 km of GOME-2A overpasses is highlighted by the red box.

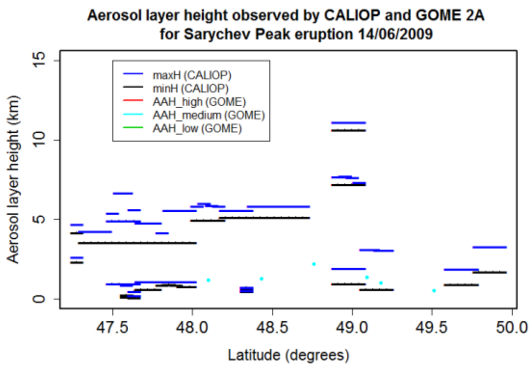

Figure 135: The aerosol layer height detected by CALIOP is shown in blue (maximum layer height) and black (minimum layer height) as a function of latitude for the 14th of June 2009. The GOME-2A AAH pixels located within 100 km of a CALIOP overpass pixel are presented in red (high reliability), cyan (medium reliability) and green (low reliability).

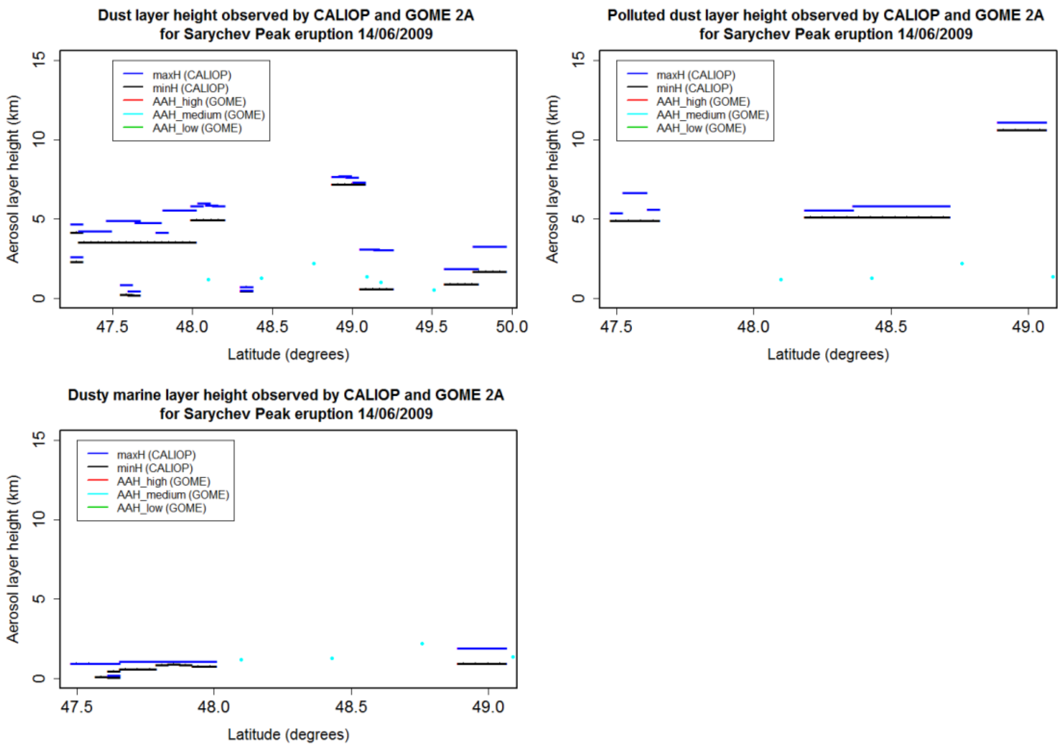

Figure 136: Detail of the dust (upper left), polluted dust (upper right) and dusty marine (lower left) layer detected by CALIOP. The maximum and minimum layer heights are shown in blue and black respectively as a function of latitude for the 14th of June 2009. The GOME-2A AAH pixels located within 100 km of a CALIOP overpass pixel are presented in red (high reliability), cyan (medium reliability) and green (low reliability).

Table 43: Height of the aerosol layer detected by CALIOP for the different aerosol species compared to the AAH detected by GOME-2A for pixels located within 100 km distance for the 14th of June 2009.

	CALIOP	AAH
Clean marine	0.6-0.7 km	1.2-2.2 km
Dust	0.2-7.7 km	0.5-2.2 km
Polluted dust	4.9-11.1 km	0.5-2.2 km
Dusty marine	0.1-1.9 km	0.5-2.2 km

On the 16th of June 2009, GOME-2A and CALIOP have overpasses within 100 km of each other close to the volcano (Figure 137). CALIOP detects dust, polluted dust, smoke, dusty marine and volcanic ash layers (Figure 138 and Table 44). Even though a volcanic ash layer was observed by CALIOP at an altitude lower than 15 km (which should be detectable by GOME-2A), the AAH from GOME-2A does not agree with the height of this layer (Figure 140). It seems that the AAH from GOME-2A agrees more with the height of the dust and polluted dust layers (Figure 140). The time difference between GOME-2A and CALIOP overpasses is 15 h.

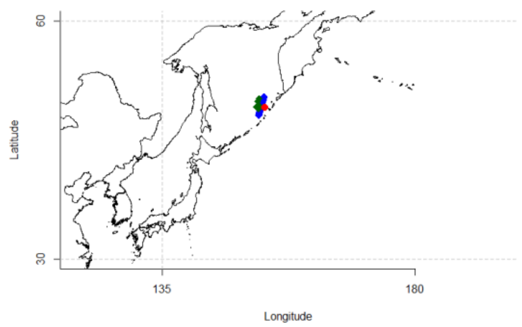

Figure 137: The location of the volcano is shown in red. The location of the CALIOP and GOME-2A overpasses for the 14th of June 2009 are shown in blue and green respectively.

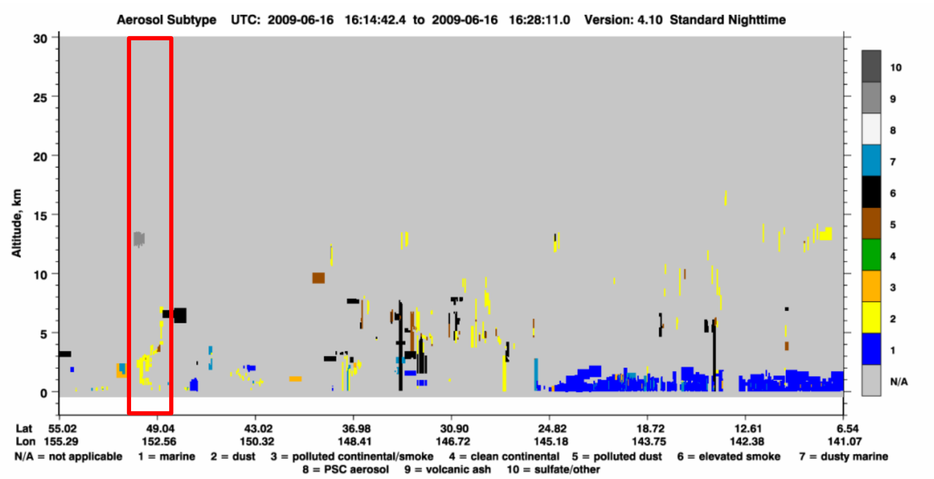

Figure 138: CALIOP overpass on the 16th of June 2009 from 16:14:42 to 16:28:11. The approximate part of the overpass within 100 km of GOME-2A overpasses is highlighted by the red box.

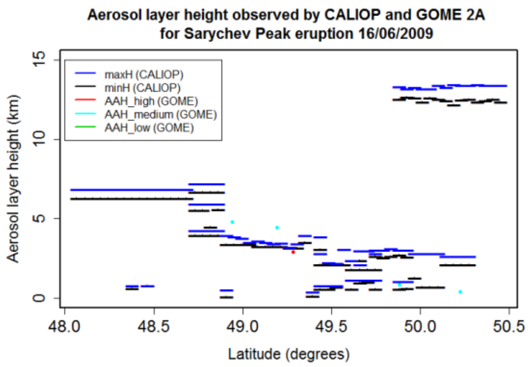

Figure 139: The aerosol layer height detected by CALIOP is shown in blue (maximum layer height) and black (minimum layer height) as a function of latitude for the 16th of June 2009. The GOME-2A AAH pixels located within 100 km of a CALIOP overpass pixel are presented in red (high reliability), cyan (medium reliability) and green (low reliability).

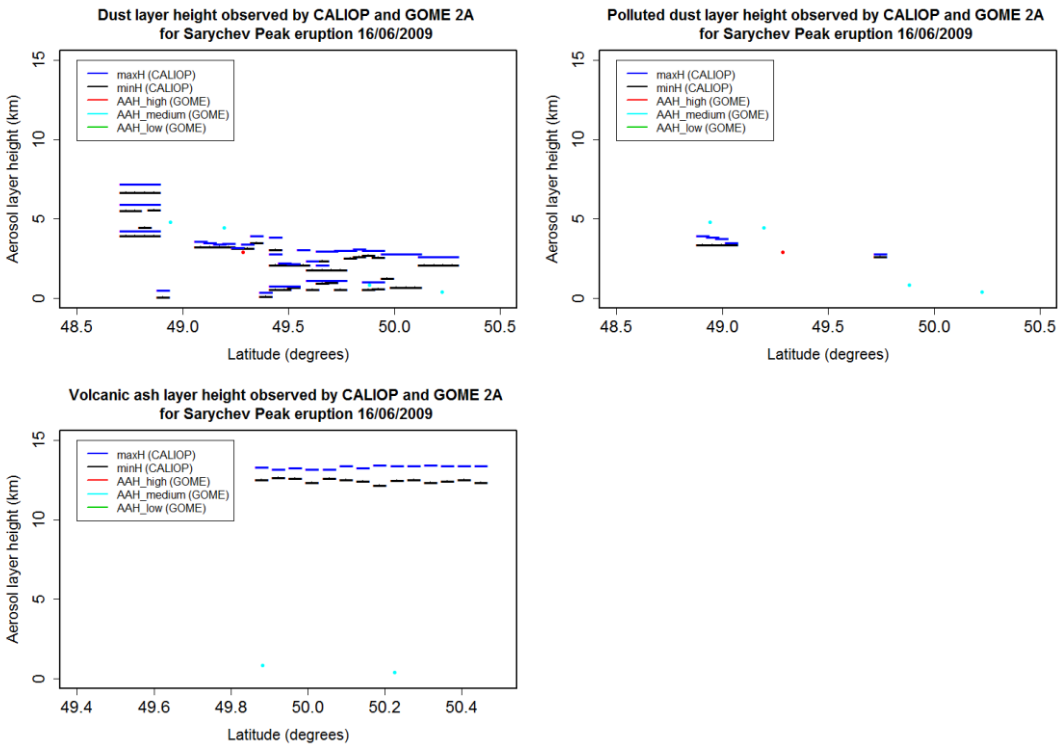

Figure 140: Detail of the dust (upper left), polluted dust (upper right) and volcanic ash (lower left) layer detected by CALIOP. The maximum and minimum layer heights are shown in blue and black respectively as a function of latitude for the 16th of June 2009. The GOME-2A AAH pixels located within 100 km of a CALIOP overpass pixel are presented in red (high reliability), cyan (medium reliability) and green (low reliability).

Table 44: Height of the aerosol layer detected by CALIOP for the different aerosol species compared to the AAH detected by GOME-2A for pixels located within 100 km distance for the 16th of June 2009.

	CALIOP	**AAH**
Dust	0.1-7.2 km	0.4-4.8 km
Polluted dust	2.7-3.9 km	0.4-4.8 km
Smoke	6.3-6.9 km	2.9-4.8 km
Dusty marine	0.6-0.8 km	2.9-4.8 km
Volcanic ash	12.2-13.5 km	0.4-2.9 km

11.13 Ubinas

The seismicity at Ubinas increased during 9-14 September 2016, characterized by an increased number of volcano-tectonic and hybrid events[15]. Data from both GOME-2A and GOME-2B from the 13th and 14th of September 2016 were studied.

1.1.1. GOME-2A

On the 13th of September 2016, GOME-2A has no overpasses within 100 km of CALIOP overpasses close to the volcano.

On the 14th of September 2016, GOME-2A and CALIOP have overpasses within 100 km of each other close to the volcano (Figure 141). CALIOP detects clean marine, dust, polluted and clan

[15] https://volcano.si.edu/volcano.cfm?vn=354020#September2016

continental, polluted dust and smoke layers (Figure 142 and Table 45). No volcanic species have been observed, however dust and polluted dust might be misclassified volcanic aerosols. It seems that the AAH from GOME-2A agrees slightly with the dust and polluted dust layers (Figure 143 and Figure 144). The time difference between GOME-2A and CALIOP overpasses is 3 or 8.5 h.

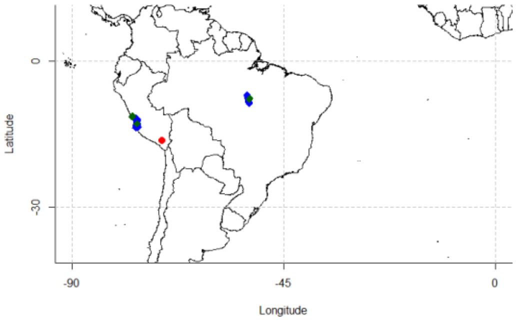

Figure 141: The location of the volcano is shown in red. The location of the CALIOP and GOME-2A overpasses for the 14th of September 2016 are shown in blue and green respectively.

Table 45: Height of the aerosol layer detected by CALIOP for the different aerosol species compared to the AAH detected by GOME-2A for pixels located within 100 km distance for the 14th of June 2009.

	CALIOP	AAH
Clean marine	0.0-1.7 km	5.1 km
Dust	0.3-10.8 km	5.0-5.2 km
Polluted continental	0.1-6.0 km	5.0-5.2 km
Clean continental	4.5-4.8 km	5.0-5.2 km
Polluted dust	1.3-6.6 km	0.8-5.2 km
Smoke	2.3-7.5 km	0.8-5.2 km

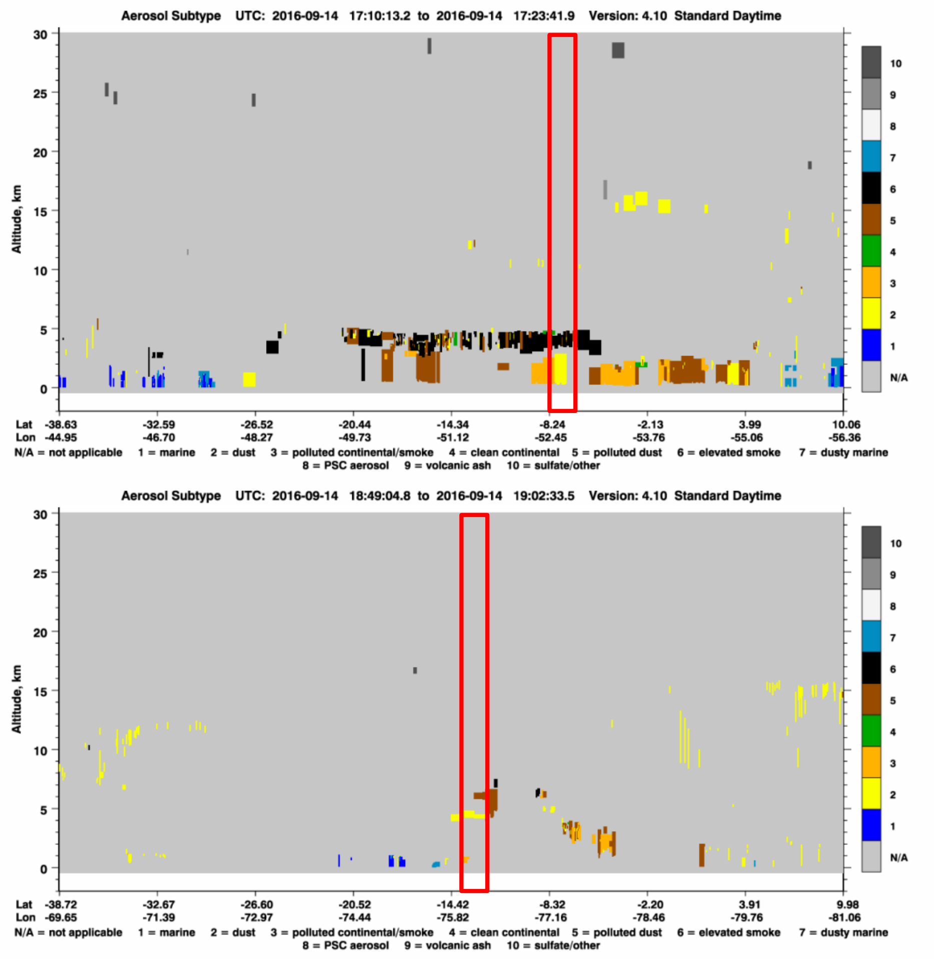

Figure 142: CALIOP overpasses on the 14th of September 2016 from 17:10:13 to 17:23:41 and from 18:49:04 to 19:02:33. The approximate part of the overpasses within 100 km of GOME-2A overpasses are highlighted by the red boxes.

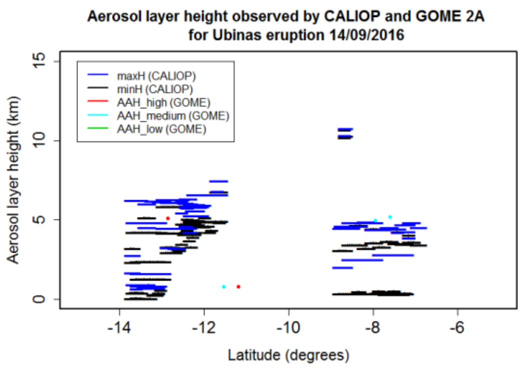

Figure 143: The aerosol layer height detected by CALIOP is shown in blue (maximum layer height) and black (minimum layer height) as a function of latitude for the 14th of September 2016. The GOME-2A AAH pixels located within 100 km of a CALIOP overpass pixel are presented in red (high reliability), cyan (medium reliability) and green (low reliability).

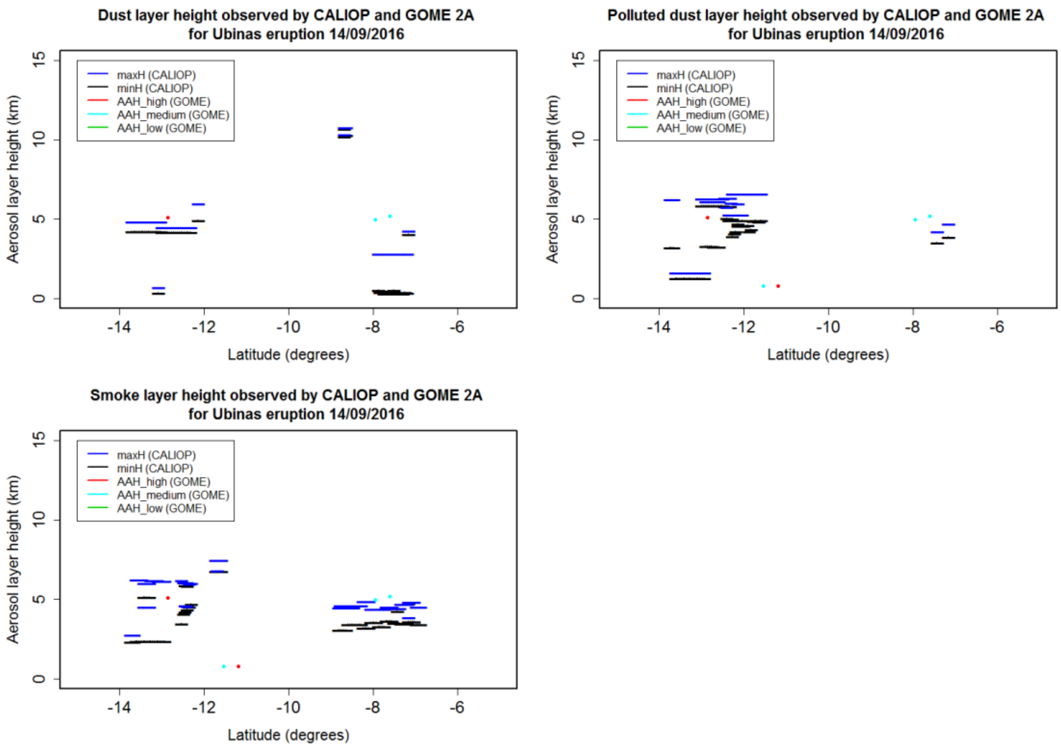

Figure 144: Detail of the dust (upper left), polluted dust (upper right) and smoke (lower left) layer detected by CALIOP. The maximum and minimum layer heights are shown in blue and black respectively as a function of latitude for the 14th of September 2016. The GOME-2A AAH pixels located within 100 km of a CALIOP overpass pixel are presented in red (high reliability), cyan (medium reliability) and green (low reliability).

11.13.1GOME-2B

On the 13th of September 2016, GOME-2B and CALIOP have overpasses within 100 km of each other close to the volcano (Figure 145). CALIOP detects mainly dust layers between 1.2 and 3.9 km (Figure 146 and Table 46). No volcanic species have been observed, however dust might be misclassified volcanic aerosols. It seems that the AAH from GOME-2B agrees with the dust layer (Figure 147). The time difference between GOME-2B and CALIOP overpasses is 3.5 h.

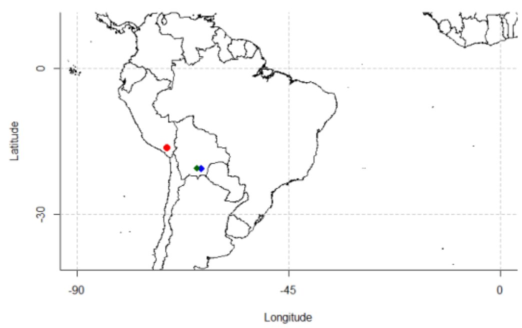

Figure 145: The location of the volcano is shown in red. The location of the CALIOP and GOME-2B overpasses for the 13th of September 2016 are shown in blue and green respectively.

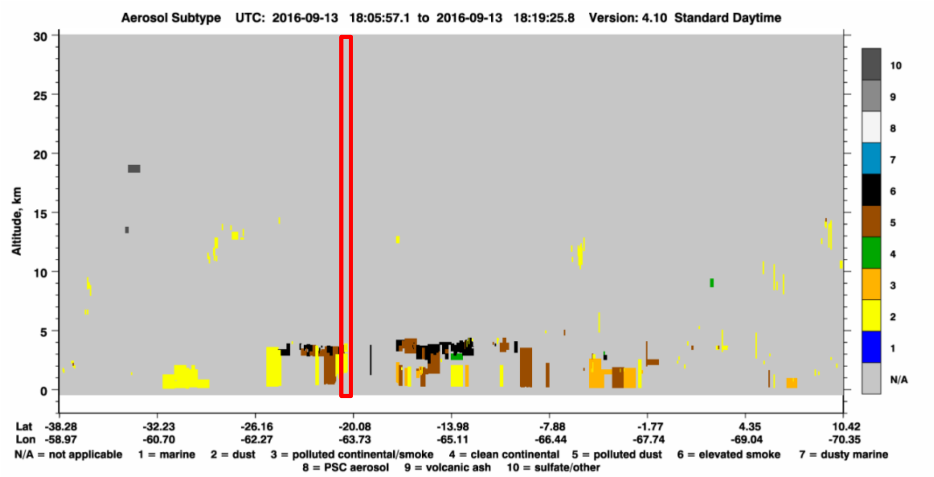

Figure 146: CALIOP overpass on the 13th of September 2016 from 18:05:57 to 18:19:25. The approximate part of the overpass within 100 km of GOME-2B overpasses is highlighted by the red box.

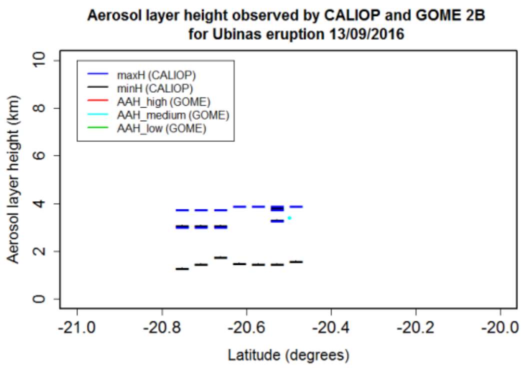

Figure 147: The aerosol layer height detected by CALIOP is shown in blue (maximum layer height) and black (minimum layer height) as a function of latitude for the 13th of September 2016. The GOME-2B AAH pixels located within 100 km of a CALIOP overpass pixel are presented in red (high reliability), cyan (medium reliability) and green (low reliability).

Table 46: Height of the aerosol layer detected by CALIOP for the different aerosol species compared to the AAH detected by GOME-2B for pixels located within 100 km distance for the 13th of June 2009.

	CALIOP	**AAH**
Dust	1.3-3.9 km	3.4 km
Polluted continental	3.3-3.8 km	3.4 km
Polluted dust	3.1-3.8 km	3.4 km

On the 14th of September 2016, GOME-2B and CALIOP have no overpasses within 100 km of each other close to the volcano.

12 Appendix B

12.1 GOME-2/MetOp AAH and AAI time series

This appendix contains the results from different case studies performed by AUTH but not discussed in the main document.

Figure 148, shows the AAI time series from the GOME-2 satellite measurements for each satellite platform. Observation pixels with AAI values below 2.0 correspond to scenes with a too low amount of aerosols to result in a reliable AAH retrieval and for this reason these pixels are excluded from the time series. The amount of data for comparison is often highly limited when only using AAH calculated under conditions with AAI>2. The time series of GOME-2 AAH for the five EARLINET stations for the study period from 2007 to 2019 is presented in Figure 149. These figures are shown in order to illustrate the extent of the GOME-2 database available once the collocation criteria are applied. In Figure 150, the effect of choosing the pixel closest spatially within the 150 km criterion is shown. It needs to be mentioned that the AAH can never be higher than 15km, an upper limit imposed by the FRESCO algorithm.

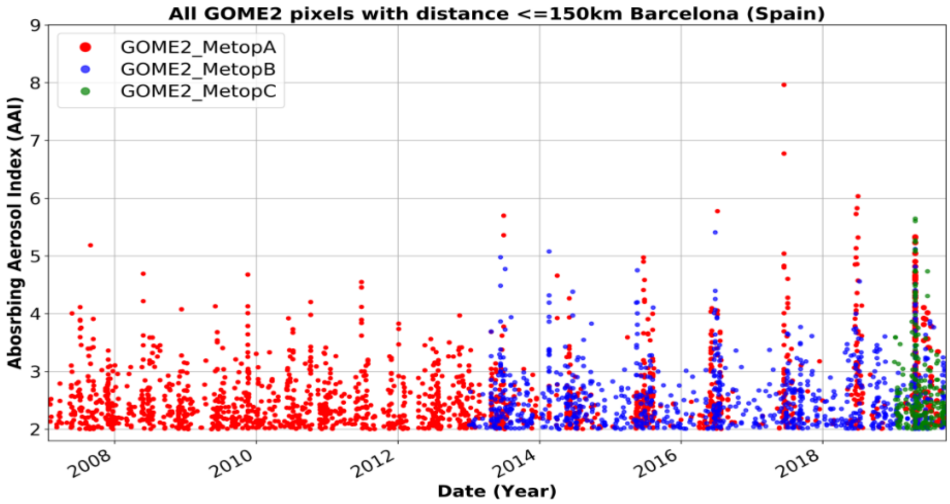

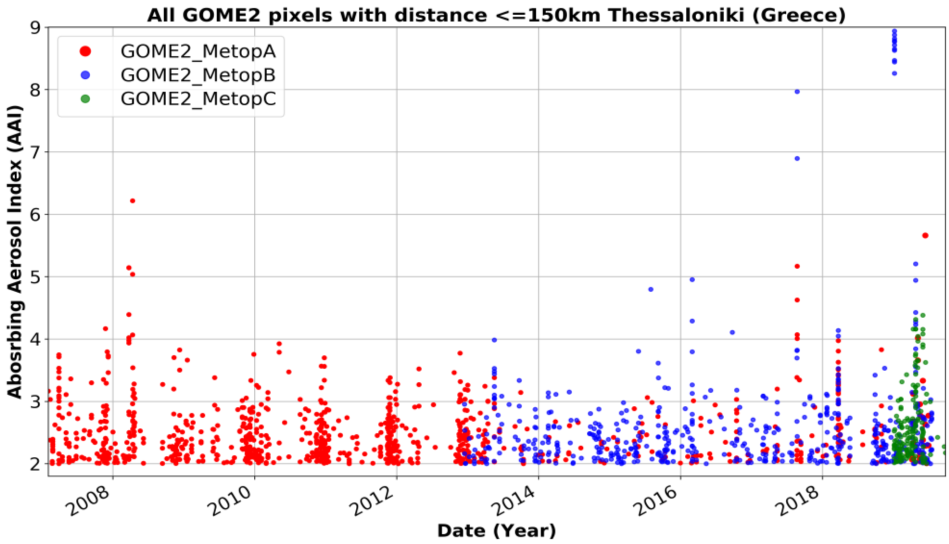

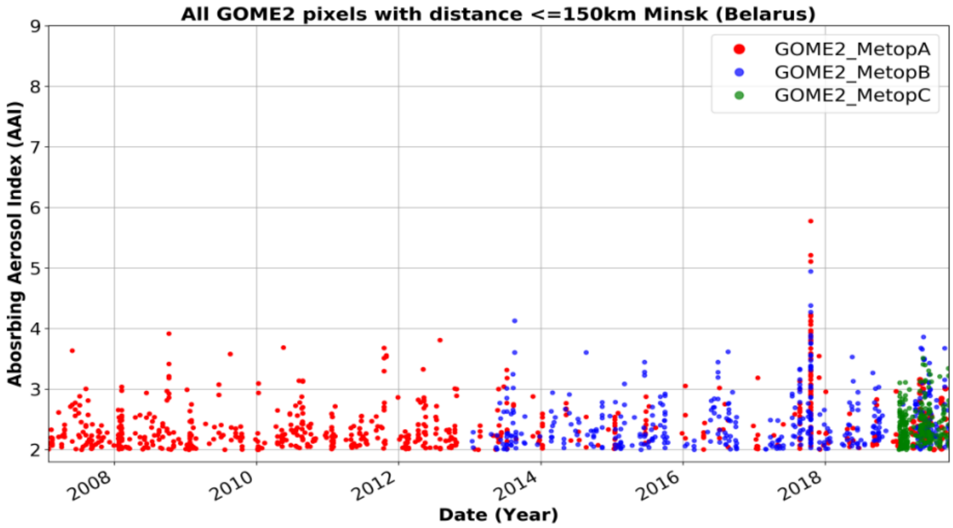

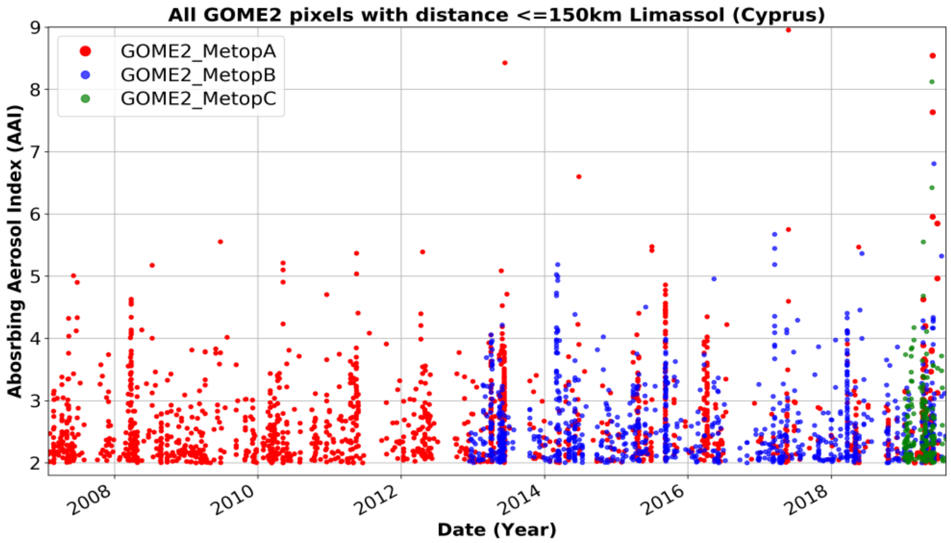

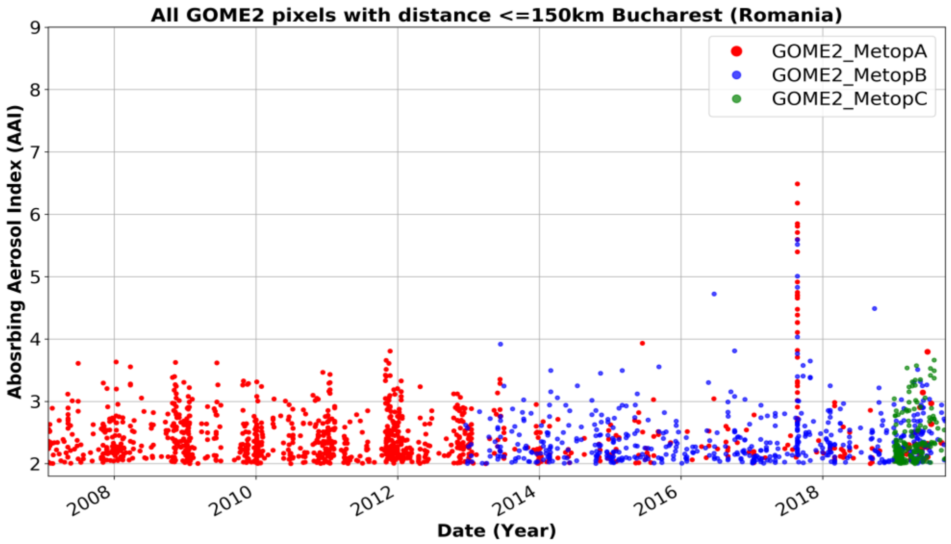

Figure 148. Time series of GOME-2 AAI for the study period from 2007 to 2019 for Barcelona, Thessaloniki, Minsk, Bucharest and Limassol EARLINET stations.

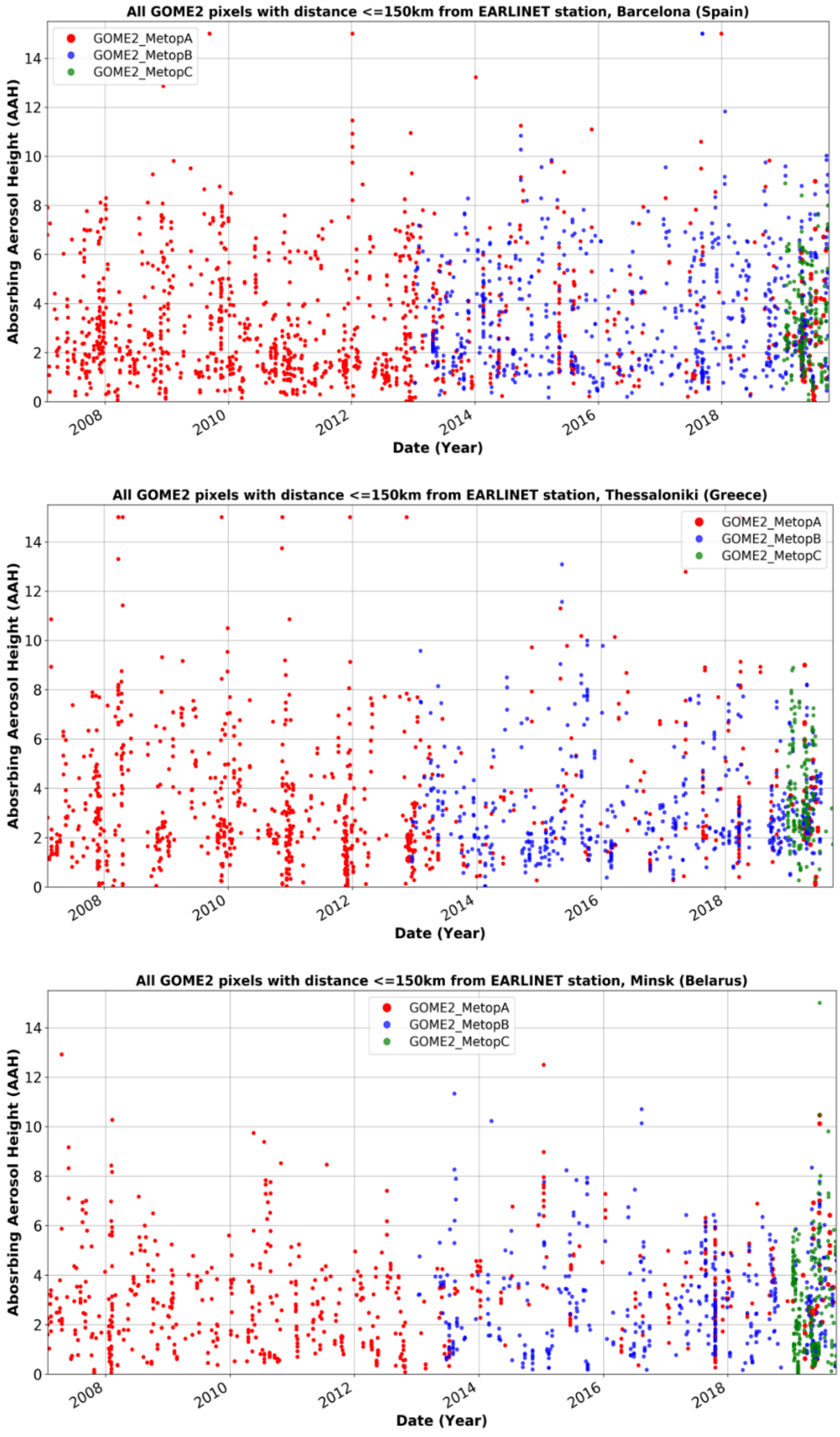

Figure 149. Time series of GOME-2 AAH for the study period from 2007 to 2019 for Barcelona, Thessaloniki, Minsk, Bucharest and Limassol EARLINET stations.

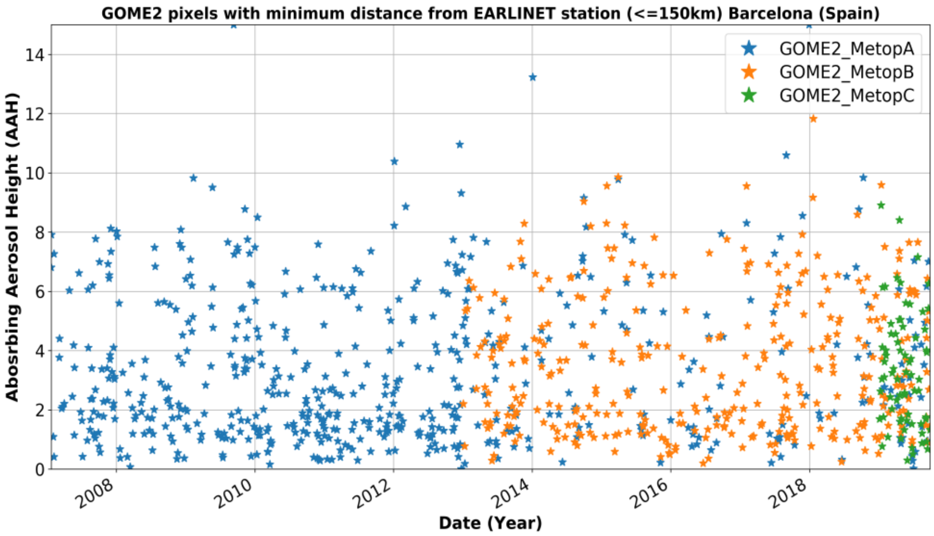
GOME2 pixels with minimum distance from EARLINET station (<=150km) Barcelona (Spain)
Abosrbing Aerosol Height (AAH)
Date (Year)
GOME2_MetopA
GOME2_MetopB
GOME2_MetopC
0
2
4
6
8
10
12
14
2008
2010
2012
2014
2016
2018

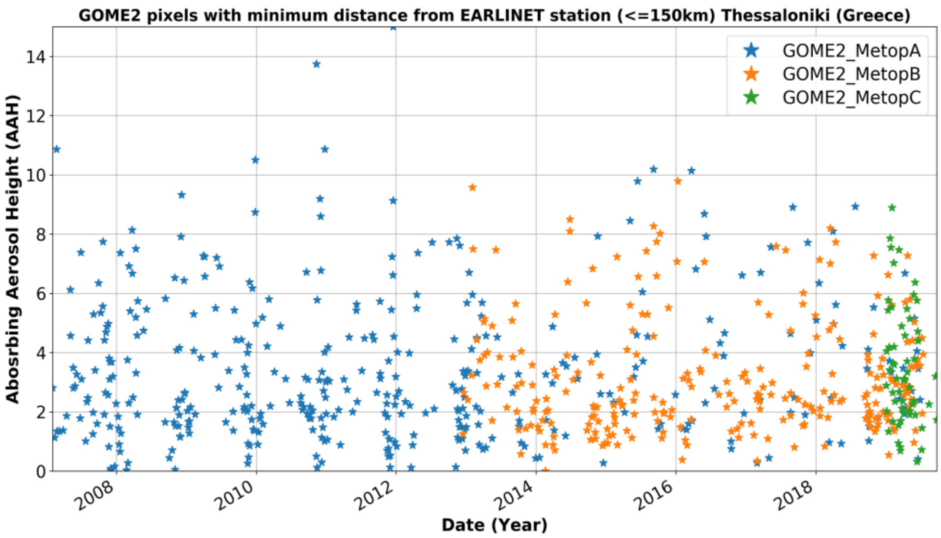
GOME2 pixels with minimum distance from EARLINET station (<=150km) Thessaloniki (Greece)
Abosrbing Aerosol Height (AAH)
Date (Year)
GOME2_MetopA
GOME2_MetopB
GOME2_MetopC
0
2
4
6
8
10
12
14
2008
2010
2012
2014
2016
2018

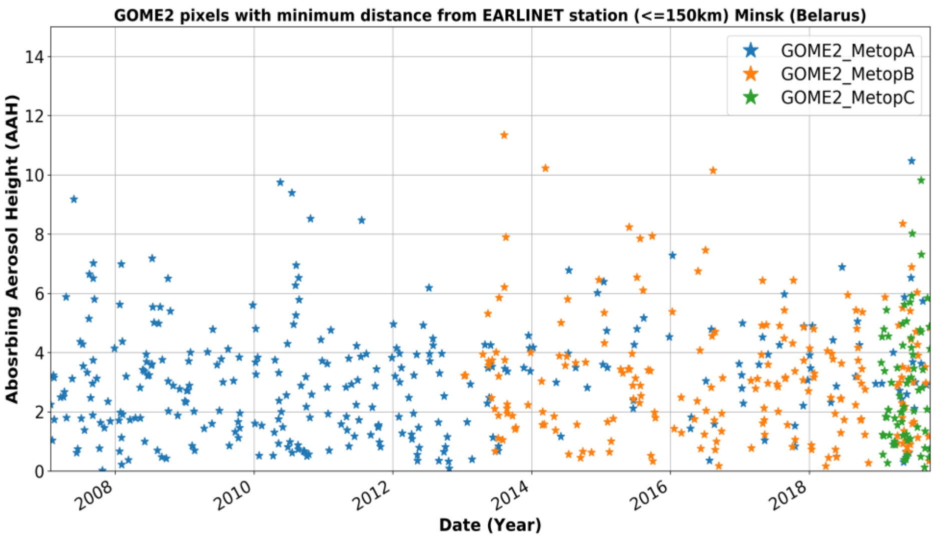
GOME2 pixels with minimum distance from EARLINET station (<=150km) Minsk (Belarus)
Abosrbing Aerosol Height (AAH)
Date (Year)
GOME2_MetopA
GOME2_MetopB
GOME2_MetopC
0
2
4
6
8
10
12
14
2008
2010
2012
2014
2016
2018

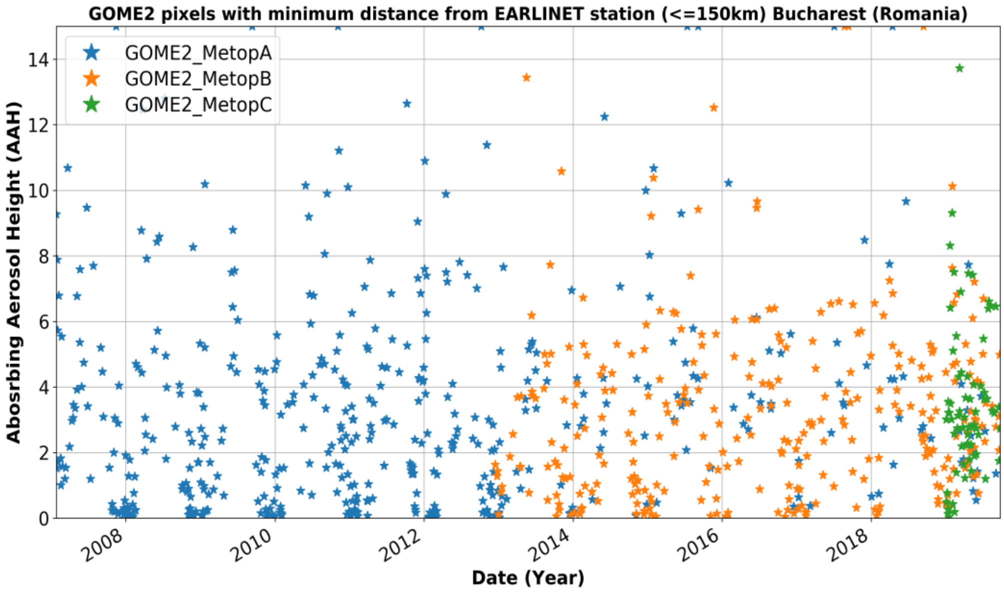

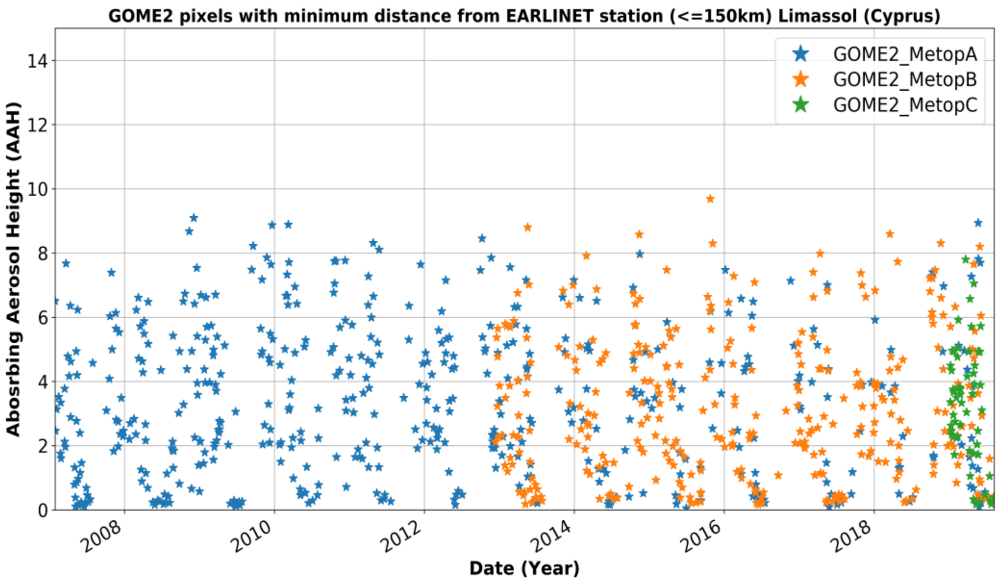

Figure 150.The time series of GOME-2 AAH for five EARLINET stations for the study period from 2007 to 2019. These values represent only the GOME-2 AAH pixels closest to each EARLINET station (Barcelona, Thessaloniki, Minsk, Bucharest and Limassol).

12.2 Saharan dust over the Iberian Peninsula, 20-23 February, 2017

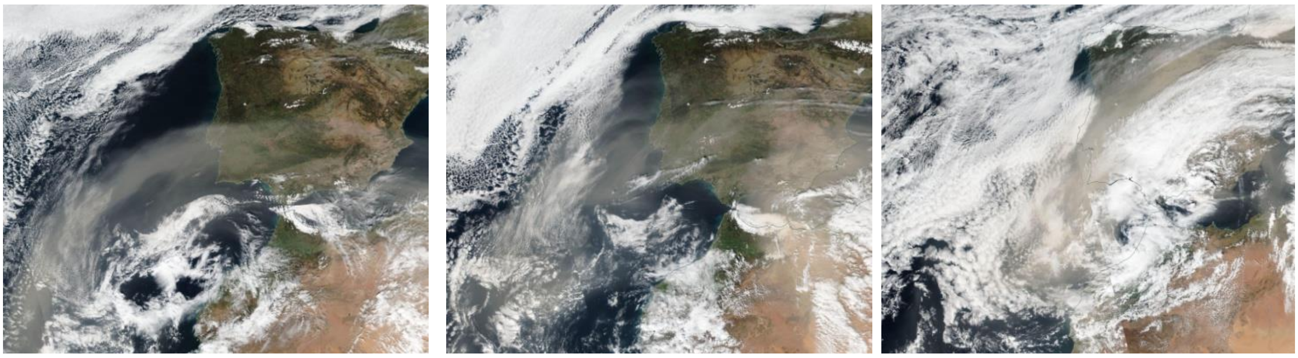

Figure 151. Images of Saharan dust transport as captured by the MODIS/Terra satellite, on the 21st [left], the 22nd [middle] and the 23rd of February 2017, over the Iberian Peninsula.

A second Saharan dust event will be discussed using the EARLINET Évora station in Portugal [38.56ºN/-7.91ºE] which took place between the 20th and the 23rd of February 2017. In Figure 151 satellite maps from MODIS/Terra sensor show the dust being transported by air masses over the Atlantic before returning towards Portugal and Spain on the 21st [left], 22nd [middle] and 23rd [right] of February 2017. A map of the AAI as seen by GOME-2A on the 23rd of February 2017 is shown in Figure 152Figure 152 where the high aerosol index values are seen to spread through a large area in the Iberian Peninsula. The ground-based observations of this dust event are shown in Figure 153 as backscatter profiles reported by the EARLINET Évora lidar for the 21st [top], the 22nd [middle] and the 23rd [bottom] of February. The 5-day NOAA HYSPLIT backward trajectories ending at the position of Évora for 10:00 UTC and the same days is shown in Figure 153.

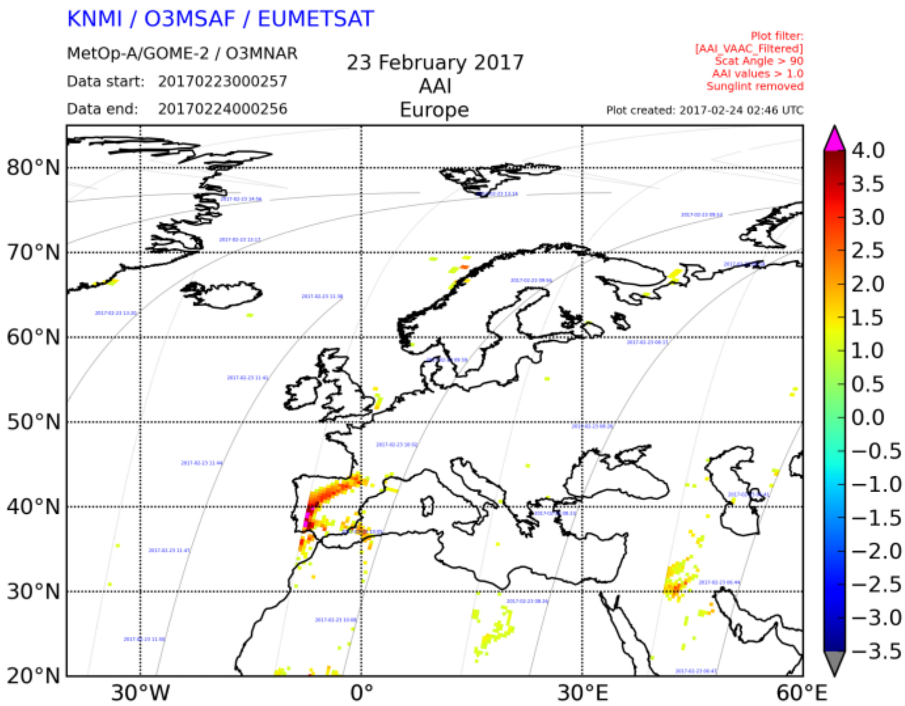

Figure 152. Map of the AAI on the 23rd of February 2017 as seen by GOME-2A. (https://temis.nl/)

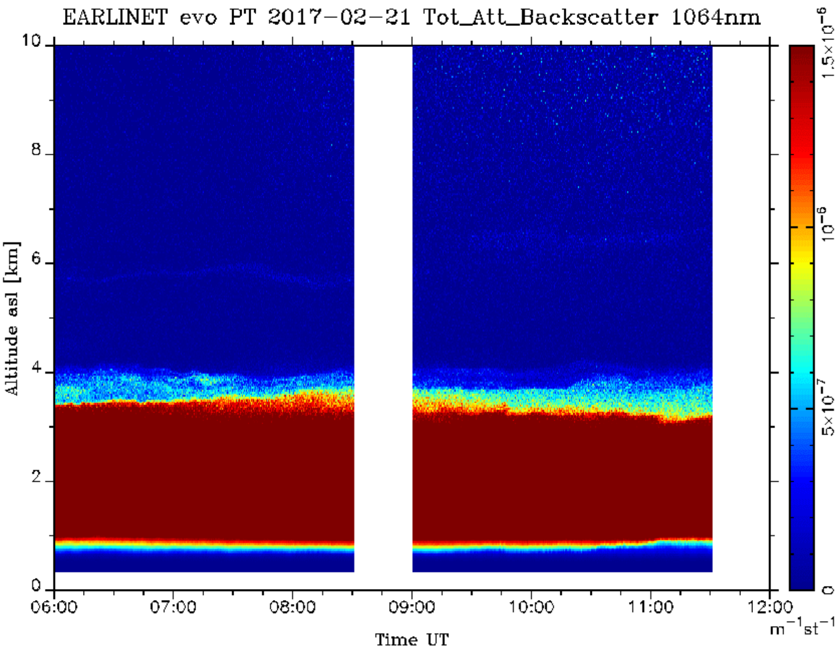
EARLINET evo PT 2017-02-21 Tot_Att_Backscatter 1064nm
Altitude asl [km]
Time UT
m^{-1}st^{-1}

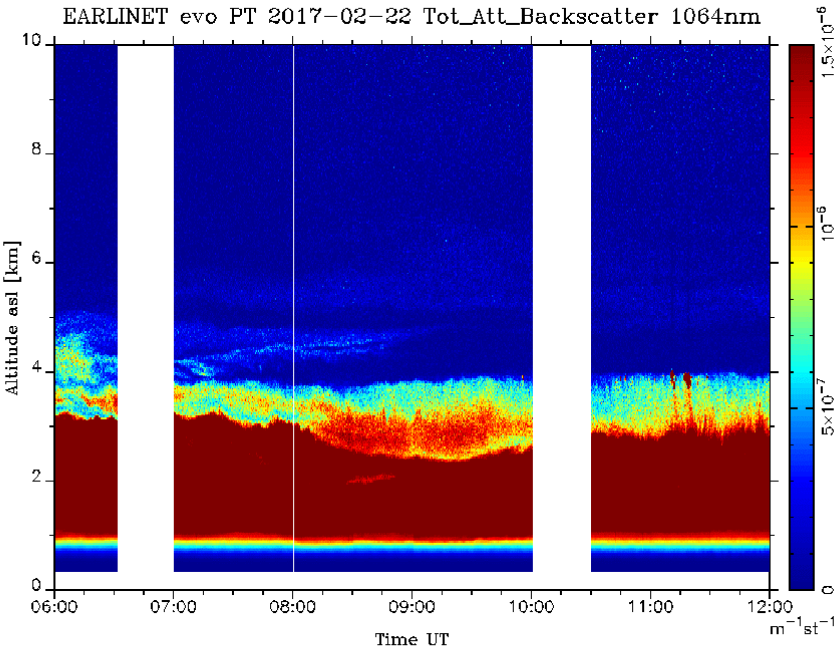
EARLINET evo PT 2017-02-22 Tot_Att_Backscatter 1064nm
Altitude asl [km]
Time UT
m^{-1}st^{-1}

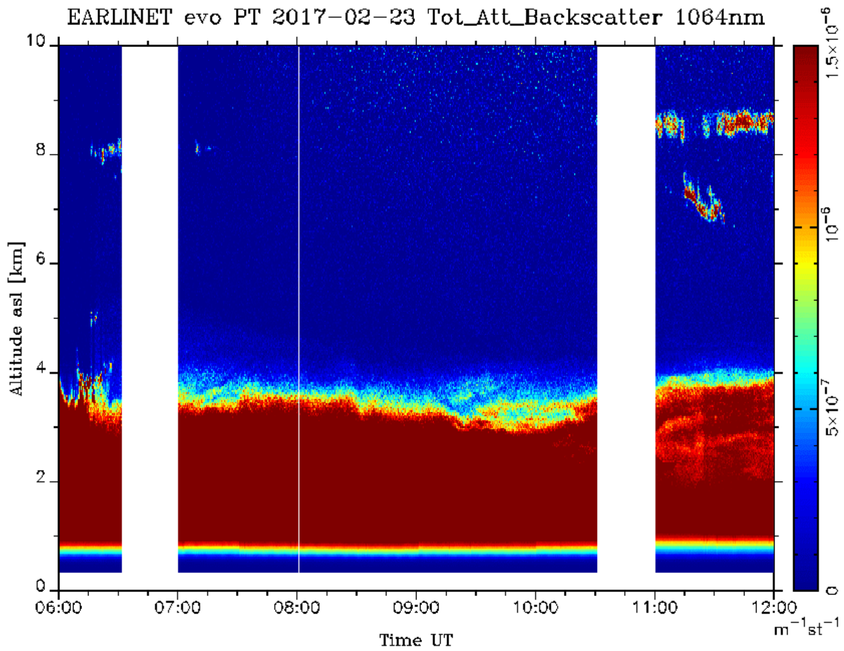

Figure 153. Quicklook images corresponding to the total attenuated backscatter at the 1064 nm by the EARLINET Évora lidar for the 21st [top], the 22nd [middle] and the 23rd [bottom] of February shown nicely the evolution of this particular dust event (https://quicklooks.earlinet.org/)

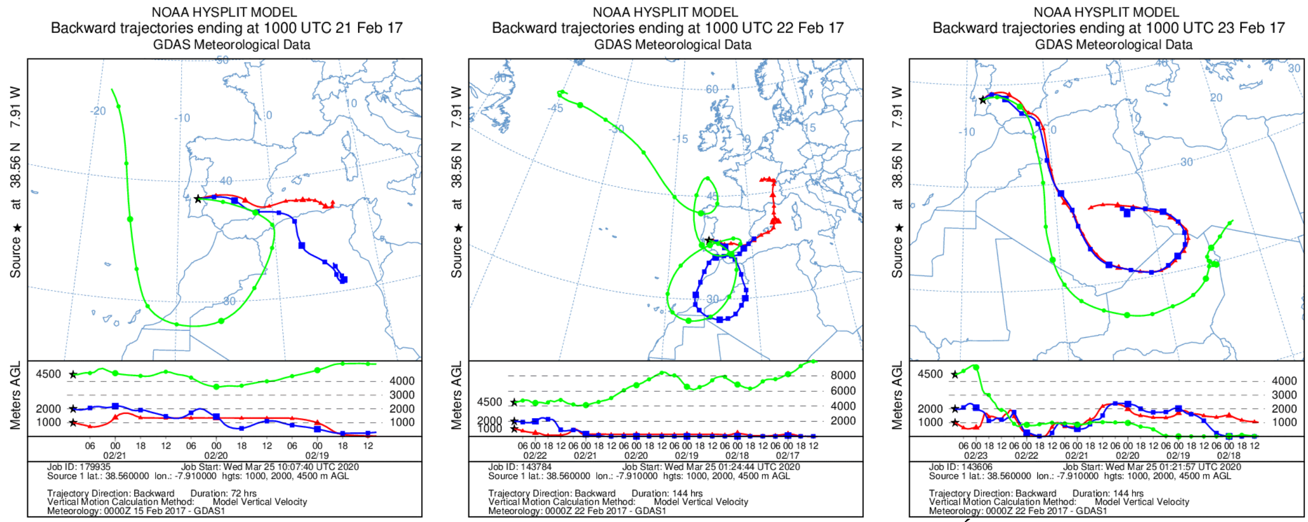

Figure 154. The 5-day NOAA HYSPLIT backward trajectories ending at the position of Évora 10:00 UTC (38.56°N, -7.91°E) for the 21st [left], the 22nd [middle] and the 23rd [right] of February show nicely the evolution of this particular dust event.

On the 21st of February, a well-defined aerosol layer is picked up by the lidar at 10:01:23 UT [Figure 155, left.] spanning between 1.5 and 3 km. The collocated GOME-2B observation between 09:59 and 10:30 UTC, at a distance of 62.7 km from the ground station, has an associated AAI value of 2.65, cloud fraction of 9% and an AAH estimate at 2.0 km, well within the range seen by the lidar at the ground. For the case of the 22nd of February, the aerosol layer appears to split into two separate plumes [Figure 154Figure 155, middle] resulting in GOME-2A reporting an AAI value of 2.07, i.e. quite close to the threshold value of 2.0. Even though the cloud fraction remains low (10%), the satellite AAH estimate is quite low (0.8 km). On the 23rd of February, [Figure 154, right] GOME-2B reports a pixel quite close to the station, at 25 km, and even though the reported AAH of 2.8 km is well within the range of the aerosol layer height reported by the lidar, the high cloud fraction of 45% and associated extreme AAI value of 5.75 makes it difficult to draw further conclusions.

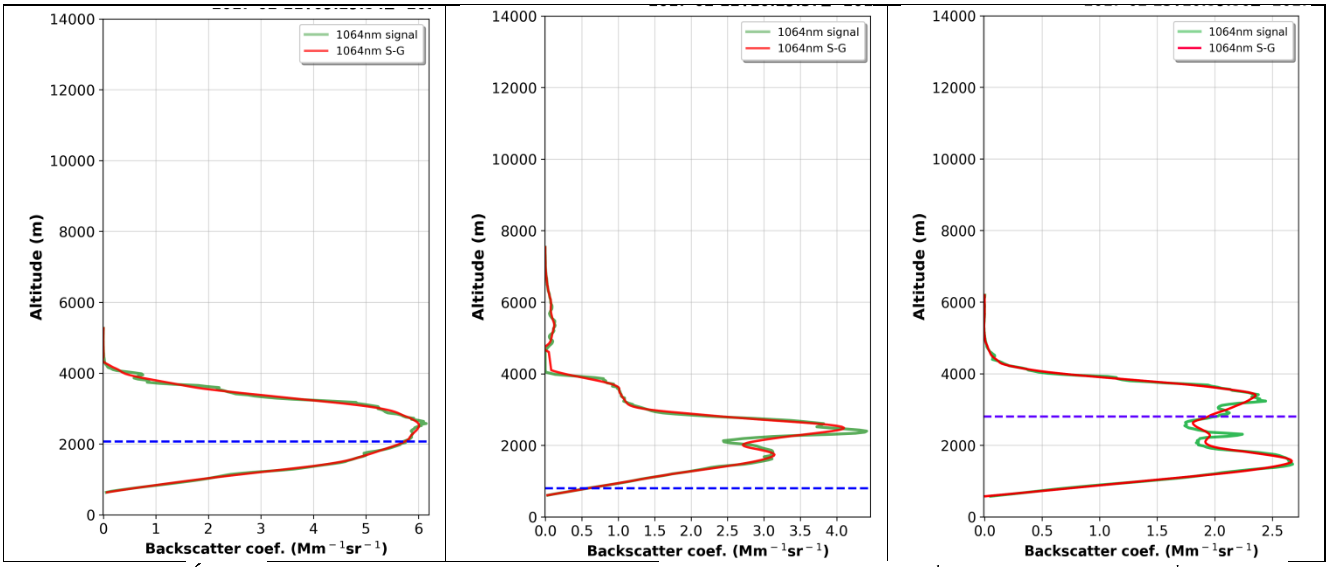

Figure 155. The Évora lidar backscatter profile at 1064 nm for the 21st [left], the 22nd [middle] and the 23rd [right] of February. The blue lines represent the GOME-2 AAH product whose details are given in Table 47.

Table 47. Satellite products from MetOp-A [middle] & MetOp-B [left and right] overpasses on February 21st, 22nd and 23rd 2019.

	21-02-2017	22-02-2017	23-02-2017
MetOp	MetOpB	MetOpA	MetOpB
Satellite Time	10:01:23 UT	10:26:50 UT	11:00:05 UT
Lidar Time	0	1	1
Distance	km	105 km	km
AAI	2.65	2.07	5.75
AAH	2.0 km	0.8 km	2.8 km
CF	0.09	0.10	0.45

The lidar system in Granada, Spain, [37.16°N/-3.60°E], also captured this event for the 20th, 21st and 22nd of February 2019. In this case, all three satellite overpasses where quite close spatially, between 60 and 70 km as shown in Table 48, with quite high associated AAI values between 2.4 and 2.8. However, for the 20th of February [Figure 156, left] the temporal collocation is not as good and, more importantly, the cloud fraction of 56% probably explains why the satellite algorithm resulted in such a high estimate for the aerosol layer [recall the important cloud structures over the area show in Figure 151.] The same cannot be postulated for the disagreement shown for the 21st of February [Figure 156, middle] where the temporal collocation is optimal and the cloud fraction is reported lower, but not cloud-free, at 34%. As a result, it cannot be claimed with certainty that the agreement of the 22nd of February [Figure 156, right] is promising as similar low cloudiness conditions were reported here as well. The 3-day NOAA HYSPLIT backward trajectories ending at the position of Granada for 10:00 UTC and the same days are shown in Figure 157.

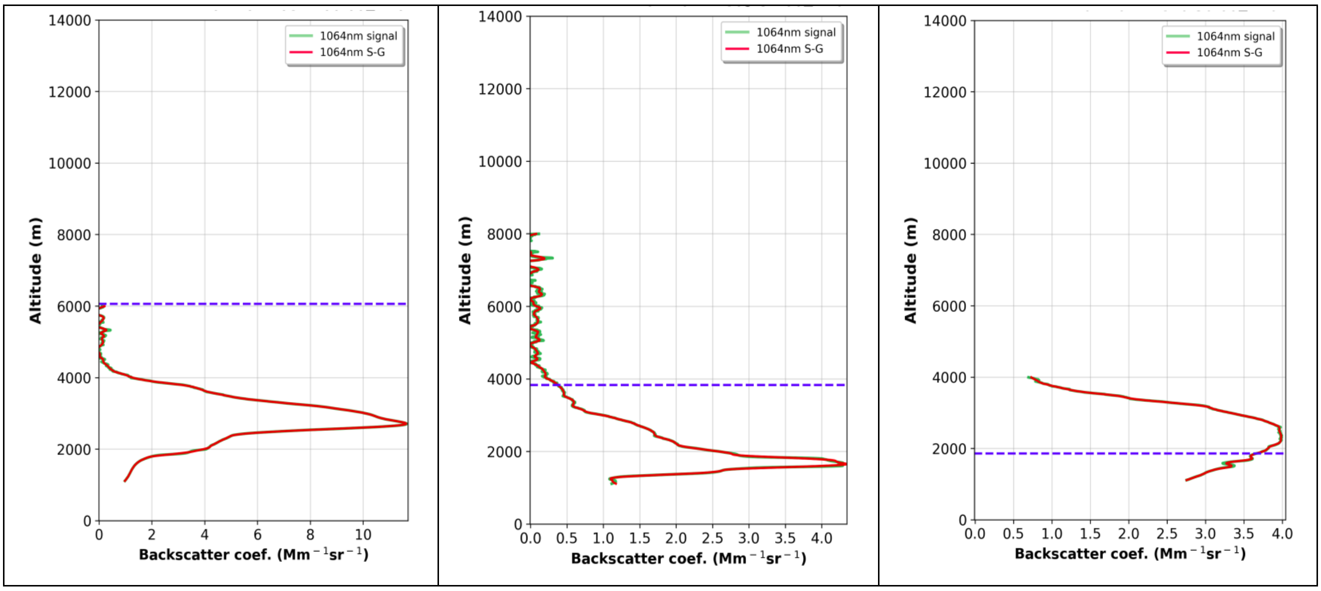

Figure 156. The Granada lidar backscatter profile at 1064 nm for the 20th [left], the 21st [middle] and the 22nd [right] of February. The blue lines represent the GOME-2 AAH product whose details are given in Table 48.

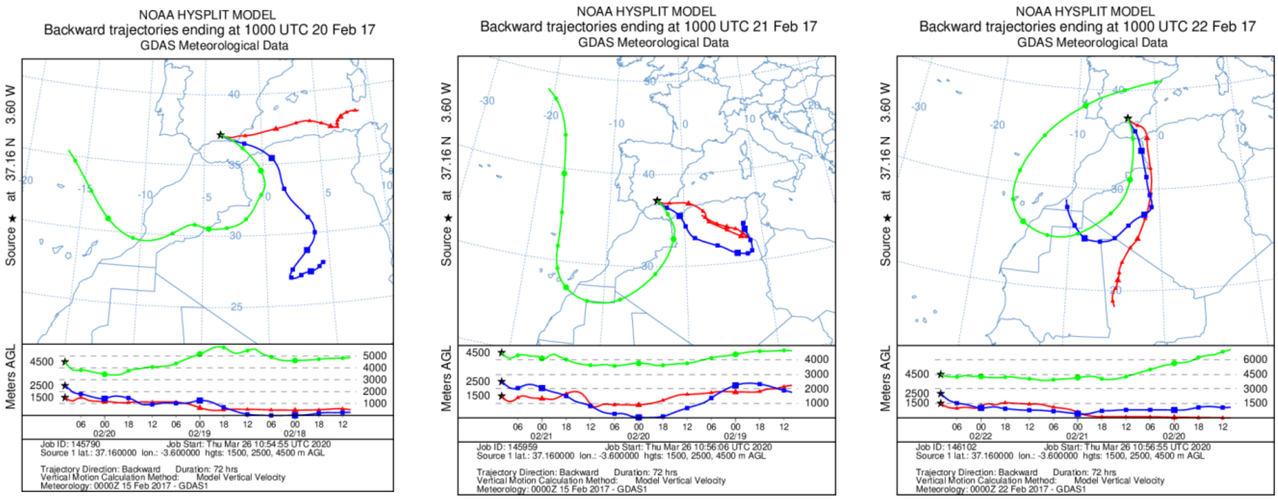

Figure 157.The 3-day NOAA HYSPLIT backward trajectories ending at the position of Granada 10:00 UTC (37.16°N, -3.60oE) for the 20th [left], the 21st [middle] and the 22nd [right] of February show nicely the evolution of this particular dust event.

Table 48. Satellite products from MetOp-A [right] & MetOp-B [left and middle] overpasses on February 20th, 21st and 22nd 2019.

	20-02-2017	**21-02-2017**	**22-02-2017**
MetOp	MetOpB	MetOpB	MetOpA
Satellite Time	10:22:03 UT	10:01:22 UT	10:26:34 UT
Lidar Time	1	UT	1
Distance	66.3 km	62.1 km	71 km
AAI	2.36	2.5	2.81
AAH	6.06 km	3.83 km	1.85 km
CF	0.56	0.34	0.27